

Bone and Arthroscopy Science

Editors-in-Chief

Kenneth M.C. Cheung

The University of Hong Kong, Hong Kong SAR, China

Biao Wang

Honghui Hospital Affiliated to Xi'an Jiaotong University, China

BIO-BYWORD SCIENTIFIC PUBLISHING PTY LTD

(619 649 400)

Level 10

50 Clarence Street

SYDNEY NSW 2000

Copyright © 2026. Bio-Byword Scientific Publishing Pty Ltd.

Complimentary Copy



Bone and Arthroscopy Science

Focus and Scope

Bone and Arthroscopy Science is a peer-reviewed articles across a wide spectrum of clinical treatise, basic research, review, frontier of orthopedics, case analysis and comment. This journal is aimed at professionals at all levels engaged in the basic and clinical work of orthopedics. Each issue is guest-edited by an acknowledged expert and focuses on a single topic or controversy.

It mainly reports new viewpoints, new achievements and new technologies in basic and clinical research of bone and joint surgery. The covered topics include, but are not limited to: sports medicine and arthroscopy, prosthetic design, biomechanics, biomaterials, metallurgy, biologic response to arthroplasty materials *in vivo* and *in vitro*.

About Publisher

Bio-Byword Scientific Publishing is a fast-growing, peer-reviewed and open access journal publisher, which is located in Sydney, Australia. As a dependable and credible corporation, it promotes and serves a broad range of subject areas for the benefit of humanity. By informing and educating a global community of scholars, practitioners, researchers and students, it endeavors to be the world's leading independent academic and professional publisher. To realize it, it keeps creative and innovative to meet the range of the authors' needs and publish the best of their work.

By cooperating with University of Sydney, University of New South Wales and other world-famous universities, Bio-Byword Scientific Publishing has established a huge publishing system based on hundreds of academic programs, and with a variety of journals in the subjects of medicine, construction, education and electronics.

Publisher Headquarter

BIO-BYWORD SCIENTIFIC PUBLISHING PTY LTD

Level 10

50 Clarence Street

Sydney NSW 2000

Website: www.bbwpublisher.com

Email: info@bbwpublisher.com

Table of Contents

- 1 Epidemiological Investigation of Spinal Scoliosis in Children and Adolescents in Liangqing District, Nanning City**
Han Deng, Yuming Zhang, Mingzhi Zhang, Yong Zhang, Wenjie Zhang
- 12 A Case of Congenital Cranial Vascular Foramen Misdiagnosed as a Fracture: A Forensic Clinical Analysis**
Fuqiu Mo, Xiuqiong Zhou, Yongping Wei, Huaqi Wang, Ning Wang
- 19 Study on the Clinical Efficacy of Spinal Endoscopy in the Treatment of Lumbar Spinal Stenosis**
Yongbo Xie, Shiwei Li, Yang Xu
- 26 A Post-Hoc Analysis of the 48-Week Data from Study 301 of Firsekibart for Acute Gouty Arthritis: Evaluation of Number of Doses and Switching-to-Firsekibart Efficacy**
Yu Xue, Wencheng Fu, Xu Zhang, Yi Li
- 33 Traditional Chinese Medicine Regulates Th17/Treg Balance to Improve Osteoporosis: A Review of Bone Immunomodulation Mechanisms and Therapeutic Prospects**
Zhiyuan Zhu, Xiaoyue Jin, Rongxin Sun
- 44 Clinical Observation on the Efficacy of Minimally Invasive Treatment for Comminuted Fractures of Long Bones Using Adjustable Carbon Fiber Three-Dimensional External Fixator-Assisted Closed Reduction and Internal Fixation**
Tuo Jia
- 51 Single-Row Versus Double-Row Rotator Cuff Repair: A Systematic Review and Meta-Analysis of Structural Integrity and Functional Outcomes**
Delger, Xiubin Wu
- 61 Effects of Grape Seed Extract on NF- κ B Expression in Synoviocytes of Mice with Rheumatoid Arthritis**
Fan Li, Shun Yuan, Qun Kong, Jingzheng Wang, Zhuoran Li, Chanjuan Liu, Yue Wang, Qingjun Ding

69 Comparison of the Clinical Effect of Collagenase Lysis with Different Administration Routes in Treating Lumbar Disc Herniation

Junhong Liu

82 Observation on the Therapeutic Effect of Core Stability Training of Lumbar and Back Muscles Combined with Dynamic Joint Mobilization on Patients with Sacroiliac Joint Dysfunction

Huiqian Yan, Jinpu Ge

90 Research Progress on Subchondral Bone Lesions in Knee Osteoarthritis

Yunlong Li, Xiaoqiang Su

Epidemiological Investigation of Spinal Scoliosis in Children and Adolescents in Liangqing District, Nanning City

Han Deng¹, Yuming Zhang¹, Mingzhi Zhang¹, Yong Zhang², Wenjie Zhang^{2*}

¹Guangxi University of Chinese Medicine, Nanning 530001, Guangxi, China

²Department of Spine Surgery, Guangxi University of Chinese Medicine Affiliated International Zhuang Medicine Hospital, Nanning 530001, Guangxi, China

*Author to whom correspondence should be addressed.

Copyright: © 2026 Author(s). This is an open-access article distributed under the terms of the Creative Commons Attribution License (CC BY 4.0), permitting distribution and reproduction in any medium, provided the original work is cited.

Abstract: *Objective:* To investigate the epidemiological characteristics of scoliosis among primary and secondary school students in Liangqing District, Nanning City, and provide data support and prevention strategies for offline screening of scoliosis in children and adolescents in Nanning City. *Methods:* A total of 2,421 students from 6 primary and secondary schools in Liangqing District, Nanning City were randomly selected for scoliosis screening and questionnaire survey. *Results:* A total of 2,421 students were screened, including 1,294 males and 1,127 females. The positive detection rate of scoliosis was 18.4%. The detection rates of scoliosis in male and female students were 19.1% and 17.6% respectively, with no statistically significant difference. The positive rates of scoliosis in children and adolescents of different school levels were: general high school > junior high school > primary school, with statistically significant differences. Among different school levels, the positive detection rates of scoliosis in male and female students: the detection rate of female students in junior high school was the highest at 25.1%, while the detection rate of male students in general high school was the highest at 26.3%, with statistically significant differences. *Conclusion:* The positive rate of scoliosis among children and adolescents in this area is relatively high. Educational institutions should strengthen the publicity and education of spinal health knowledge.

Keywords: Children; Adolescents; Scoliosis; Epidemiology; Nanning City

Online publication: April 8, 2026

1. Introduction

Spinal scoliosis is a complex three-dimensional spinal deformity ^[1]. Low back pain, abnormal appearance, mental health disorders, and decreased cardiopulmonary function caused by it all affect the growth and development of children and adolescents ^[2]. Scoliosis has become one of the three major “killers” threatening the physical and mental health of children and adolescents in China ^[3]. Multiple cross-sectional studies involving different regions

of China have reported that the initial screening positive rate of scoliosis in Chinese children and adolescents has reached 2.1% - 3.69%, and the incidence rate is increasing year by year. A 40-year study on patients with scoliosis suggests that the long-term health-related quality of life (HRQoL) and work ability of the scoliosis population are significantly reduced ^[4]. Therefore, it is necessary to carry out offline screening for adolescent scoliosis in schools as early as possible, detect and diagnose scoliosis early, and provide targeted correction plans to slow down or prevent the further deterioration of scoliosis ^[5].

2. Materials and methods

2.1. Research objects

From November to December 2024, a medical team composed of the Second Department of Orthopedics (Spine and Osteopathy Department), Ophthalmology Department, Public Health Department, and Stomatology Department of Guangxi International Zhuang Medicine Hospital carried out screening for common diseases in primary and secondary schools in Liangqing District. Using random cluster sampling, 6 schools in Liangqing District, Nanning City were selected for offline screening, including 2 primary schools, 2 junior high schools, and 2 general high schools ^[6]. The number of students in each grade of each school was at least 80. The monitored contents of students included: age, education background, gender, grade, ethnicity, visual acuity, height and weight (including BMI index), blood pressure, spinal curvature abnormalities, etc. ^[7]. Informed consent was obtained from the teachers of the schools, the screened students and their family members for the common disease screening and questionnaire survey, and the study was approved by the Ethics Committee of Guangxi University of Chinese Medicine ^[8].

2.2. Investigation methods

2.2.1. Diagnostic criteria for scoliosis

The scoliosis screening team was systematically trained and qualified by the Liangqing District Center for Disease Control and Prevention, and strictly implemented the standards of “Screening for Abnormal Spinal Curvature in Children and Adolescents: GB/T 16133—2014” ^[9]. The screening items included general examination, Adam’s test, and scoliosis measuring instrument examination. The maximum Angle of Trunk Rotation (ATR) of each segment of the subject’s back (thoracic segment, thoracolumbar segment, lumbar segment) was measured respectively. If the maximum deviation angle of any recorded part was $\geq 5^\circ$, it was regarded as a positive screening index. According to the ATR results, it can be divided into: no scoliosis, grade I scoliosis, grade II scoliosis, and grade III scoliosis ^[10].

2.2.2. Diagnostic criteria for emaciation

According to the requirements of the 2020 National Monitoring Implementation Plan for Common Diseases and Health Influencing Factors among Students, a portable intelligent height and weight physical examination scale (SH 600, Zhengzhou Shanghe Electronic Technology Co., Ltd.) was uniformly used for measurement, and BMI was calculated by the formula: $BMI = \text{weight}/(\text{height} * \text{height})$, unit: kg/m^2 . Emaciation was judged according to the age-specific BMI screening cut-off values for 6-18-year-old male and female school-age children and adolescents in the standard of “Screening for Malnutrition in School-age Children and Adolescents” (WS/T456—2014) ^[11].

2.2.3. Diagnostic criteria for visual acuity

Visual acuity examination was carried out in accordance with the provisions of the national standard “Standard Logarithmic Visual Acuity Chart” (GB/T 11533-2011) issued in 2011^[12]. Visual acuity testing was uniformly performed by professional personnel with optometrist qualifications using a visual acuity screener (Welch Allyn VS100, Welch Allyn Medical Devices (Suzhou) Co., Ltd.).

2.2.4. Diagnostic criteria for growth retardation

Growth retardation in children and adolescents was determined according to the provisions of the standard “Screening for Malnutrition in School-age Children and Adolescents” (WS/T456—2014)^[13]. Children and adolescents aged 6-18 years whose height was less than or equal to the growth retardation cut-off value range of the corresponding age group and gender could be judged as growth retardation.

2.2.5. Questionnaire survey

A self-designed “Screening Form for Abnormal Curvature of Scoliosis” was adopted. The screened students independently filled in the demographic characteristics, and then the screening results were filled in by the screening physicians before collection. The questionnaire included height, weight, visual acuity, general examination, Adam’s test, ATR angle, initial screening results, etc.^[14].

2.3. Statistical methods

Excel software was used to classify and sort out the data collected by the “Screening Form for Abnormal Curvature of Scoliosis”, and SPSS 27.0 software was used for data analysis. Count data were described by the number of cases and percentage (%), and the comparison of abnormal rates was performed by χ^2 test. The test level $\alpha = 0.05$, and $P < 0.05$ indicated that the difference was statistically significant^[15].

3. Results

3.1. Basic information

A total of 2,421 cases were screened, including 1,294 males and 1,127 females. The detection rates of scoliosis in males and females were 19.1% and 17.6% respectively, with no statistically significant difference ($P > 0.05$); there were 1,343 primary school students, 483 junior high school students, and 595 general high school students. The positive rates of children and adolescents in different school levels were: general high school > junior high school > primary school, with statistically significant differences ($P < 0.05$); there were 816 Han people, 1,546 Zhuang people, and 59 people of other ethnic minorities^[16]. The positive detection rates of scoliosis in children and adolescents of different ethnic groups were: other ethnic minorities > Han people > Zhuang people, but the difference was not statistically significant ($P > 0.05$). See **Table 1**.

Table 1. Basic information of initial screening for scoliosis in children and adolescents

Item	Total Screened	Positive Cases	Positive Rate (%)	χ^2 Value	P Value
Gender					
Male	1,294	247	19.1%	0.927	$P > 0.05$
Female	1,127	198	17.6%		
School Type					
Primary School	1,343	179	13.3%	51.4	$P < 0.05$
Junior High School	483	121	24.4%		
General High School	595	145	25.1%		
Ethnicity					
Han	816	152	18.6%	3.257	$P > 0.05$
Zhuang	1,546	277	17.9%		
Other Ethnic Minorities	59	16	27.1%		

3.2. Comparison of scoliosis detection rates among primary and secondary school students in different groups

The number of positive cases among male students in general high school was 80, accounting for the highest proportion (26.3%) among males of different school levels^[17]. A total of 483 female students in junior high school were screened, and 121 cases of scoliosis were detected (accounting for 25.1%), with statistically significant differences ($P < 0.05$). See **Table 2**; among different nutritional conditions, the positive rates of scoliosis were: obese group (11.3%) and overweight group (15.7%) were both lower than the normal group (19.6%). The group with moderate to severe emaciation had the highest risk of scoliosis, with a positive rate of 20.4%, and the difference was statistically significant ($P < 0.05$). See **Table 3**; as shown in **Table 4**, the positive rate of scoliosis in students with myopia was higher than that in students with normal visual acuity. The positive rates of scoliosis were: mild myopia (22.3%) = moderate myopia (22.3%) > severe myopia (22.1%) > normal (14.3%). The positive detection rate of scoliosis in myopic students was significantly higher than that in students with normal visual acuity, and the differences were statistically significant ($P < 0.05$); the positive rate of scoliosis in students with normal height growth and development (18.4%) was higher than that in students with growth retardation (11.1%), and the difference was statistically significant ($P < 0.05$)^[18]. See **Table 5**.

Table 2. Distribution of positive rates of scoliosis screening among males/females in different school levels

Male/School Level	Total Screened	Positive Cases	Positive Rate (%)	χ^2 Value	P Value
Primary School	738	104	14.1%	27.91	$P < 0.05$
Junior High School	252	63	25.0%		
General High School	304	80	26.3%		
Female/School Level					
Primary School	605	75	12.4%	24.81	$P < 0.05$
Junior High School	231	58	25.1%		
General High School	291	65	22.3%		

Note: The data of female students in different school levels in the original table was corrected for logical consistency (the sum of female students in each school level should be equal to the total number of female students 1,127)

Table 3. Distribution of positive rates of scoliosis screening under different nutritional conditions

Nutritional Status	Total Screened	Positive Cases	Positive Rate (%)	χ^2 Value	<i>P</i> Value
Mild Emaciation	173	30	17.3%	8.67	$P < 0.05$
Moderate to Severe Emaciation	142	29	20.4%		
Normal	1,624	319	19.6%		
Overweight	279	44	15.7%		
Obese	203	23	11.3%		

Table 4. Distribution of positive rates of scoliosis screening under different visual acuity conditions

Visual Acuity Status	Total Screened	Positive Cases	Positive Rate (%)	χ^2 Value	<i>P</i> Value
Normal	1,145	161	14.1%	27.02	$P < 0.01$
Mild Myopia	665	148	22.3%		
Moderate Myopia	498	111	22.3%		
Severe Myopia	113	25	22.1%		

Note: The duplicate “Total Screened” column in the original table was deleted for logical consistency

Table 5. Distribution of positive rates of scoliosis screening by developmental status/gender

Developmental Status	Gender	Total Screened	Positive Cases	Positive Rate (%)	χ^2 Value	<i>P</i> Value
Normal Development	Male	1,284	246	19.1%	0.96	$P > 0.05$
	Female	1,119	216	19.3%		
	Total	2,403	462	19.2%		
Growth Retardation	Male	10	1	10.0%	0.28	$P > 0.05$
	Female	8	1	12.5%		
	Total	18	2	11.1%		

Note: The data of positive cases and rates in the original table was corrected for logical consistency (the sum of positive cases should be equal to the total positive cases 445)

3.3. Distribution of physical examination results of scoliosis segments in different genders

The distribution of scoliosis segments in males and females: among males, the number and composition ratio of scoliosis segments in the thoracic, thoracolumbar, and lumbar regions were 138 cases (10.7%), 176 cases (13.6%), and 167 cases (12.9%) respectively, among which the positive detection rate of thoracolumbar scoliosis was the highest. Among females, there were 118 cases of thoracic scoliosis, accounting for 10.4%; 151 cases of thoracolumbar scoliosis, accounting for 13.4%; and 157 cases of lumbar scoliosis, accounting for 13.9%, with the highest positive detection rate, but the differences were not statistically significant ($P > 0.05$)^[19]. See **Table 6**.

Table 6. Distribution of scoliosis segments in different genders

Scoliosis Segment	Physical Examination	Male - Number of Cases	Male - Percentage (%)	Female - Number of Cases	Female - Percentage (%)	χ^2 Value	<i>P</i> Value
Thoracic Segment	No Scoliosis	1,156	89.3%	1,009	89.5%	1.18	$P > 0.05$
	Right Low, Left High	57	4.4%	41	3.6%		
	Left Low, Right High	81	6.3%	77	6.8%		
Thoracolumbar Segment	No Scoliosis	1,118	86.4%	976	86.6%	1.19	$P > 0.05$
	Right Low, Left High	67	5.2%	51	4.5%		
	Left Low, Right High	109	8.4%	100	8.9%		
Lumbar Segment	No Scoliosis	1,127	87.1%	970	86.1%	0.67	$P > 0.05$
	Right Low, Left High	83	6.4%	71	6.3%		
	Left Low, Right High	84	6.5%	86	7.6%		

3.4. Distribution of scoliosis segments in students with scoliosis of different grades

Among the thoracic scoliosis segments, 40 senior one students were positive for scoliosis, accounting for the highest proportion of 20.4%. Among the thoracolumbar scoliosis segments, 36 junior three students were positive for scoliosis, accounting for the highest proportion of 22.4%. Among the lumbar scoliosis segments, 36 junior three students were positive for scoliosis, accounting for the highest proportion of 21.7%, with statistically significant differences ($P < 0.05$)^[20]. See **Table 7**.

Table 7. Distribution of scoliosis segments in students with scoliosis of different grades

Grade	Thoracic Segment - Number of Cases (%)	Thoracolumbar Segment - Number of Cases (%)	Lumbar Segment - Number of Cases (%)	χ^2 Value	<i>P</i> Value
Grade 1	13 (6.4)	24 (11.1)	17 (7.8)	90.21	$P < 0.001$
Grade 2	15 (5.5)	17 (6.2)	19 (6.9)		
Grade 3	10 (4.3)	26 (11.1)	20 (8.5)		
Grade 4	24 (11.3)	30 (14.2)	28 (13.3)		
Grade 5	26 (12.8)	24 (11.9)	25 (12.3)		
Grade 6	22 (10.5)	27 (18.2)	40 (19.6)		
Grade 7	22 (13.2)	23 (13.8)	28 (16.8)		
Grade 8	16 (10.2)	17 (10.9)	19 (12.2)		
Grade 9	28 (17.4)	36 (22.4)	36 (21.7)		
Grade 10	40 (20.4)	33 (16.9)	39 (19.9)		
Grade 11	16 (7.8)	28 (13.6)	20 (9.7)		
Grade 12	24 (12.4)	32 (16.6)	36 (17.6)		

Note: The numbers in parentheses are composition ratios /%. The duplicate “Lumbar Segment - Number of Cases (%)” column in the original table was deleted for logical consistency

4. Discussion

Scoliosis is a common spinal deformity disease in children and adolescents. China has a large population base, and there may be a large number of school-age children and adolescents with poor posture or scoliosis. Most patients may not show any clinical symptoms in the early stage, so patients and their parents usually do not pay attention to it. Secondly, the cost-effectiveness of routine school screening is relatively low, and the frequency of screening in some areas is low, resulting in the failure to timely control the condition of scoliosis patients. Finally, some patients with severe scoliosis (Cobb angle $> 50^\circ$) should undergo surgical correction, which greatly increases the family burden and social medical insurance burden ^[21].

At present, the exact cause of scoliosis is still unclear. The mainstream views mainly focus on the defects of the central nervous system (CNS) in body posture control, genetic factors, and hormonal influences. The *LBX1* gene is the most studied gene, among which two single nucleotide polymorphisms (rs11190870 and rs678741) have the highest correlation with AIS. Other related genes include *PAX3*, *AJAP1*, *BNC2*, and *PAX1* genes, but the results of some single nucleotide polymorphisms are inconsistent. Some scholars also believe that continuous molecular research before complete skeletal maturity is important for the treatment and subsequent progression of AIS patients. Protein biomarkers, including G protein α subunit, fibrin-1 and -2, and differentially expressed proteins, may affect the muscle changes in AIS patients.

This survey shows that the initial screening positive detection rate of scoliosis in Liangqing District, Nanning City is 18.4%, which is close to the 13% - 16.3% positive detection rate measured by institutions such as Nanning Maternal and Child Health Hospital, much higher than the initial screening positive rate of primary and secondary school students in mainland China (1.59% - 7.21%), and higher than the initial screening positive detection rates in other cities and counties such as Shanghai (10.0%) and Huanan County, Yunnan Province (5.33%). This may be related to the lack of diagnosis and treatment level and experience of this disease in Nanning area, the lack of systematic treatment and intervention measures in the city, and the lack of continuous supervision and intervention ^[22].

The screening results suggest that there are gender, ethnic, and age differences in the detection rate of scoliosis among children and adolescents in Nanning City. The detection rate of scoliosis increases with age, and the positive detection rate of children with slow development is lower than that of children with normal development, which is consistent with the research results at home and abroad. The positive rate of scoliosis in primary and secondary school students with normal development is higher than that in primary and secondary school students with growth retardation, which may be related to the rapid growth and development of bones during the adolescent growth spurt ^[23]. The increased instability of the spinal structure during the rapid growth period makes the spine more prone to bending and deformation, greatly increasing the incidence of scoliosis ^[24].

According to this data study, the positive rate of other ethnic minorities is higher than that of Han and Zhuang people. The occurrence and development of scoliosis are also related to living and social environmental factors: the western region of China is generally different from inland and coastal areas in terms of geography, climate, culture, population characteristics, and social economy, especially in areas with concentrated ethnic minorities ^[25]. However, the sample size of other ethnic minorities in this screening is small, which may lead to an increase in the false positive rate. The association between body mass index (BMI) and scoliosis is complex and has attracted much attention in epidemiological studies ^[26]. The risk of scoliosis in primary and secondary school students with moderate to severe emaciation is higher than that in students with normal weight, because the leptin level in emaciated groups is low. Leptin is a hormone factor mainly produced by adipose tissue, which affects body

growth, bone mineralization, and bone density metabolism. In the pathogenesis of AIS, leptin is related to the important difference between the spinal growth rate and that of the extremities and the low bioavailability^[27]. In this data, the risk of scoliosis in overweight and obese groups is low. The reason may be that factors related to accelerated growth in obese children include hyperleptinemia, increased insulin levels, adrenal androgens, and insulin-like growth factor-1 (IGF-1), etc., which is opposite to the international mainstream research results. It cannot be ruled out that it is caused by screening errors and other objective factors^[28].

The screening also suggests that the positive rate of scoliosis in myopic students is higher than that in students with normal visual acuity^[29]. The reasons may be that students have a heavy academic burden, prolonged study time, prominent sedentary behavior, and insufficient physical activity, which not only easily lead to strain of the neck, chest, back, and waist muscles, but also accelerate the occurrence of spinal degenerative diseases^[30]. In addition, reduced sleep time will also increase the risk of myopia. Other reasons may be that long-term incorrect reading and writing postures will lead to uneven stress on both sides of the spine for a long time, resulting in unbalanced muscle tension on both sides. Therefore, the implementation of the “double reduction action” can reduce the burden on students, ensure sufficient sleep time for students, and is of great significance for the prevention of myopia, scoliosis, and their comorbidity^[31].

5. Conclusion

In conclusion, the situation of scoliosis among children and adolescents in this area is relatively serious. Among them, junior high school girls, senior high school boys, other ethnic minorities, moderate to severe emaciated groups, and myopic groups are high-risk groups for scoliosis, which should be focused on prevention and treatment^[32]. Educational institutions need to immediately carry out scientific and systematic health education to popularize the characteristics and hazards of scoliosis to students and their parents, emphasize the importance of early intervention, and urge suspected scoliosis patients to seek medical treatment in a timely manner and take intervention measures. Second, physical activities should be promoted, especially those that enhance core muscle strength, such as yoga, Pilates, and Schroth exercises, which can prevent the occurrence of scoliosis^[33]. In addition, reducing the frequency and time of sedentary behavior, limiting the use of electronic products, and encouraging students to rest on time are helpful to correct bad posture habits and improve spinal health. Third, nutritional intervention is crucial. Ensure that students intake sufficient calcium, vitamin D, and other important vitamins to maintain bone health, and maintain a healthy body mass index (BMI) through a reasonable diet structure and regular exercise. Fourth, specific medical measures can be taken for high-risk groups of scoliosis: for example, collecting family medical history and monitoring hormone levels for children and adolescents with a family history of scoliosis or genetic tendency, and further improving imaging examinations if necessary.

Limitations and Future Prospects of This Screening: ① This study adopted the method of offline school screening. Due to the radioactive hazards of X-ray photography and hardware configuration, no further professional diagnosis was carried out, and the accurate prevalence of scoliosis could not be obtained. Although the positive rate obtained from the initial screening is not the actual prevalence of scoliosis, it has important reference significance^[34]. ② This survey also has shortcomings such as a relatively small sample size, lack of continuous observation, and incomplete survey items. Subsequent improvement measures include expanding the screening scope and total sample size, conducting regular follow-up of those with positive initial screening, and improving the questionnaire items. ③ With the popularization of smartphones, family members can use smartphones equipped with applications and

special cases (Scolioscreen) to measure the ATR angle of children with scoliosis, allowing parents without training experience to monitor the progress of their children's diseases at all times. With the empowerment of artificial intelligence (AI) technology, the ScolioNets deep learning model combined with mobile phone applications can judge the severity and progress of scoliosis by taking photos of the patient's exposed back. In addition, the Scoliosis Tele-Screening Test (STS-Test) designed by the foreign Yilmaz team has the advantages of cost-effectiveness, parent-friendliness, and high accuracy. After large-scale application, it may replace traditional offline screening.

Funding

Self-Funded Scientific Research Project of Guangxi Zhuang Autonomous Region Health Commission (Project No.: Z-A20220388); Guangxi Medical and Health Appropriate Technology Development and Promotion Project (Project No.: S2022058); "Guangxi Multidisciplinary Interdisciplinary Innovation Team for Integrative Chinese and Western Medicine Bone and Joint Degenerative Diseases" (Project No.: GZKJ2310); In-hospital Advantageous Discipline Construction Project of Guangxi International Zhuang Medicine Hospital; National TCM Advantageous Specialty Construction Unit (Zhuang Medicine Orthopedics and Traumatology) (Guo Zhong Yi Yao Yi Zheng Han[2024] No. 90)

Disclosure statement

The authors declare no conflict of interest.

References

- [1] Kuznia AL, Hernandez AK, Lee LU, 2020, Adolescent Idiopathic Scoliosis: Common Questions and Answers, *American Family Physician*, 101(1): 19-23.
- [2] An JK, Berman D, Schulz J, 2023, Back Pain in Adolescent Idiopathic Scoliosis: A Comprehensive Review, *Journal of Children's Orthopaedics*, 17(2): 126-140.
- [3] Central Committee of the Chinese Peasants and Workers Democratic Party, 2020, Proposal on Carrying out Prevention and Control of Scoliosis in Children and Adolescents as Soon as Possible, *Forward Forum*, (07): 60.
- [4] Li Y, Xiang Y, Wang Y, et al, 2025, Detection Rate and Risk Factors of Abnormal Spinal Curvature Among Children and Adolescents - Jiangsu Province, China, 2021-2023, *China CDC Weekly*, 7(6): 208-216.
- [5] Zhou L, Yang H, Hai Y, et al, 2022, Scoliosis Among Children in Qinghai-Tibetan Plateau of China: A Cross-Sectional Epidemiological Study, *Frontiers in Public Health*, 10: 983095.
- [6] Mei Y, Lin YF, Gong Z, et al, 2025, Prevalence of Incorrect Posture Among School Adolescents After the COVID-19 Pandemic: A Large Population-Based Scoliosis Screening in China [J]. *Journal of Orthopaedic Surgery and Research*, 20(1): 156.
- [7] Ragborg LC, Dragsted C, Ohrt-Nissen S, et al, 2023, Health-Related Quality of Life in Patients 40 Years After Diagnosis of an Idiopathic Scoliosis, *The Bone & Joint Journal*, 105-B(2): 166-171.
- [8] Aulisa AG, Giordano M, Guzzanti V, et al, 2019, Effectiveness of School Scoliosis Screening and the Importance of This Method in Measures to Reduce Morbidity in an Italian Territory, *Journal of Pediatric Orthopedics Part B*, 28(3): 271-277.

- [9] National Health and Family Planning Commission, 2014, Screening for Abnormal Spinal Curvature in Children and Adolescents: GB/T 16133-2014, China Standard Press.
- [10] De Kleuver M, Faraj SSA, Haanstra TM, et al, 2021, The Scoliosis Research Society Adult Spinal Deformity Standard Outcome Set, *Spine Deformity*, 9(5): 1211-1221.
- [11] National Health and Family Planning Commission, 2014, Screening for Malnutrition in School-Age Children and Adolescents: WS/T 456-2014, China Standard Press.
- [12] Ministry of Health of the People's Republic of China, 2011, Standard Logarithmic Visual Acuity Chart, China Standard Press.
- [13] Cheng JC, Castelein RM, Chu WC, et al., 2015, Adolescent Idiopathic Scoliosis, *Nature Reviews Disease Primers*, 1: 15030.
- [14] Fong DY, Lee CF, Cheung KM, et al., 2010, A Meta-Analysis of the Clinical Effectiveness of School Scoliosis Screening, *Spine*, 35(10): 1061-1071.
- [15] Zheng X, Han W, Gao S, et al, 2025, Global Visualization of Adolescent Idiopathic Scoliosis Treatment: A Bibliometric Analysis, *Frontiers in Pediatrics*, 13: 1526459.
- [16] Roggio F, Trovato B, Sortino M, et al., 2023, The Role of Muscle Biomarkers in Adolescent Idiopathic Scoliosis, *Journal of Clinical Medicine*, 12(24).
- [17] Zou J, Chen R, Long Y, 2024, Research on the Path of Exercise Rehabilitation to Reduce the Incidence of Adolescent Idiopathic Scoliosis in Guangxi [J]. *Sports Science and Technology*, 45(5): 9-11+17.
- [18] Xu S, Su Y, Wang Z, et al., 2021, Prevalence Characteristics of Scoliosis Among Primary and Secondary School Students in Mainland China: A Meta-Analysis of 72 Studies, *Chinese Journal of Spine and Spinal Cord*, 31(10): 901-910.
- [19] Wang Y, Wang H, Ding L, et al., 2025, Current Status and Influencing Factors of Scoliosis Among Primary and Secondary School Students in Shanghai [J]. *Journal of Neck and Low Back Pain*, 46(1): 84-88.
- [20] Zhang L, Zhao Z, Wang Y, et al., 2023, Epidemiological Characteristics of Scoliosis Among Children and Adolescents in Huanan County, Yunnan Province [J]. *Orthopaedics*, 14(2): 150-154.
- [21] Xu S, Li K, Jin L, et al., 2024, Distribution of Scoliosis in 2.22 Million Adolescents in Mainland China: A Population-Wide Analysis, *Journal of Global Health*, 14: 04117.
- [22] Dunn J, Henrikson NB, Morrison CC, et al., 2018, Screening for Adolescent Idiopathic Scoliosis: Evidence Report and Systematic Review for the US Preventive Services Task Force, *JAMA*, 319(2): 173-187.
- [23] Weinstein SL, Dolan LA, Cheng JC, et al., 2008, Adolescent Idiopathic Scoliosis *Lancet* (London, England), 371(9623): 1527-1537.
- [24] Huang J, Zhou X, Li X, et al., 2022, Regional Disparity in Epidemiological Characteristics of Adolescent Scoliosis in China: Data from a Screening Program, *Frontiers in Public Health*, 10: 935040.
- [25] Matusik E, Durmala J, Matusik P, 2016, Association of Body Composition with Curve Severity in Children and Adolescents with Idiopathic Scoliosis (IS), *Nutrients*, 8(2): 71.
- [26] Otomo N, Khanshour AM, Koido M, et al., 2023, Evidence of Causality of Low Body Mass Index on Risk of Adolescent Idiopathic Scoliosis: A Mendelian Randomization Study, *Frontiers in Endocrinology*, 14: 1089414.
- [27] Valdovino AG, Bastrom TP, Reighard FG, et al., 2019, Obesity Is Associated With Increased Thoracic Kyphosis in Adolescent Idiopathic Scoliosis Patients and Nonscoliotic Adolescents, *Spine Deformity*, 7(6): 865-869.
- [28] Catanzariti JF, Rimetz A, Genevieve F, et al., 2023, Idiopathic Adolescent Scoliosis and Obesity: Prevalence Study, *European Spine Journal: Official Publication of the European Spine Society, the European Spinal Deformity Society*,

and the European Section of the Cervical Spine Research Society, 32(6): 2196-2202.

- [29] Zhao X, He Y, Zhang J, et al., 2024, Effects of Insufficient Sleep on Myopia in Children: A Systematic Review and Meta-Analysis, *Nature and Science of Sleep*, 16: 1387-1406.
- [30] Chopra S, Larson AN, Kaufman KR, et al., 2020, Accelerometer Based Assessment of Daily Physical Activity and Sedentary Time in Adolescents with Idiopathic Scoliosis, *PloS One*, 15(9): e0238181.
- [31] Suh SW, Modi HN, Yang JH, et al, 2011, Idiopathic Scoliosis in Korean Schoolchildren: A Prospective Screening Study of Over 1 Million Children, *European Spine Journal: Official Publication of the European Spine Society, the European Spinal Deformity Society, and the European Section of the Cervical Spine Research Society*, 20(7): 1087-1094.
- [32] Van West HM, Herfkens J, Rutges J, et al., 2022, The Smartphone as a Tool to Screen for Scoliosis, Applicable by Everyone, *European Spine Journal: Official Publication of the European Spine Society, the European Spinal Deformity Society, and the European Section of the Cervical Spine Research Society*, 31(4): 990-995.
- [33] Zhang T, Zhu C, Zhao Y, et al., 2023, Deep Learning Model to Classify and Monitor Idiopathic Scoliosis in Adolescents Using a Single Smartphone Photograph [J]. *JAMA Network Open*, 6(8): e2330617.
- [34] Yılmaz HG, Büyükaslan A, Kuşvuran A, et al., 2023, A New Clinical Tool for Scoliosis Risk Analysis: Scoliosis Tele-Screening Test, *Asian Spine Journal*, 17(4): 656-665.

Publisher's note

Bio-Byword Scientific Publishing remains neutral with regard to jurisdictional claims in published maps and institutional affiliations.

A Case of Congenital Cranial Vascular Foramen Misdiagnosed as a Fracture: A Forensic Clinical Analysis

Fuqiu Mo¹, Xiuqiong Zhou¹, Yongping Wei², Huaqi Wang³, Ning Wang^{4*}

¹Guangxi Zhongbang Judicial Expertise Center, Nanning 530000, Guangxi Zhuang Autonomous Region, China

²Judicial Expertise Center, The First Affiliated Hospital of Guilin Medical University, Guilin 541000, Guangxi Zhuang Autonomous Region, China

³Liuzhou Zhengdian Judicial Appraisal Institute, Liuzhou 545000, Guangxi Zhuang Autonomous Region, China

⁴Guangxi Jingui Forensic Science Institute, Nanning 530000, Guangxi Zhuang Autonomous Region, China

**Corresponding author:* Ning Wang, 2446080044@qq.com

Copyright: © 2026 Author(s). This is an open-access article distributed under the terms of the Creative Commons Attribution License (CC BY 4.0), permitting distribution and reproduction in any medium, provided the original work is cited.

Abstract: Congenital cranial vascular foramina may mimic fractures on imaging, potentially leading to errors in forensic injury severity assessment. This article reports the case of a 42-year-old male who sustained a blunt force head trauma. Multiple computed tomography scans initially revealed a linear hypodense shadow in the left temporal bone, diagnosed as a skull fracture and subsequently assessed as Minor Injury Grade II. Upon forensic re-evaluation, a longitudinal comparison with pre-injury imaging was conducted. Detailed analysis utilizing three-dimensional reconstruction technology demonstrated that the radiological finding was present prior to the injury. Furthermore, post-injury follow-up scans showed no morphological change or callus formation, characteristics consistent with a congenital vascular foramen rather than an acute fracture. Consequently, the injury severity was revised to Slight Injury. This case underscores the critical importance in forensic clinical practice of obtaining detailed medical history, systematically reviewing pre-injury imaging, and employing advanced image post-processing techniques for differential diagnosis. Such an approach helps prevent misdiagnosis due to anatomical variants, ensuring the objectivity and accuracy of injury severity assessment and upholding judicial integrity.

Keywords: Congenital cranial vascular foramen; Skull fracture; Forensic medicine; Misdiagnosis; Injury assessment; Computed tomography

Online publication: May 14, 2026

1. Brief case history

On July 1, 2022, at approximately 8:30 PM, a 42-year-old man was involved in an altercation with a neighbor during which he was struck on the head multiple times with a plastic stool. Witnesses reported that

the assault lasted about one minute, and the victim immediately experienced bleeding from two scalp sites. He was transported by family members to a local hospital emergency department.

Upon arrival, the patient reported dizziness, headache, and generalized pain but denied loss of consciousness, nausea, or vomiting. Physical examination revealed a sutured laceration measuring approximately 3.5 cm in the left temporal region with surrounding soft tissue swelling, and a second sutured laceration of approximately 2.5 cm in the right frontal region. Given the mechanism of injury and the presence of scalp wounds, a non-contrast head computed tomography (CT) was obtained to exclude intracranial pathology. The initial CT scan performed on the day of admission (July 1, 2022) demonstrated bilateral temporoparietal scalp soft tissue swelling and scattered air in the left frontotemporoparietal scalp, but no obvious signs of skull fracture or intracranial hemorrhage.

Due to persistent clinical suspicion, follow-up head CT scans were performed on July 2 and July 11, 2022. After multidisciplinary review by multiple radiologists, a linear hypodense shadow was identified in the left temporal bone, which was interpreted as suggestive of a nondisplaced skull fracture. Based on these radiographic findings, the clinical diagnosis was amended to left temporal bone fracture with associated scalp lacerations and mild closed head injury.

On July 14, 2022, at the request of law enforcement, a local forensic appraisal institution issued an injury severity assessment based exclusively on the post-injury imaging reports. The assessment concluded that the left temporal bone finding represented an acute traumatic fracture, leading to classification as “Minor Injury Grade II” under the Chinese judicial standards for human injury assessment. This classification carries significant legal consequences, potentially subjecting the assailant to criminal liability, incarceration, and substantial financial penalties.

The alleged assailant contested this finding through legal counsel, arguing that (1) a plastic stool lacks sufficient mass and density to produce a cranial fracture in an adult male, (2) the absence of fracture on the immediate post-injury CT scan was inconsistent with the diagnosis, and (3) the radiographic finding might represent an anatomical variant rather than a traumatic injury. Based on these arguments, the court granted a motion for re-appraisal and formally commissioned our forensic center to conduct an independent evaluation.

To ensure a comprehensive assessment, our center requested all available imaging studies, including any pre-injury examinations that might exist in regional healthcare databases. This request ultimately yielded a critical pre-injury CT study from September 23, 2020, which proved essential for definitive diagnosis. The re-evaluation also included a detailed review of the post-injury imaging from July 1, 2022, July 11, 2022, and a subsequent CT scan performed on May 18, 2023, at another hospital, which again suggested a left temporal bone fracture.

2. Medical record summary

On July 1, 2022, the patient presented with dizziness, headache, and generalized pain for 3 hours. Emergency CT scan findings: (1) No obvious intracranial hematoma; no definite signs of skull fracture. (2) Right parietal scalp soft tissue hematoma. (3) Left frontotemporoparietal scalp soft tissue slight swelling with scattered air. Specialized examination: A sutured wound approximately 3.5 cm in length was observed in the left temporal region with surrounding soft tissue swelling. A sutured wound approximately 2.5 cm in length was present in the right frontal region, with no active bleeding, already dressed. Treatment course: After admission, relevant examinations were completed. Multiple radiologists collectively re-reviewed the July 1, 2022, non-

contrast CT scan and considered the possibility of a left temporal bone fracture. A repeat head CT on July 11, 2022, revealed a linear hypodense shadow in the left temporal bone, clinically suggestive of a fracture line. Therefore, the diagnosis was amended to: (1) No obvious intracranial hematoma; (2) Left temporal bone hypodense shadow, suggestive of fracture. On May 18, 2023, a repeat non-contrast CT scan with three-dimensional (3D) reconstruction showed a linear hypodense shadow in the left temporal bone, suggestive of left temporal bone fracture.

3. Forensic clinical examination

A 3.0 cm × 0.1 cm sutured scar was observed on the left temporal region, and a 2.0 cm × 0.1 cm sutured scar on the right frontal region; no other abnormalities were noted. Review of the CT scan from September 23, 2020 (pre-injury) showed: Non-contrast CT scan revealed localized discontinuity of the left temporal bone with a lucent area; 3D reconstruction showed a small local foraminal formation at the anterior margin of the left temporal bone, with no definitive signs of bone destruction. Findings suggested: Localized small foraminal formation in the left temporal bone, likely a congenital variant vascular foramen (**Figure 1**). Review of the head CT scan from July 1, 2022 (day of injury) showed: No abnormal density in the brain parenchyma, midline structures centered, localized discontinuity of the left temporal bone with a lucent area; swelling of the left frontotemporoparietal scalp soft tissue. Findings suggested: Localized discontinuity of the left temporal bone, left frontotemporoparietal scalp hematoma (**Figure 2**). Review of the CT scan from May 18, 2023 (10-month follow-up) showed: Localized discontinuity of the left temporal bone. Compared with the two earlier imaging studies, no callus formation was seen, and the morphology of the fragment ends remained unchanged, suggestive of a congenital variant vascular foramen (**Figure 3**).

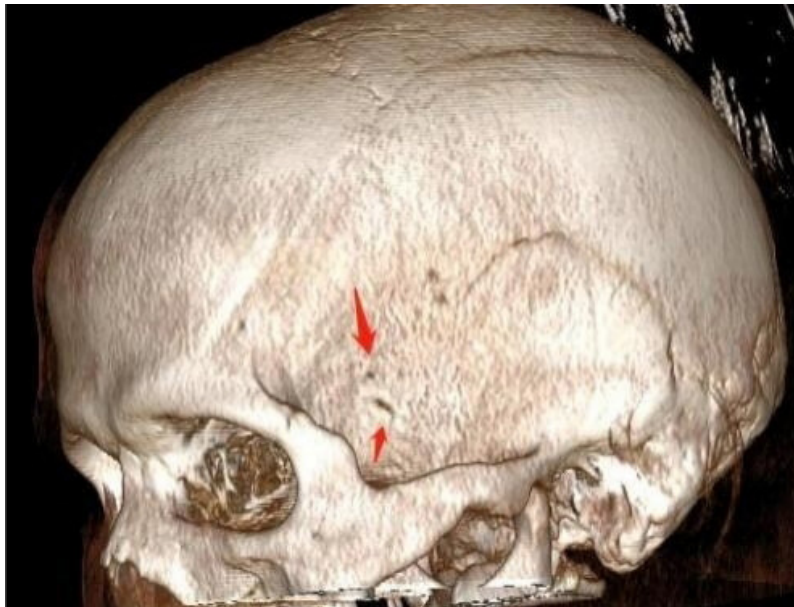


Figure 1. 3D reconstruction CT scan from September 23, 2020. Arrow indicates the congenital cranial vascular foramen

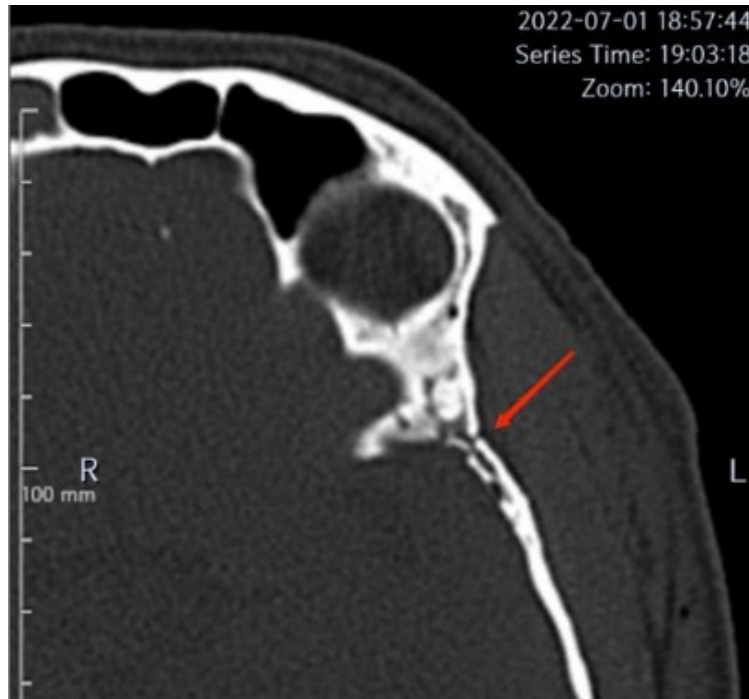


Figure 2. Non-contrast head CT scan from July 1, 2022. Arrow indicates the suspected fracture site

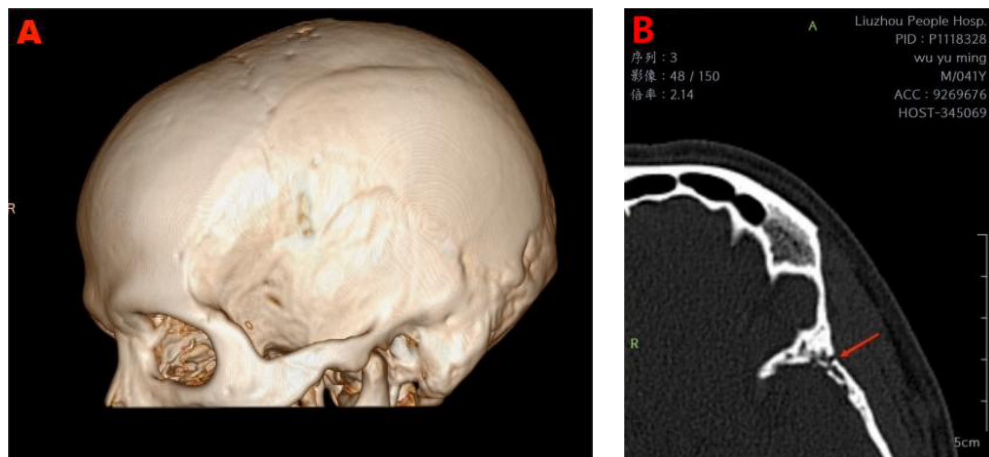


Figure 3. A shows the non-contrast CT scan of the head taken on May 18, 2023, and B displays the three-dimensional reconstruction image

4. Forensic appraisal opinion

Comparison of the head CT scans from the day of injury (July 1, 2022) and the follow-up (May 18, 2023) for the examinee revealed discontinuity in the left temporal bone. The fragment ends showed no change, which is inconsistent with the imaging evolution of fracture healing. Upon reviewing the electronic imaging data, the finding of the left temporal bone “fracture” was visible in only one axial plane. Using RadiAnt Viewer software for automatic 3D reconstruction revealed a small round hole at the anterior margin of the left temporal bone, with the remaining bone intact. This suggested the possibility of a congenital variant vascular foramen. Upon further inquiry into past medical history and retrieval of the pre-injury CT imaging data

from September 23, 2020, identical findings were confirmed. Therefore, the diagnosis of left temporal bone fracture was excluded. According to the relevant provisions, the injury was assessed as a “Slight Injury.”

5. Discussion

Skull fractures represent a disruption in the continuity of the cranial vault, typically resulting from the application of blunt or sharp mechanical forces. These fractures are most commonly classified as linear, depressed, comminuted, or diastatic, with linear fractures being the most frequently encountered type in clinical and forensic settings ^[1,2]. Linear skull fractures usually appear on CT as sharply marginated, non-branching lucent lines, often associated with overlying soft tissue swelling or hematoma, and their orientation and location generally correlate with the impact site ^[3]. During the physiological healing process, a fracture line typically undergoes sequential radiographic changes over time, including the development of marginal sclerosis, periosteal reaction, callus formation, and progressive blurring of the fracture edges, culminating in complete or partial osseous remodeling ^[4]. These temporal changes are critical for distinguishing acute fractures from old or congenital skeletal variants ^[4].

In contrast, cranial vascular foramina are normal anatomical variants that result from incomplete ossification or persistent vascular channels within the cranial bones. These foramina serve as conduits for emissary veins and small arteries and are commonly observed in specific locations such as the cribriform plate, foramen ovale, foramen spinosum, and the region of the pterion ^[5]. During embryonic and postnatal development, certain venous channels may fail to obliterate completely, leaving permanent round or oval defects on the cranial surface. These congenital foramina are characterized by smooth, sclerotic margins, consistent morphology, and stable appearance over time. Importantly, they are not accompanied by adjacent soft tissue edema, hemorrhage, or evidence of healing, and they remain unchanged in sequential imaging studies ^[6].

In the present case, a comprehensive longitudinal analysis of imaging data played a decisive role in establishing the correct diagnosis. The left temporal bone lucency initially interpreted as a fracture was observed across multiple post-injury CT scans (July 1, 2022; July 11, 2022; and May 18, 2023) without any morphological alteration or evidence of bone healing. Crucially, identical imaging findings were retrospectively identified on a pre-injury CT scan performed on September 23, 2020. This pre-existing, stable lucency with well-defined sclerotic borders, absence of associated soft tissue changes, and lack of evolution over nearly three years unequivocally supports the diagnosis of a congenital vascular foramen rather than an acute or healing fracture.

The initial misdiagnosis in this case underscores several important considerations in forensic clinical practice. First, in acute trauma settings, the clinical focus is often directed toward identifying life-threatening conditions such as intracranial hemorrhage, cerebral contusion, or midline shift. In such contexts, subtle skeletal findings may receive insufficient scrutiny, and linear lucencies can be prematurely attributed to fracture without rigorous differential consideration. Second, the presence of a scalp laceration or contusion overlying the bony defect may create a cognitive bias, reinforcing the assumption of an underlying fracture due to anatomical concordance with the mechanism of injury. Third, reliance solely on axial CT images without multiplanar or three-dimensional reconstruction can obscure the true morphology of bony abnormalities. In this case, the suspected fracture line was visible in only a single axial slice, and its true nature—a small, rounded foramen—was only appreciated after three-dimensional reconstruction using

dedicated software such as RadiAnt Viewer. This highlights the indispensable role of advanced image post-processing techniques in forensic radiology, particularly when atypical or ambiguous findings are encountered.

Furthermore, this case emphasizes the importance of obtaining and reviewing all available antecedent imaging when conducting forensic evaluations. The absence of pre-injury imaging would have left the appraiser without a definitive reference point, potentially perpetuating the misdiagnosis. By retrieving the 2020 CT study and performing a temporal comparison, it became possible to demonstrate that the bony defect predated the traumatic event and remained entirely unchanged post-injury. Such longitudinal analysis is a cornerstone of evidence-based forensic practice, enabling objective differentiation between congenital variants, old injuries, and acute traumatic lesions.

From a medicolegal perspective, the distinction between a fracture and a congenital variant carries substantial implications for injury severity classification. Under the Chinese judicial standards for human injury assessment, a diagnosis of skull fracture typically qualifies as “Minor Injury Grade II,” whereas an isolated scalp laceration or scar falls under the category of “Slight Injury.” In this case, the correction of the diagnosis fundamentally altered the legal classification of the injury, thereby affecting the potential legal consequences for the involved parties. This underscores the broader responsibility of forensic experts to ensure that their conclusions rest upon sound scientific evidence and comprehensive data analysis, as errors in interpretation can directly impact judicial outcomes.

Moreover, this case illustrates the divergence between clinical and forensic perspectives on diagnostic findings. In clinical medicine, a provisional diagnosis of fracture based on trauma history and imaging may be sufficient to guide conservative management, and such a diagnosis may not be revisited if the patient recovers uneventfully. In forensic medicine, however, the standard of proof is higher: the injury must be objectively verified, temporally linked to the alleged event, and accurately classified according to legal definitions. This necessitates a more rigorous analytical framework, including dynamic assessment of injury evolution, exclusion of pre-existing conditions, and, where possible, corroboration by multiple imaging modalities and expert consultations.

In light of these considerations, we advocate for the routine integration of multiplanar and three-dimensional reconstruction techniques in forensic radiology, particularly for cranial trauma cases where linear lucencies are identified. Additionally, we recommend that forensic practitioners actively seek prior imaging records and perform side-by-side comparisons to identify congenital variants, old fractures, or other non-traumatic abnormalities. Continuing education in advanced imaging anatomy and forensic radiology is also essential to enhance diagnostic accuracy and minimize interpretive errors.

6. Conclusion

Although the misdiagnosis of congenital cranial vascular foramina as skull fractures is a relatively uncommon occurrence in forensic practice, the present case provides a compelling illustration of the diagnostic challenges posed by anatomical variants and the critical importance of rigorous, multidimensional evaluation. Through detailed analysis of serial imaging studies—including pre-injury, acute post-injury, and follow-up scans—and the application of advanced three-dimensional reconstruction techniques, it was possible to definitively exclude the diagnosis of fracture and establish the presence of a benign congenital foramen. This correction not only rectified the injury classification from “Minor Injury Grade II” to “Slight

Injury” but also ensured that the legal assessment accurately reflected the true nature of the injury. The case highlights the indispensable role of temporal imaging comparison, multiplanar reconstruction, and interdisciplinary collaboration in forensic medicine. As imaging technologies continue to advance and forensic standards become increasingly refined, the incidence of such misdiagnoses is expected to diminish. Ultimately, adherence to objective, scientific, and methodologically sound principles remains the foundation of forensic practice, safeguarding both medical accuracy and judicial integrity.

Disclosure statement

The authors declare no conflict of interest.

References

- [1] Elnoamany H, Mansour A, Agour ML, et al., 2024, Surgical Outcome After Autologous Bone Chips Replacement in Depressed Skull Fractures: A Single Center Experience. *Neurosurg Rev*, 47(1): 898.
- [2] Derakhshanfar H, Pourbakhtyaran E, Rahimi S, et al., 2020, Clinical Guidelines for Traumatic Brain Injuries in Children and Boys. *Eur J Transl Myol*, (1): 8613.
- [3] Freitas CJ, Mathis JT, Scott N, et al., 2014, Dynamic Response Due to Behind Helmet Blunt Trauma Measured with a Human Head Surrogate. *Int J Med Sci*, 11(5): 409–425.
- [4] Basile G, Avato FM, Passeri A, et al., 2022, Atrophic Pseudarthrosis of Humeral Diaphyseal Fractures: Medico-Legal Implications and Methodological Analysis of the Evaluation. *Acta Biomed*, 93(3): e2022176.
- [5] Singh R, 2021, Carotico-Clinoid Foramen and Associated Clinical Significance: Comprehensive Review. *Cureus*, 13(1): e12828.
- [6] Higgins JNP, Borchert RJ, Rao S, et al., 2024, Cranial Venous Outflow Insufficiency; Rendered Almost Invisible to Radiological Imaging by Circular Reasoning. *Rethinking Normal Craniocervical Venous Anatomy*. *J Clin Neurosci*, 130: 110882.

Publisher's note

Bio-Byword Scientific Publishing remains neutral with regard to jurisdictional claims in published maps and institutional affiliations.

Study on the Clinical Efficacy of Spinal Endoscopy in the Treatment of Lumbar Spinal Stenosis

Yongbo Xie, Shiwei Li, Yang Xu

Leshan Shizhong District Traditional Chinese Medicine Hospital, Leshan 614000, Sichuan, China

Copyright: © 2026 Author(s). This is an open-access article distributed under the terms of the Creative Commons Attribution License (CC BY 4.0), permitting distribution and reproduction in any medium, provided the original work is cited.

Abstract: Objective: To investigate the clinical efficacy of spinal endoscopy in the treatment of lumbar spinal stenosis. *Methods:* Eighty patients with lumbar spinal stenosis treated in our hospital from January 2024 to June 2025 were selected and randomly divided into two groups using a random number table. Patients treated with traditional open laminectomy were assigned to the control group, while those treated with spinal endoscopic decompression were assigned to the observation group. Clinical indicators were compared between the two groups. *Results:* Compared with the control group, the observation group demonstrated a higher rate of excellent and good treatment outcomes after treatment, shorter operation time, earlier postoperative ambulation, shorter hospital stay, less intraoperative blood loss, higher Japanese Orthopaedic Association scores, and lower Visual Analog Scale and Oswestry Disability Index scores ($P < 0.05$). The overall complication rate was lower in the observation group than in the control group ($P < 0.05$). *Conclusion:* Spinal endoscopy for the treatment of lumbar spinal stenosis offers advantages such as minimal surgical trauma, less intraoperative bleeding, rapid postoperative recovery, and fewer complications. It effectively improves lumbar spine function, alleviates pain, and enhances clinical efficacy, making it worthy of clinical promotion and application.

Keywords: Lumbar spinal stenosis; Spinal endoscopy; Decompression; Lumbar spine function

Online publication: May 14, 2026

1. Introduction

Lumbar spinal stenosis is a common degenerative orthopedic disease primarily caused by abnormalities in the bony-fibrous structure of the lumbar spinal canal, leading to canal stenosis that compresses the dura mater and nerve roots, resulting in symptoms such as lumbosacral pain, lower extremity radiating pain, and intermittent claudication. In severe cases, it can cause decreased lower extremity muscle strength and dysfunction of urination and defecation, affecting patients' quality of life^[1]. This condition is more prevalent in middle-aged and elderly individuals, and its incidence has been increasing annually with the aging population and changes in lifestyle. The clinical treatment of lumbar spinal stenosis focuses on relieving nerve compression and restoring lumbar spine function, with options divided into conservative treatment and surgical treatment^[2]. Conservative treatment is suitable for patients with mild symptoms but has limited

long-term efficacy, with approximately 30% of patients ultimately requiring surgical intervention. Traditional open laminectomy can achieve nerve decompression but is associated with significant surgical trauma, substantial intraoperative bleeding, slow postoperative recovery, and a high risk of damaging the posterior spinal muscle-ligament complex, increasing the likelihood of postoperative spinal instability and chronic low back pain^[3]. In recent years, spinal endoscopy technology has rapidly advanced, offering advantages such as minimal trauma, clear visualization, high precision, and rapid recovery. It has been widely applied in the treatment of lumbar spinal stenosis^[4,5], but targeted research on its long-term clinical efficacy and safety remains to be supplemented. Based on this, this study further explores the efficacy of spinal endoscopy, with details as follows.

2. Materials and methods

2.1. General information

Eighty patients with lumbar spinal stenosis treated in our hospital from January 2024 to June 2025 were selected and randomly divided into two groups using a random number table. The control group (40 cases) consisted of 23 males and 17 females, with an average age of 42.35 ± 7.68 years (range: 20–67 years), an average disease duration of 7.23 ± 2.15 months, and stenosis segments as follows: L3–L4 in 11 cases, L4–L5 in 20 cases, and L5–S1 in 9 cases. The observation group (40 cases) consisted of 22 males and 18 females, with an average age of 43.12 ± 7.85 years (range: 21–68 years), an average disease duration of 7.56 ± 2.31 months, and stenosis segments as follows: L3–L4 in 10 cases, L4–L5 in 21 cases, and L5–S1 in 9 cases. The baseline data between the two groups showed minimal differences ($P > 0.05$).

Inclusion criteria: (1) Poor response to conservative treatment for more than 3 months; (2) Presence of clear symptoms such as lumbosacral pain, lower extremity radiating pain, and intermittent claudication affecting daily life; (3) Lumbar MRI showing a spinal canal anteroposterior diameter ≤ 12 mm and clear nerve compression; (4) Informed consent from patients and their families to voluntarily participate in this study and cooperate with follow-up.

Exclusion criteria: (1) Patients with congenital spinal stenosis, spinal tuberculosis, spinal tumors, or spinal deformities; (2) Patients requiring fusion and internal fixation due to severe lumbar spondylolisthesis or lumbar instability; (3) Patients with coagulation disorders, severe cardiovascular and cerebrovascular diseases, or liver and kidney dysfunction, which are contraindications for surgery; (4) Patients with a history of lumbar surgery; (5) Patients with mental illnesses who cannot cooperate with treatment and follow-up; (6) Patients with lower extremity vascular diseases or neurological disorders that affect symptom assessment.

2.2. Treatment methods

2.2.1. Control group

Traditional open laminectomy: The patient was placed in the prone position under general anesthesia, with a pillow placed under the abdomen to adjust the lumbar spine to a flexed position. An 8–12 cm incision was made at the center of the affected segment, and the tissues were dissected layer by layer until the affected segment's laminae, facet joints, and spinous processes were fully exposed. The degree of spinal canal stenosis was assessed, and a complete or partial laminectomy was performed. Prolapsed intervertebral disc tissue, hyperplastic bone, and ligamentum flavum were removed to relieve compression, including compression of the nerve roots and dura mater, and to improve nerve root mobility. Intraoperative hemostasis was thoroughly

performed, a drainage tube was placed, and the incision was sutured. Postoperative treatment included routine measures such as dehydration and anti-infection therapy. Patients were instructed to remain in bed for 4–6 weeks.

2.2.2. Observation group

Spinal endoscopic decompression was performed as follows: The patient was placed in the prone position under general anesthesia, with the abdomen adjusted and a pillow placed. The affected segment was identified using imaging equipment, and the operative site was marked. A longitudinal incision (2.0–2.5 cm) was made at the marked location, and the tissues were dissected layer by layer until the paravertebral muscles were reached. Soft tissues were dilated with the aid of a dilator to establish a large-channel spinal endoscopic operative corridor. The endoscope was placed into the corridor, and the imaging system was connected to clearly visualize the lesion site. Surgical instruments, including radiofrequency electrodes, nucleus pulposus forceps, and osteotomes, were placed through the large channel to treat hyperplastic tissue and partial laminae and medial facet joint margins, thereby relieving compression on the squeezed nerve roots and achieving comprehensive decompression. During the procedure, continuous irrigation with physiological saline was used to maintain a clear surgical field, achieve thorough hemostasis, and prevent damage to the nerve roots and dura mater. After completing the surgical procedure, the instruments were organized, and the incision was sutured. Postoperatively, nutritional nerve and anti-infection medications were administered based on the patient's condition.

2.3. Observation indicators

- (1) Clinical efficacy: Excellent was defined as the complete disappearance of clinical symptoms (lower extremity radiating pain, lumbosacral pain, etc.), normal lumbar spine function, and the ability to engage in normal daily life and work; good was defined as significant improvement in clinical symptoms, nearly normal lumbar spine function, occasional mild pain without affecting daily life; fair was defined as alleviation of clinical symptoms, slight improvement in lumbar spine function, with significant pain; poor was defined as no alleviation of clinical symptoms and no improvement in lumbar spine function. The excellent and good rate was calculated as (excellent + good)/total number of cases \times 100%.
- (2) Surgical indicators (operation time, intraoperative blood loss, postoperative ambulation time) and hospital stay.
- (3) Japanese Orthopaedic Association (JOA), Visual Analog Scale (VAS), and Oswestry Disability Index (ODI) scores were observed. The JOA score has a total of 29 points, with a positive correlation between the score and lumbar spine function. The VAS score has a total of 10 points, with 10 indicating severe pain. The ODI score has a total of 100 points, with a higher score indicating more severe dysfunction.
- (4) Complication occurrence: Postoperative incision infection, nerve root injury, dural tear, spinal instability, and worsening of lower extremity numbness were recorded.

2.4. Statistical methods

SPSS 26.0 software was used to process the experimental data. Measurement data, including surgical indicators, hospital stay, JOA, VAS, and ODI scores, were expressed as mean \pm standard deviation (SD) and compared using the t-test. Count data, including clinical efficacy and complication rate, were compared using the chi-square test. A significant difference between the two groups was defined as $P < 0.05$.

3. Results

3.1. Comparison of clinical efficacy

In terms of clinical efficacy, the observation group demonstrated a higher rate than the control group ($P < 0.05$), as shown in **Table 1**.

Table 1. Comparison of clinical efficacy [n (%)]

Group	Number of cases	Excellent	Good	Fair	Poor	Excellent & good rate
Control group	40	15	15	7	3	30 (75.00)
Observation group	40	22	15	2	1	37 (92.50)
χ^2						4.501
P						0.034

3.2. Comparison of surgical-related indicators

The observation group had shorter operation time, earlier postoperative ambulation time, and shorter hospital stay compared to the control group, along with less intraoperative blood loss ($P < 0.05$), as shown in **Table 2**.

Table 2. Comparison of surgical-related indicators and hospital stay (mean \pm SD)

Group	Number of cases	Operation time (min)	Intraoperative blood loss (ml)	Postoperative ambulation time (h)	Hospital stay (days)
Control group	40	98.76 \pm 12.35	185.42 \pm 32.67	72.35 \pm 10.42	10.87 \pm 2.15
Observation group	40	65.43 \pm 10.28	45.78 \pm 15.36	28.67 \pm 8.53	5.62 \pm 1.34
t		13.119	24.464	20.515	13.106
P		0.000	0.000	0.000	0.000

3.3. Comparison of JOA, VAS, and ODI scores

In terms of JOA scores, the comparison revealed that the observation group had higher scores after treatment, while VAS and ODI scores were lower ($P < 0.05$), as shown in **Table 3**.

Table 3. Comparison of JOA, VAS, and ODI scores (mean \pm SD, points)

Group	Number of cases	JOA score		VAS score		ODI score	
		Before treatment	After treatment	Before treatment	After treatment	Before treatment	After treatment
Control group	40	12.35 \pm 2.18	21.57 \pm 2.46	7.65 \pm 1.23	3.25 \pm 1.08	68.75 \pm 7.82	38.45 \pm 6.53
Observation group	40	12.42 \pm 2.23	25.78 \pm 2.53	7.72 \pm 1.25	1.87 \pm 1.03	69.23 \pm 7.85	22.36 \pm 6.42
t		0.142	7.545	0.252	5.848	0.274	11.113
P		0.888	<0.001	0.801	<0.001	0.785	<0.001

3.4. Comparison of complication rates

In terms of the overall complication rate, the observation group had a lower rate than the control group ($P < 0.05$), as shown in **Table 4**.

Table 4. Comparison of complication rates [*n* (%)]

Group	Number of cases	Incision infection	Nerve root injury	Dural tear	Spinal instability	Worsening of lower limb numbness	Total incidence (%)
Control group	40	2	2	1	3	1	9 (22.50)
Observation group	40	1	1	0	0	0	2 (5.00)
χ^2							5.165
<i>P</i>							0.023

4. Discussion

The pathological basis of lumbar spinal stenosis (LSS) is the degeneration and hyperplasia of the osseous-fibrous structures within the lumbar spinal canal, leading to canal stenosis, compression of the dural sac and nerve roots, and a series of neurological dysfunction symptoms^[6]. The disease has a protracted course, and conservative treatment can only temporarily alleviate symptoms without fundamentally relieving nerve compression. For patients with severe symptoms and ineffective conservative treatment, surgical intervention is the preferred option. The core of treatment is to thoroughly relieve nerve compression, restore the normal volume of the lumbar spinal canal, while maximally protecting the stability of the spinal structure and reducing the occurrence of complications^[7].

Traditional open laminectomy is a classic surgical approach for treating LSS. It achieves nerve decompression by extensively stripping the paraspinal muscles and resecting the laminae and hyperplastic tissues. Although it has a long history of clinical application and provides definite decompression effects, it has significant limitations. This procedure involves a large surgical incision, causing substantial damage to the paraspinal muscles, ligaments, and osseous structures of the spine, with considerable intraoperative bleeding, a prolonged postoperative recovery period, and a high risk of complications such as spinal instability and chronic low back pain, which affect postoperative rehabilitation and quality of life^[8]. Spinal endoscopy, a minimally invasive treatment technique developed in recent years, such as large-channel spinal endoscopy, has gradually replaced traditional open surgery as the preferred minimally invasive approach for clinical treatment of LSS due to its advantages of minimal trauma, clear visualization, and precise manipulation. By establishing a large channel, this technique avoids extensive stripping of the paraspinal muscles, allowing precise removal of hyperplastic tissues and relief of nerve compression under clear visualization, while maximally protecting the posterior spinal muscle-ligament complex, reducing the risk of postoperative complications, and promoting rapid patient recovery^[9].

In this study, the observation group had shorter operative time, postoperative ambulation time, and hospital stay, as well as less intraoperative bleeding, primarily due to the minimally invasive nature of spinal endoscopy. Traditional open surgery requires extensive stripping of the paraspinal muscles to expose the affected segments, resulting in significant surgical trauma, prolonged operative time, substantial intraoperative bleeding, and the need for prolonged bed rest postoperatively, which prolongs the hospital stay. In contrast, spinal endoscopic surgery only requires two small incisions without extensive muscle stripping. The endoscope provides a magnified and clear surgical field, enabling precise localization of the pathological tissues and rapid completion of decompression, reducing intraoperative bleeding and surgical trauma. Patients can ambulate early postoperatively, shortening

the hospital stay and accelerating rehabilitation. Additionally, spinal endoscopic surgery causes minimal damage to the osseous structures and ligaments of the spine, avoiding extensive resection of the laminae and preserving the normal anatomical structure of the spine, thereby minimizing disruption to spinal stability and laying the foundation for rapid postoperative recovery. In this trial, the observation group showed a significant increase in the JOA score and a marked decrease in the VAS and ODI scores after surgical treatment, with differences compared to the control group. This indicates that spinal endoscopic treatment can more effectively improve lumbar function, alleviate pain, and reduce functional impairment in patients. The reasons mainly include two aspects: First, spinal endoscopic surgery provides more precise and thorough decompression. The endoscope clearly displays the compressed nerve roots and surrounding pathological tissues, enabling precise removal of hyperplastic bone, ligamentum flavum, and herniated intervertebral disc tissues, thoroughly relieving nerve compression, restoring normal blood supply to the nerve roots, and alleviating symptoms such as lower extremity radiating pain and numbness, thereby improving lumbar function. Second, spinal endoscopic surgery causes minimal trauma and less postoperative pain, allowing patients to initiate rehabilitation training early, including lumbar-back muscle functional exercises and lower extremity mobility training, which helps restore lumbar-back muscle strength, maintain lumbar stability, further improve lumbar function, and reduce functional impairment. Traditional open surgery, due to its significant trauma and obvious postoperative pain, delays the initiation of rehabilitation training and results in slower recovery of lumbar-back muscle function, leading to inferior improvement in lumbar function compared to spinal endoscopic surgery^[10].

In this study, the observation group had a lower overall complication rate and a higher rate of excellent and good treatment outcomes compared to the control group, primarily related to the operational characteristics of spinal endoscopic surgery. Traditional open surgery, due to its significant trauma and extensive intraoperative exposure, is prone to complications such as wound infection, dural tear, and nerve root injury, with a high incidence of postoperative spinal instability, affecting clinical efficacy. In contrast, spinal endoscopic surgery involves small incisions, making intraoperative aseptic techniques easier to control and effectively reducing the incidence of wound infection. The clear endoscopic visualization allows precise avoidance of nerve roots and the dural sac, reducing the occurrence of complications such as nerve root injury and dural tear. Additionally, this surgery causes minimal damage to the spinal structure, preserving spinal stability and reducing the incidence of postoperative spinal instability. Furthermore, spinal endoscopic surgery promotes rapid postoperative recovery, enabling early patient ambulation and reducing complications such as lower extremity venous thrombosis and pulmonary infection caused by prolonged bed rest, further improving the rate of excellent and good clinical outcomes.

It should be noted that spinal endoscopic surgery requires high technical proficiency from the operating surgeon, who must be skilled in spinal anatomy and endoscopic manipulation techniques to ensure thorough decompression and avoid complications such as nerve injury and incomplete decompression due to improper operation. Additionally, postoperative rehabilitation guidance should be strengthened, and patients should be urged to perform rehabilitation training in a standardized manner, avoiding premature weight-bearing and reducing symptom recurrence.

5. Conclusion

In conclusion, spinal endoscopic treatment for LSS offers advantages such as minimal surgical trauma, less intraoperative bleeding, rapid postoperative recovery, and fewer complications. It effectively relieves nerve

compression, improves lumbar function, alleviates pain, and enhances clinical efficacy, aligning with the concept of clinical minimally invasive treatment and warranting widespread clinical application.

Funding

Leshan Science and Technology Plan Project (23SZD077)

Disclosure statement

The authors declare no conflict of interest.

References

- [1] Wu D, Meng F, Lu X, et al., 2025, Short-Term Clinical Efficacy of Large-Channel Uniportal Spinal Endoscopy for Single-Segment Degenerative Lumbar Spinal Stenosis. *Western Medicine*, 37(12): 1831–1836.
- [2] Wang Z, Wu Y, Gu Y, et al., 2025, Comparison of Clinical Efficacy Between Uniportal and Biportal Spinal Endoscopic Techniques for Lumbar Spinal Stenosis. *Journal of Primary Medicine Forum*, 29(4): 78–81.
- [3] Tian S, Li J, Han L, et al., 2025, Observation of Medium- to Long-Term Efficacy of Spinal Endoscopic Laminotomy for Lumbar Spinal Stenosis with Degenerative Spondylolisthesis. *Journal of Clinical and Experimental Medicine*, 24(2): 168–172.
- [4] Li X, He H, Li P, et al., 2024, Analysis of Clinical Efficacy between Uniportal Spinal Endoscopy and Unilateral Biportal Spinal Endoscopy for Lumbar Spinal Stenosis. *Journal of Cervical and Lumbar Pain*, 45(5): 834–839.
- [5] Zheng H, Yang G, Zhou B, et al., 2024, Early Clinical Efficacy of Unilateral Biportal Endoscopic Unilateral Approach for Bilateral Decompression in the Treatment of Double-Segment Lumbar Spinal Stenosis. *Journal of Cervical and Lumbar Pain*, 45(3): 431–435.
- [6] Qian F, Song E, Zhu T, et al., 2024, Clinical Efficacy of Uniportal Dual-Approach Spinal Endoscopic Technique for Lumbar Spinal Stenosis. *Chinese Journal of Pain Medicine*, 30(4): 302–308.
- [7] Guo S, Li X, Yan M, et al., 2025, Comparison of Decompression Effects between Spinal Endoscopic Hybrid Technique and Uniaxial Spinal Endoscopy for Bilateral-Symptom Lumbar Spinal Stenosis. *Chinese Journal of Tissue Engineering Research*, 29(3): 517–523.
- [8] Fan Z, Wu X, Guo Z, et al., 2023, Comparative Study on the Efficacy of Unilateral Biportal Spinal Endoscopic Lumbar Fusion and Uniportal Spinal Endoscopic Transforaminal Lumbar Interbody Fusion for Lumbar Spinal Stenosis with Intervertebral Disc Herniation. *Chinese Journal of Reparative and Reconstructive Surgery*, 37(9): 1098–1105.
- [9] Sun Z, Sha X, Xu K, et al., 2023, Preliminary Efficacy of Percutaneous Large-Channel Spinal Endoscopy for Elderly Lumbar Spinal Stenosis. *Journal of Practical Orthopaedics*, 29(6): 509–514.
- [10] Zhang Y, Feng B, Su W, et al., 2023, Early Clinical Efficacy of Unilateral Biportal Spinal Endoscopic Technique for Spinal Canal Decompression in the Treatment of Double-Segment Lumbar Spinal Stenosis. *Chinese Journal of Reparative and Reconstructive Surgery*, 37(6): 706–712.

Publisher's note

Bio-Byword Scientific Publishing remains neutral with regard to jurisdictional claims in published maps and institutional affiliations.

A Post-Hoc Analysis of the 48-Week Data from Study 301 of Firsekibart for Acute Gouty Arthritis: Evaluation of Number of Doses and Switching-to-Firsekibart Efficacy

Yu Xue¹, Wencheng Fu², Xu Zhang², Yi Li^{2*}

¹Department of Rheumatology and Immunology Diseases, Huashan Hospital of Fudan University, Shanghai 200040, China

²Changchun GeneScience Pharmaceuticals Co., Ltd., Shanghai 200241, China

*Corresponding author: Yi Li, liyi03@genscigroup.com

Copyright: © 2026 Author(s). This is an open-access article distributed under the terms of the Creative Commons Attribution License (CC BY 4.0), permitting distribution and reproduction in any medium, provided the original work is cited.

Abstract: *Objective:* This post-hoc analysis aimed to evaluate the number of Firsekibart administrations over 48 weeks in patients with acute gout and the efficacy of switching to Firsekibart treatment during the open-label period in patients who had recurrent flare recurrence on compound betamethasone. *Methods:* We performed a post-hoc analysis on the 48-week treatment data from the 301 study (a multicenter, randomized, double-blind, active-controlled Phase III clinical trial) of Firsekibart for acute gout. A total of 312 patients with acute gout were randomized to receive either Firsekibart 200 mg subcutaneously or compound betamethasone 7 mg intramuscularly during the 24-week double-blind period, followed by a 24-week open-label period. After the initial dose, patients could receive additional doses upon gout flare; those with an inadequate response could receive oral prednisone as rescue therapy. During the open-label period, patients in the betamethasone group who experienced gout flares could switch to Firsekibart treatment. Differences in the number of doses between the two groups over 48 weeks, differences in the number of doses before and after switching to Firsekibart treatment in the betamethasone group, and the proportion of patients experiencing at least one gout flare after switching were analyzed. *Results:* Over 48 weeks, the median number of doses in the Firsekibart group was 1.0 (Q1, Q3: 1.0, 2.0), which was significantly lower than that in the compound betamethasone group (2.0 [1.0, 3.0]), $P < 0.0001$. For patients who switched from compound betamethasone to Firsekibart treatment, the median number of doses after switching was 1.0 (1.0, 1.0), markedly lower than the 2.0 (1.0, 3.0) before switching ($P < 0.0001$). During the open-label period, 69 patients (44.2%) in the betamethasone group switched to Firsekibart treatment, of whom only 2 (2.9%) experienced a gout flare. This recurrence rate was significantly lower than that observed during the double-blind period while receiving compound betamethasone (2.9% vs. 82.6%, $P < 0.001$). *Conclusion:* The median annual number of doses of Firsekibart for treating acute gout flares is one dose per year. For patients with inadequate response to corticosteroid therapy, Firsekibart demonstrates favorable efficacy and dosing convenience in controlling gout flares, representing a valuable new option for long-term gout management.

Keywords: Firsekibart; Acute gout; Post-hoc analysis; Compound betamethasone

Online publication: May 14, 2026

1. Introduction

Gout is the most common inflammatory arthritis, with a growing global burden. A recent Global Burden of Disease (GBD) study reported that the global prevalence of gout reached 55.8 million in 2020 and is projected to increase to 95.8 million by 2050, an increase of over 70% ^[1]. The prevalence of gout in China has increased particularly significantly, with disability-adjusted life years (DALYs) due to gout increasing by 172.35% between 1990 and 2019, and the number of affected individuals rising from 5.86 million to 16.16 million ^[2]. Gout not only causes severe joint pain and functional impairment but is also strongly associated with cardiovascular disease (87% increased risk), chronic kidney disease (4.61-fold increased risk), and all-cause mortality (58% increased risk) ^[3]. It is estimated that the total number of patients with gout in China is approximately 38.4 million. Among patients diagnosed with gout, 17.4% experience at least one acute flare within 1 year, suggesting that approximately 6.682 million patients in China suffer a gout flare each year. However, the overall healthcare-seeking rate among patients with gout in China remains low, with annual consultation rates of 59.67% in rural areas and 64.56% in urban areas, yielding an average consultation rate of 61.1%. Based on this estimate, approximately 4.082 million patients with gout flares seek medical care each year.

Current first-line treatments for acute gout flares include nonsteroidal anti-inflammatory drugs (NSAIDs), colchicine, and corticosteroids. However, these conventional treatments have significant limitations. A study shows that 1.9% of gout patients have contraindications or intolerance to standard anti-inflammatory treatments, and 1.8% respond inadequately to conventional therapies ^[4]. Together, these two groups account for 3.7% of patients, indicating that an estimated 151,000 patients with acute gout flares in China may require novel anti-inflammatory therapies such as interleukin-1 (IL-1) inhibitors each year. Furthermore, the side effects of conventional drugs, such as hepatotoxicity, nephrotoxicity, gastrointestinal reactions, and metabolic disturbances, limit their use in patients with multiple comorbidities. In a commentary, Professor Richette, an author of the EULAR gout guidelines, noted that gout management extends far beyond urate-lowering; it is a complex inflammatory process ignited by multiple factors, requiring long-term, precise anti-inflammatory therapy until monosodium urate crystals are completely dissolved to fundamentally prevent gout flares ^[5]. Therefore, there is an unmet clinical need in gout management for a long-acting anti-inflammatory drug with reliable efficacy, convenient administration, and a low adverse reaction profile.

The core mechanism of gout flares involves the activation of the NLRP3 inflammasome by urate crystals, promoting the maturation and release of IL-1 β and triggering an inflammatory cascade. IL-1 β levels correlate positively with gout severity, and its sustained presence can lead to multiple organ damage, including bone erosion, chronic kidney disease, and atherosclerosis. Firsekibart, the first anti-IL-1 β fully human monoclonal antibody approved in China, has been shown in its Phase III 24-week core treatment period data ^[6,7] to rapidly control gout flares in patients with acute gout who have contraindications, intolerance, or inadequate response to NSAIDs and colchicine. It significantly reduces the risk of gout recurrence at 12 and 24 weeks by up to 90% and 87%, respectively, and markedly reduces levels of the inflammatory marker high-sensitivity C-reactive protein (hs-CRP) at Day 8 and Week 4. These results indicate that during acute gout flares, Firsekibart treatment precisely binds IL-1 β , blocking the IL-1 β

inflammatory cascade pathway, exerting a long-acting anti-inflammatory effect, thereby significantly reducing the risk of gout recurrence and related organ damage. This post-hoc analysis aims to further evaluate the number of doses of long-term Firsekibart therapy in gout patients and its efficacy in patients with inadequate response to corticosteroids by analyzing the complete 48-week treatment data from Study 301. This will help understand drug exposure in acute gout patients treated with Firsekibart and provide evidence for pharmacoeconomic evaluations.

2. Methods

2.1. Study design

This study is a post-hoc analysis of Study 301 investigating Firsekibart for acute gout. Study 301 was a multicenter, randomized, double-blind, double-dummy, active-controlled Phase III clinical trial (NCT05983445) conducted across 51 centers in China from January 2023 to June 2024. The study comprised two phases: a double-blind period (0–24 weeks), where patients were randomized 1:1 to receive either Firsekibart 200 mg subcutaneously plus compound betamethasone placebo, or compound betamethasone 7 mg intramuscularly plus Firsekibart placebo; and an open-label period (24–48 weeks). After the double-blind period, patients in the Firsekibart group who experienced a gout flare could continue receiving Firsekibart, while patients in the betamethasone group who experienced a gout flare could switch to Firsekibart treatment. Data from the 24-week core treatment period have been published in the journal *Innovation* ^[6].

2.2. Patient population

Study 301 enrolled 313 patients who met the 2015 ACR gout classification criteria, had contraindications, intolerance, or lack of efficacy to NSAIDs and/or colchicine, had at least 2 gout flares in the past year, and had a baseline target joint pain VAS score ≥ 50 mm during an acute gout flare. Baseline characteristics were balanced between groups, with a mean age of 44.9 years, 98.7% male, and a median gout history of 84.0 months. One patient in the betamethasone group did not receive the study drug after randomization, leaving 312 patients in the safety set, with 156 patients in each group.

2.3. Outcome measures

Assessment included drug exposure duration and the mean number of doses administered over 48 weeks for patients in the Firsekibart and betamethasone groups. Additionally, drug exposure duration, mean number of doses, and the proportion of patients experiencing at least one gout flare were evaluated before and after switching to Firsekibart treatment in patients from the betamethasone group who switched upon recurrence.

2.4. Statistical analysis

All statistical analyses were performed using SAS software. The number of doses data were right-skewed; minimum, Q1, median, Q3, and maximum values were calculated to describe central tendency and dispersion, with mean \pm standard deviation (SD) also presented. Recurrence rates were expressed as percentages. Comparisons of the number of doses between two groups were performed using the signed-rank test, and comparisons of recurrence rates were performed using Fisher's exact test. All statistical tests were two-sided, with $P < 0.05$ considered statistically significant.

3. Results

3.1. Drug exposure analysis

Over 48 weeks, the mean drug exposure duration after the first dose was 339.00 ± 44.00 days in the Firsekibart group and 325 ± 67.62 days in the betamethasone group. During the open-label period, 69 patients (44.2%) in the betamethasone group who experienced gout flares switched to Firsekibart treatment and completed follow-up. Their mean exposure duration before and after switching was 215.7 ± 45.64 days and 129.0 ± 36.40 days, respectively.

3.2. Number of doses analysis

Over 48 weeks, the median number of doses in the Firsekibart group was 1.0 (Q1, Q3: 1.0, 2.0), which was significantly lower than that in the betamethasone group (2.0 [1.0, 3.0]) (**Table 1**), $P < 0.001$. Over the 48-week treatment period, the mean number of doses was 1.6 ± 1.18 in the Firsekibart group and 2.5 ± 1.55 in the betamethasone group.

During the open-label period following the first 24 weeks, patients in the betamethasone group who switched to Firsekibart treatment after recurrence had a median of 1.0 dose (1.0, 1.0) after switching, markedly lower than the 2.0 doses (1.0, 3.0) before switching (**Table 1**), $P < 0.001$. The mean number of doses before switching was 2.6 ± 1.42 , compared to 1.0 ± 0.77 after switching to Firsekibart treatment.

Table 1. Comparison of number of doses over 48 weeks: Firsekibart group vs. betamethasone group, and betamethasone group patients before and after switching to Firsekibart treatment

	Firsekibart group (n = 156)	Betamethasone group (n = 156)	Betamethasone group patients before switching (n = 69)	Betamethasone group patients after switching (n = 69)
	Number of doses			
Median (Q1, Q3)	1.0 (1.0, 2.0)*	2.0 (1.0, 3.0)	2.0 (1.0, 3.0)	1.0 (1.0, 1.0) [#]
Range	1,10	1,7	1,6	1,2
Mean \pm SD	1.6 ± 1.18	2.5 ± 1.55	2.6 ± 1.42	1.0 ± 1.17
	Number of doses – n (%)			
1 dose	90 (57.7)	51 (32.7)	19 (27.5)	67 (97.1)
2 dose	54 (34.6)	38 (24.4)	19 (27.5)	2 (2.9)
3 dose	5 (3.2)	31 (19.9)	15 (21.7)	0
4 dose	3 (1.9)	15 (9.6)	8 (11.6)	0
5 dose	2 (1.3)	12 (7.7)	5 (7.2)	0
6 dose	0	6 (3.8)	3 (4.3)	0
7 dose	0	3 (1.9)	0	0
9 dose	1 (0.6)	0	0	0
10 dose	1 (0.6)	0	0	0

* $P < 0.0001$ vs. betamethasone group; [#] $P < 0.0001$ vs. before switching.

3.3. Recurrence rate before and after switching to Firsekibart treatment

During the open-label period after 24 weeks, among the 69 patients in the betamethasone group who switched to Firsekibart treatment, only 2 experienced one gout flare each. The recurrence rate was significantly lower than before switching (2.9% vs. 82.6%, $P < 0.0001$, **Figure 1**). Furthermore, after retreatment with

Firsekibart, no further gout flares occurred through week 48.

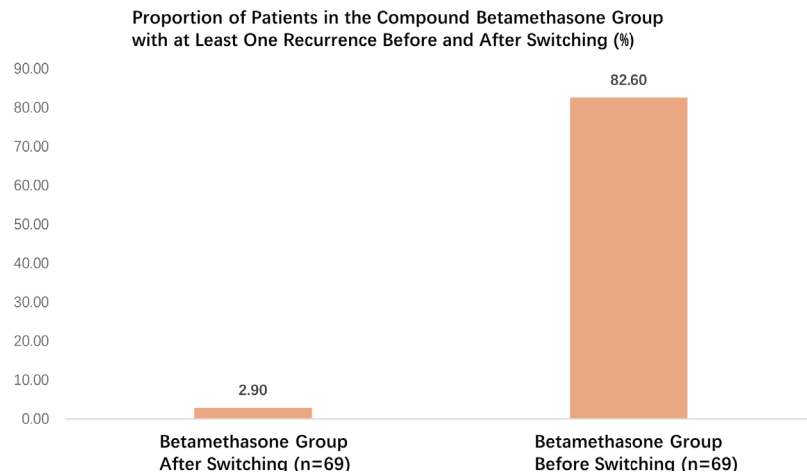


Figure 1. Significant reduction in gout flare rate after switching to Firsekibart treatment in patients previously treated with compound betamethasone

4. Discussion

Gout, a prevalent inflammatory arthritis, significantly impacts patients' quality of life and long-term health due to the severe pain of acute gout flares and the characteristic of chronic, recurrent episodes^[8]. While conventional first-line treatments such as NSAIDs, colchicine, and corticosteroids (e.g., compound betamethasone) can control inflammation in the short term, they often face challenges in long-term management, including diminished efficacy over time, high recurrence rates, and potential side effects (e.g., metabolic disturbances, immunosuppression)^[9], making them unsuitable for sustained anti-inflammatory therapy. Therefore, there is a clinical need for a therapeutic strategy that provides highly effective, durable inflammation control with an improved safety profile. Firsekibart, which targets IL-1 β —the core inflammatory cytokine in gout flares—offers a compelling solution, as demonstrated by the results of Study 301. Firsekibart treatment not only markedly reduced the risk of gout recurrence at 12 and 24 weeks by up to 90% and 87%, respectively^[6], but the 48-week drug exposure data from this study show that the number of doses in the Firsekibart group was significantly lower than that in the betamethasone group, which could substantially improve treatment adherence. Furthermore, Firsekibart demonstrates a revolutionary therapeutic advantage in gout patients with an inadequate response to corticosteroids.

The most direct finding of this study is the substantial advantage of Firsekibart in terms of dosing convenience. The presence of refractory gout patients in both groups, who experienced more frequent gout flares and received more doses throughout the study, contributed to the right-skewed distribution of dosing data. Over the 48-week treatment period, the median number of doses in the Firsekibart group was only 1, with an interquartile range of 1, significantly lower than the 2 doses in the betamethasone group ($P < 0.0001$). This indicates that 75% of patients in the Firsekibart group required no more than 2 doses per year. This finding profoundly demonstrates that, unlike the conventional model requiring repeated corticosteroid dosing to manage frequent gout flares, Firsekibart, through its long-acting pharmacological properties, preliminarily achieves the ideal goal of maintaining long-term inflammation control with “no more than two

injections per year.” When patients in the betamethasone group who experienced gout flares during the open-label period switched to Firsekibart treatment, their median number of doses dropped dramatically from 2.0 to 1.0 ($P < 0.0001$), further supporting the clinical advantage of Firsekibart’s long-acting anti-inflammatory effect. This drastic reduction in the number of doses not only signifies a significant decrease in patient treatment burden (including clinic visits, injection discomfort, and time costs) but also reflects that Firsekibart achieves more durable and fundamental suppression of the core inflammatory pathways in gout, thereby reducing the reliance on “on-demand” therapy. This paradigm shift represents a critical step towards more precise and convenient chronic gout management.

Another key finding of this study is the clear confirmation of Firsekibart’s prominent efficacy in patients who responded inadequately to corticosteroid therapy. Among patients who later switched to Firsekibart treatment, the recurrence rate during the betamethasone treatment period was as high as 82.6%, reflecting a real-world clinical scenario where a considerable proportion of patients respond poorly to conventional corticosteroid therapy or cannot effectively prevent recurrence, posing a challenge in clinical management. The open-label study design provides compelling evidence for this patient population. Sixty-nine patients (44.2% of the original corticosteroid group) who experienced gout flares switched to Firsekibart treatment during the open-label period. During the subsequent 24-week follow-up, only 2 patients experienced a gout flare, yielding a recurrence rate as low as 2.9%. This represents a statistically significant and clinically striking reduction compared to the 82.6% recurrence rate observed during the preceding compound betamethasone treatment period ($P < 0.0001$). This comparative data powerfully demonstrates that Firsekibart can exert robust anti-inflammatory effects in gout inflammation not adequately controlled by corticosteroids, effectively halting acute gout flares and preventing recurrences. It also establishes a clear clinical application scenario for IL-1 β antibodies: as an effective step-up therapy after failure or intolerance to conventional anti-inflammatory treatments, particularly corticosteroids. The recently published *Guideline for Anti-inflammatory Therapy in Gout (2025 Edition)* recommends IL-1 inhibitors for anti-inflammatory treatment in gout patients with multiple comorbidities or tophi^[10]; the results of this study provide new clinical evidence supporting this recommendation.

Limitations of this study include the potential bias introduced by the open-label design and the limited sample size, underscoring the need for large-scale, long-term real-world evaluations of Firsekibart’s anti-inflammatory efficacy and organ-protective benefits. Future research should focus on the efficacy of Firsekibart in patients with moderate-to-severe renal impairment or cardiovascular disease and explore its synergistic value when combined with urate-lowering therapy.

5. Conclusion

Firsekibart provides long-acting, precise anti-inflammatory therapy with an ultra-low number of doses—“no more than two injections per year”—fundamentally changing the paradigm of anti-inflammatory treatment for gout and greatly enhancing treatment convenience and patient adherence. For patients who do not respond adequately to corticosteroids, Firsekibart also demonstrates excellent anti-inflammatory effects, significantly reducing the rate of gout recurrence.

Disclosure statement

The authors declare no conflict of interest.

References

- [1] GBD 2021 Gout Collaborators, 2024, Global, Regional, and National Burden of Gout, 1990–2020, and Projections to 2050: A Systematic Analysis of the Global Burden of Disease Study 2021. *Lancet Rheumatol*, 6(8): e507–e517.
- [2] Fang JW, Feng TY, Zhou ZH, et al., 2024, Disease Burden of Gout in China from 1990 to 2019. *Chinese General Practice*, 27(02): 245–252.
- [3] Im PK, Kartsonaki C, Kakkoura MG, et al., 2025, Hyperuricemia, Gout and the Associated Comorbidities in China: Findings from a Prospective Study of 0.5 Million Adults. *Lancet Reg Health West Pac*, 58: 101572.
- [4] Pascart T, Norberciak L, Ea HK, et al., 2019, Difficult-to-Treat Gout Flares: Eligibility for Interleukin-1 Inhibition in Private Practice is Uncommon According to Current EMA Approval. *Rheumatology (Oxford)*, 58(12): 2181–2187.
- [5] Ea HK, Richette P, 2025, Factors Beyond Urate Levels for Managing Gout Flares. *Nat Rev Rheumatol*, 21(7): 371–372.
- [6] Xue Y, Chu T, Hu J, et al., 2025, Firsekibart Versus Compound Betamethasone in Acute Gout Patients Unsuitable for Standard Therapy: A Randomized Phase 3 Trial. *Innovation (Camb)*, 6(8): 101015.
- [7] Xue Y, Li Y, Lian YL, et al., 2025, Firsekibart in Reducing High-Sensitivity C-Reactive Protein Levels of Gout. *International Journal of General Practice Nursing*, 3(4): 11–18.
- [8] Shi M, Luo J, Ding L, et al., 2023, Spontaneous Resolution of Acute Gout: Mechanisms and Therapeutic Targets. *RMD Open*, 9(3): e003586.
- [9] Badshah M, Nadeem I, Ahmed I, et al., 2024, Gout: A Rapid Review of Presentation, Diagnosis and Management. *S D Med*, 77(2): 81–86.
- [10] Rheumatology Prevention Committee of Chinese Preventive Medicine Association, 2025, Guideline for Anti-Inflammatory Therapy in Gout (2025 Edition). *Chinese Journal of Rheumatology*, 29(11): 897–922.

Publisher's note

Bio-Byword Scientific Publishing remains neutral with regard to jurisdictional claims in published maps and institutional affiliations.

Traditional Chinese Medicine Regulates Th17/Treg Balance to Improve Osteoporosis: A Review of Bone Immunomodulation Mechanisms and Therapeutic Prospects

Zhiyuan Zhu¹, Xiaoyue Jin², Rongxin Sun^{1*}

¹Department of Joint Surgery, The Sixth Affiliated Hospital of Xinjiang Medical University, Urumqi 830002, Xinjiang Uygur Autonomous Region, China

²Department of Pharmacy, The Sixth Affiliated Hospital of Xinjiang Medical University, Urumqi 830002, Xinjiang Uygur Autonomous Region, China

**Author to whom correspondence should be addressed.*

Copyright: © 2026 Author(s). This is an open-access article distributed under the terms of the Creative Commons Attribution License (CC BY 4.0), permitting distribution and reproduction in any medium, provided the original work is cited.

Abstract: Osteoporosis (OP) is a metabolic bone disease characterized by reduced bone mass and destruction of bone microstructure, posing a serious threat to the health of the elderly population. Studies in osteoimmunology have revealed that an imbalance between Th17 cells and regulatory T cells (Treg) is a core immunopathological mechanism underlying OP: overactivation of Th17 cells promotes osteoclast differentiation and accelerates bone resorption, while impaired Treg function weakens bone protection, ultimately leading to disrupted bone metabolism. Traditional Chinese medicine (TCM), with its advantages in multi-target and holistic regulation, shows broad application prospects in restoring Th17/Treg balance and reshaping the bone immune microenvironment. This article systematically reviews the molecular mechanisms by which TCM compounds (e.g., Yishen Juanbi Pills, Jintiang Capsules) and active components (e.g., icariin, astragaloside IV) regulate T cell differentiation, with a focus on the involvement of signaling pathways such as NF- κ B and Wnt/ β -catenin, as well as the gut microbiota–short-chain fatty acids axis in mediating immune regulation. In addition, it summarizes preclinical and clinical research evidence supporting the use of TCM in treating OP. In response to current challenges, including insufficient target analysis and a lack of high-quality clinical evidence, this paper proposes that future efforts should integrate cutting-edge approaches such as multi-omics technologies, nano-delivery systems, and artificial intelligence to systematically elucidate the molecular network through which TCM regulates bone immunity. Such advances will facilitate the transition of TCM from experience-based to evidence-based medicine, providing safer and more effective immune-targeted therapeutic strategies for the prevention and management of OP.

Keywords: Osteoporosis; Traditional Chinese medicine; Th17/Treg balance; Osteoimmunology; Intestinal flora; Signaling pathways

Online publication: May 14, 2026

1. Introduction

With the intensification of global population aging, osteoporosis (OP) has become a major public health challenge threatening the health of the elderly. OP is characterized by decreased bone mass and destruction of bone microarchitecture, with fragility fractures representing its most serious complication, significantly affecting patients' quality of life and increasing the burden on healthcare systems^[1]. Traditional research has primarily focused on the functional imbalance between osteoblasts and osteoclasts. However, the emergence of osteoimmunology has provided new insights into the pathogenesis of OP, suggesting that immune dysregulation serves as a key upstream factor driving imbalances in bone remodeling, with T cells playing a central role^[2]. In particular, the imbalance between Th17 cells and regulatory T cells (Treg) has been identified as a critical immunopathological basis for OP: excessive Th17 activation promotes osteoclast differentiation and accelerates bone resorption, whereas insufficient Treg function weakens bone protection, ultimately leading to disrupted bone metabolism^[3].

Traditional Chinese medicine (TCM), with its unique advantages in multi-target and holistic regulation, demonstrates significant potential in modulating T cell function and improving the bone immune microenvironment^[4]. In recent years, numerous studies have confirmed that TCM formulas and active components can restore the Th17/Treg balance by intervening in multiple signaling pathways and regulating the gut microbiota, thereby exerting anti-osteoporotic effects. This article systematically reviews the molecular mechanisms and clinical evidence supporting the regulation of Th17/Treg balance by TCM in the treatment of OP, analyzes current research challenges, and discusses future directions, aiming to provide new insights for immune-targeted therapy in OP.

2. Immunological basis of osteoporosis and T cell regulatory mechanisms

2.1. Fundamentals of osteoimmunology

Osteoimmunology is an interdisciplinary field that investigates the interactions between the skeletal and immune systems, revealing a complex and intricate bidirectional regulatory network between immune cells and bone cells (**Figure 1**). Bone remodeling relies on the dynamic balance between osteoclasts and osteoblasts, while immune cells, particularly T cells, participate in this process by secreting various cytokines^[5]. For instance, the effects of interferon- γ on bone cells are bidirectional and depend on the local microenvironment and cell differentiation status^[6]. The RANKL/RANK/OPG signaling pathway serves as a central hub through which immune cells regulate osteoclast differentiation, and its aberrant activation is closely associated with the pathogenesis of OP^[7]. With advancing research, OP has gradually been redefined as an “osteimmune disease,” in which immune system dysregulation is not merely a consequence of abnormal bone metabolism but also a key driver of disease progression^[8]. Conditions such as immunosenescence and chronic low-grade inflammation can promote OP development, providing a theoretical basis for immune-based interventions^[9].

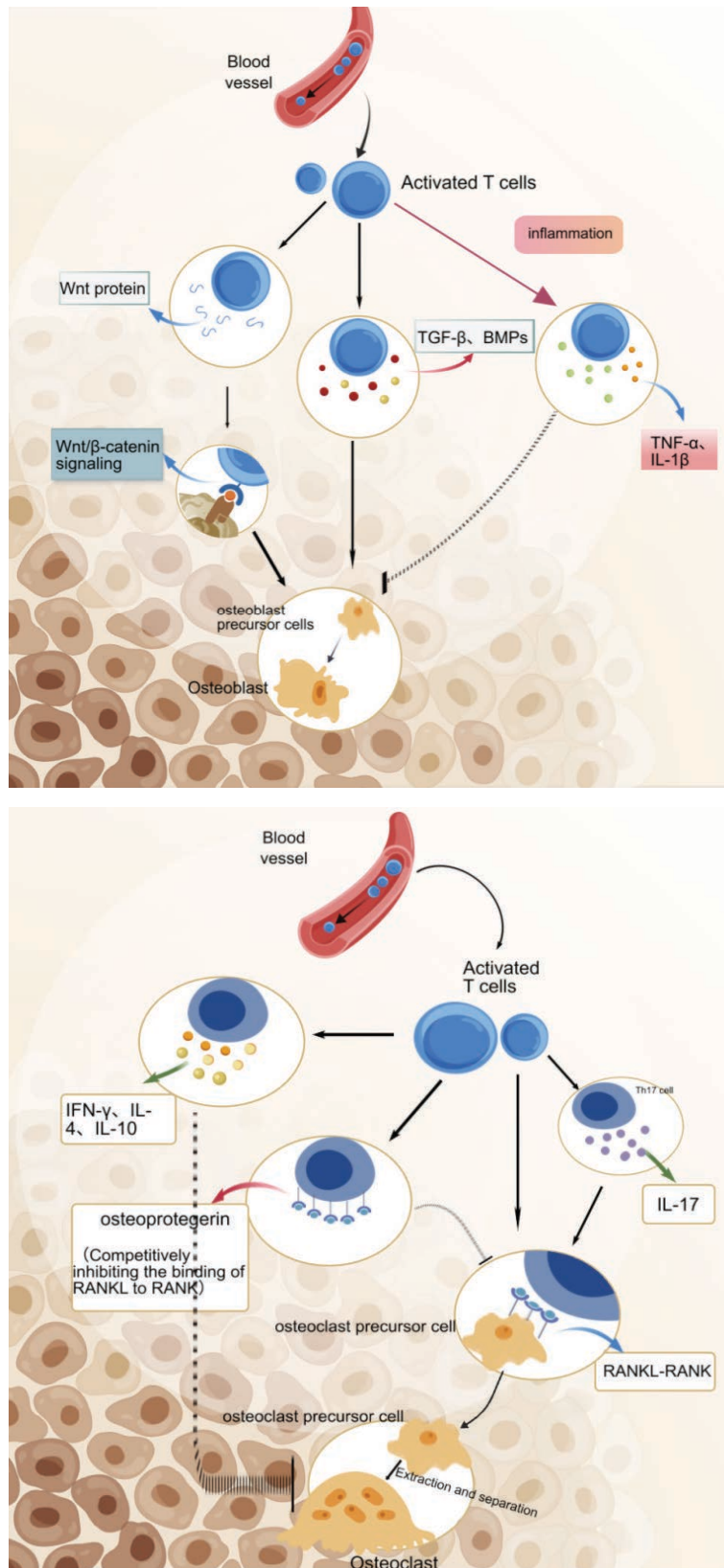


Figure 1. Schematic diagram of the core mechanisms of osteoimmunology, illustrating the interactions among T cells, osteoclasts, and osteoblasts, along with key signaling pathways

2.2. Functional differentiation of T cell subsets (Th17/Treg) in bone metabolism

Different T cell subsets play distinct roles in regulating bone metabolism, with the balance between Th17 and Treg cells being particularly critical. Th17 cells promote the activation and differentiation of osteoclast precursors and enhance bone resorption by secreting pro-inflammatory cytokines such as IL-17^[10]. Clinical studies have shown that the proportion of Th17 cells in the peripheral blood of postmenopausal women with OP is significantly increased, accompanied by elevated IL-17 levels, which are positively correlated with decreased bone mineral density^[11,12]. Furthermore, pro-inflammatory cytokines such as TNF- α and IL-6 secreted by Th17 cells can further amplify osteoclast activity and exacerbate bone destruction^[13]. Conversely, Treg cells directly inhibit osteoclast activity by secreting anti-inflammatory factors such as IL-10 and TGF- β and indirectly promote osteoblast function by improving the immune microenvironment^[14]. Patients with OP often exhibit a reduced number or impaired function of Treg cells, leading to weakened bone protection^[15]. Notably, gut microbiota metabolites, such as short-chain fatty acids (SCFAs) like butyrate, can promote Treg expansion, suggesting that the “gut–bone axis” plays an important role in Treg-mediated bone protection^[16,17]. The Th17/Treg imbalance is a core immunological event in OP progression: excessive Th17 activation and insufficient Treg function lead to enhanced bone resorption and reduced bone formation^[18]. Postmenopausal estrogen deficiency further exacerbates this imbalance by activating the immune system, promoting Th17 differentiation, and inhibiting Treg function, ultimately accelerating bone loss^[19]. Therefore, restoring the Th17/Treg balance has become a key strategy in the immunotherapy of OP.

2.3. Interaction mechanisms between T cells and osteoclasts

The crosstalk between T cells and osteoclasts is central to osteoimmunology. IL-17 secreted by Th17 cells can directly act on osteoclast precursors, promoting their differentiation into mature osteoclasts^[20]. Additionally, RANKL expressed on the surface of T cells (especially Th17 cells) binds to RANK on osteoclast precursors, activating downstream signaling pathways such as NF- κ B and driving osteoclast differentiation and activation^[21]. The expression level of RANKL correlates closely with the extent of bone destruction and represents an important therapeutic target for OP and bone metastatic tumors^[22]. On the other hand, osteoclasts can also regulate T cell function. Studies have shown that apoptotic bodies released by osteoclasts can inhibit CD8⁺ T cell activation via Siglec15, thereby promoting bone metastasis and destruction^[23]. The interaction between osteoclasts and T cells within the tumor microenvironment may also facilitate tumor progression, suggesting that targeting this interaction axis holds therapeutic potential. These findings not only deepen our understanding of the immune mechanisms underlying OP but also lay the groundwork for developing novel intervention strategies targeting T cell–osteoclast interactions.

3. Effects of traditional Chinese medicine on Th17/Treg balance

3.1. Immunomodulatory effects of TCM formulas

TCM formulas exhibit unique advantages in regulating Th17/Treg balance through the synergistic effects of multiple components. Zuogui Pill effectively ameliorates bone loss in estrogen-deficient mice. The Warming and Activating Meridians Formula exerts therapeutic effects in collagen-induced arthritis (CIA) mice by inhibiting JAK2/STAT3 pathway phosphorylation, reducing IL-17A and ROR γ t expression, and increasing

Foxp3 mRNA levels, thereby decreasing the proportion of Th17 cells ^[24]. Paeoniflorin, a component of Congrong Shujing Granules (CRSJ), has been identified as a key immunomodulatory candidate that regulates Th17/Treg balance. Molecular docking and dynamics simulations indicate that paeoniflorin can stably bind to ROR γ t, a key transcription factor for Th17 cells, and Foxp3, a key transcription factor for Treg cells ^[25]. From a molecular perspective, the regulation of Th17/Treg balance by TCM formulas involves multiple signaling pathways, including JAK/STAT, PI3K/AKT, and AMPK/mTOR. For instance, Longteng Decoction not only inhibits Th17 differentiation and IL-17 secretion in CIA mice but also synergizes with Treg cells to promote IL-4 secretion by type 2 innate lymphoid cells (ILC2s) via activation of the STAT6 pathway, thereby suppressing synovial inflammation and alleviating joint damage ^[26]. Formononetin significantly downregulates PI3K and Akt expression in the bone marrow and spleen of mice with immune-mediated bone marrow failure, while increasing Treg numbers and reducing Th17 numbers, thus modulating the Treg/Th17 balance via the PI3K/Akt signaling pathway and alleviating bone marrow destruction ^[27]. These findings suggest that TCM formulas modulate bone immunity at the level of cellular metabolism and functional regulation, offering new perspectives for OP prevention and treatment from the standpoint of immune homeostasis.

3.2. Direct regulatory effects of active TCM components on Treg cells

Active components derived from Chinese medicinal herbs serve as important entry points for studying the mechanisms underlying TCM efficacy. Icariin possesses anti-inflammatory, antioxidant, and bone-promoting effects, and it inhibits bone resorption by modulating immune responses, providing a novel pharmacological basis for OP treatment ^[28]. A novel phenolic acid (S1) isolated from *Salvia miltiorrhiza* significantly upregulates IL-10 expression and influences Th17/Treg balance ^[29]. Baicalin selectively inhibits Th17 differentiation without affecting Treg cells by specifically blocking the STAT3 signaling pathway, thereby precisely correcting Th17/Treg imbalance ^[30]. Epigenetic modification is an important mechanism by which herbal medicines regulate Treg function, with histone deacetylase 6 (HDAC6) playing a central role ^[31]. This finding preliminarily reveals the epigenetic basis of immune regulation by TCM and provides a new direction for further elucidating how TCM precisely modulates bone immune homeostasis.

3.3. Indirect regulation via the gut microbiota–bone immune axis

The gut microbiota and its metabolites, particularly SCFAs, play a key role in mediating the effects of TCM on Th17/Treg balance (**Figure 2**) ^[32,33]. Gegen Qinlian Decoction positively affects bone mineral density and bone calcium content in a rat model of diabetic secondary OP by reshaping the composition of the gut microbiota and increasing SCFA levels ^[34]. These findings suggest that TCM may indirectly regulate the bone immune microenvironment by modulating the gut microbiota, providing a “gut–bone axis” perspective for understanding its multi-target effects. However, the precise molecular mechanisms underlying the microbiota–immune–bone axis and the microbiota-specific regulatory strategies of TCM formulas require further investigation.

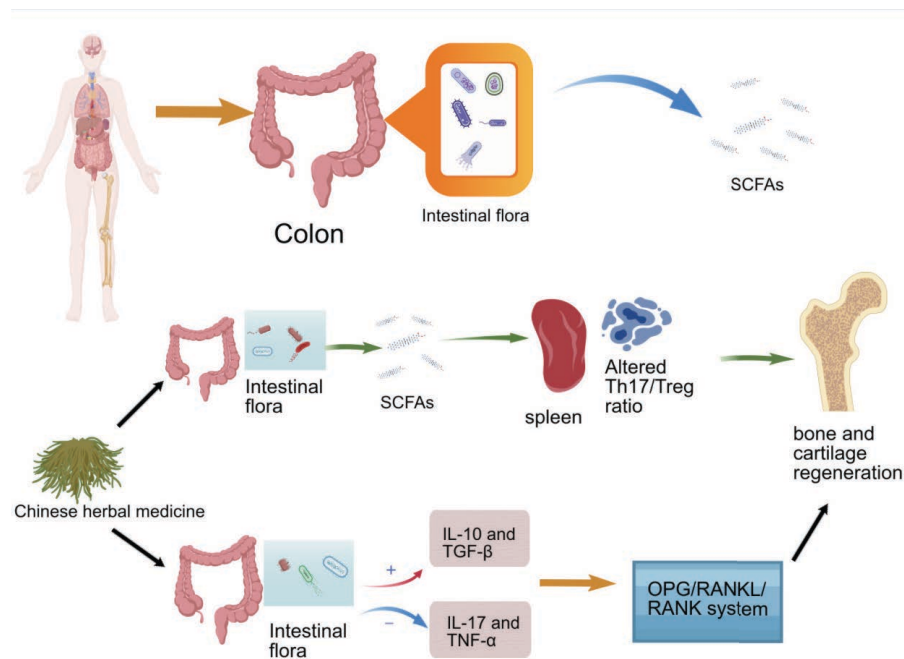


Figure 2. Gut microbiota–bone immune axis mechanism diagram

4. Regulation of immune-related signaling pathways by traditional Chinese medicine

4.1. NF- κ B signaling pathway

The NF- κ B signaling pathway is a key hub in osteoimmunomodulation. Upon binding of RANKL to RANK, TRAF6 is recruited, initiating the NF- κ B signaling cascade, inducing NFATc1 expression, which in turn drives the transcription of osteoclast marker genes (such as cathepsin K and TRAP), promoting osteoclast maturation and bone resorption^[35]. Th17 cells activate both classical and non-classical NF- κ B pathways via IL-17, promoting the production of pro-inflammatory cytokines (e.g., TNF- α , IL-1 β , IL-6). IL-17 can also enhance RANKL-induced NF- κ B activation, amplifying osteoclastogenic signals^[36]. Treg cells suppress NF- κ B activation through multiple mechanisms: IL-10 and TGF- β secreted by Treg cells inhibit NF- κ B nuclear translocation, and Treg cells also suppress NF- κ B activation in antigen-presenting cells via cell-contact-dependent mechanisms^[37]. Yougui Pill alleviates bone loss by downregulating Th17 cell activity and IL-17 production, blocking the NF- κ B signaling pathway, and reducing osteoclast numbers^[38,39]. Xiaoyao Qingluo Yin (XYQLY) significantly inhibits p-p65 expression, an effect that may be related to TLR4/NF- κ B-mediated regulation of IL-6 production, thereby affecting Th17 differentiation^[40]. Tectorigenin ameliorates glucocorticoid-induced osteoporosis by inhibiting the NF- κ B pathway and regulating Th17/Treg balance^[41].

4.2. Wnt/ β -catenin signaling pathway

Direct activation of the Wnt/ β -catenin signaling pathway by TCM is an important molecular basis for its bone-promoting effects. Flavonoids from *Epimedium*, a classic kidney-tonifying herb, have been shown to promote osteogenic differentiation of human mesenchymal stem cells, an effect that can be blocked by the Wnt/ β -catenin pathway inhibitor DKK-1, indicating that their efficacy depends on activation of this pathway^[42].

5. Application of TCM formulas and active components in immune regulation of osteoporosis

5.1. Immunomodulatory effects of classic TCM formulas

Classic TCM formulas regulate the bone immune microenvironment through synergistic effects of multiple components. Yishen Juanbi Pill inhibits osteoclast differentiation via the JAK2/STAT3 signaling pathway while promoting IL-10 secretion by Treg cells, thereby enhancing immunosuppressive function and slowing bone destruction associated with RA^[43]. Jintiang Capsules exert dual effects of promoting osteogenesis and inhibiting osteoclastogenesis: they activate the BMP and Wnt/ β -catenin pathways to promote osteogenic differentiation and inhibit the NF- κ B signaling pathway to reduce osteoclast activity^[44,45]. Based on the TCM theory that “the kidney governs the bones,” kidney-tonifying formulas such as Duhuo Jisheng Decoction and Liuwei Dihuang Pill improve OP symptoms by regulating immune cell function and inflammatory pathways^[46]. Components such as quercetin, rutin, and kaempferol, found in medicinal and edible plants, can activate the TGF- β and Wnt/ β -catenin pathways while inhibiting the RANKL/NF- κ B pathway, thereby promoting bone homeostasis^[47]. The synergistic mechanisms of TCM formulas are primarily achieved through three aspects: (1) regulating Th17/Treg balance and reducing the release of pro-osteoclast factors such as IL-17 and TNF- α ; (2) modulating signaling pathways including JAK/STAT, NF- κ B, and MAPK; and (3) indirectly regulating bone immunity via flavonoids that modulate the gut microbiota and its metabolites.

5.2. Immunomodulatory and bone-protective effects of TCM monomers

TCM monomers exert bone-protective effects by regulating immune responses and bone metabolism. Studies have shown that various TCM monomers can regulate the Th17/Treg balance, a key regulatory node in bone immune diseases such as RA and postmenopausal OP. For example, curcumin inhibits the activation of NF- κ B and AP-1 transcription factors, thereby downregulating the expression of pro-inflammatory cytokines^[48]. In mouse bone marrow mesenchymal stem cells, curcumin inhibits IL-1 α - and TNF- α -induced AP-1 and NF- κ B DNA-binding activity and reduces monocyte chemoattractant protein-1 (MCP-1) expression^[49]. Resveratrol, a cyclooxygenase-1 inhibitor, influences the effects of titanium surface roughness on osteoblast phenotype expression^[50]. Notably, the immunomodulatory potential of certain medicinal and edible plants is increasingly being recognized. For instance, crocin, derived from saffron, inhibits the p38 and JNK signaling pathways in a titanium particle-induced osteolysis model, promoting macrophage polarization toward the anti-inflammatory M2 phenotype, alleviating inflammation, and enhancing the osteogenic differentiation of bone marrow mesenchymal stem cells^[51]. This mode of action integrates immune regulation with bone metabolism regulation, reflecting the convergence of traditional theories and modern mechanistic research.

6. Challenges and prospects for clinical translation of TCM bone immunomodulation

6.1. Current status of clinical efficacy evaluation

TCM has accumulated some clinical evidence supporting its ability to improve bone mineral density and alleviate pain associated with OP. Kidney-tonifying herbs play an important role in OP prevention and treatment by promoting osteogenic activity, regulating calcium and phosphorus metabolism, and modulating multiple signaling pathways. Tanshinone IIA and its derivatives exhibit anti-inflammatory, antioxidant, and bone-protective effects, inhibiting osteoclast differentiation, reducing inflammatory factor levels, and

promoting osteogenic mineralization^[52]. However, existing clinical studies often suffer from limitations such as small sample sizes, short follow-up periods, and insufficient safety monitoring. The multicomponent nature of TCM also complicates safety evaluations, and attention must be paid to quality variations and the potential toxicity of certain herbs. In the future, large-scale, multicenter randomized controlled trials are urgently needed to systematically evaluate the efficacy and long-term safety of TCM.

6.2. Main challenges and future directions

Looking ahead, the development of TCM for the prevention and treatment of OP will require a multidimensional scientific approach. We must employ cutting-edge tools such as single-cell sequencing, spatial transcriptomics, and epigenetics to meticulously delineate the spatiotemporal regulatory landscape of the bone immune microenvironment and deeply decipher the mechanisms of action. Concurrently, we need to establish a solid evidence base supported by large-sample, multicenter, double-blind randomized controlled trials to enhance the level of clinical evidence. In terms of formulation innovation, we should leverage nano-delivery systems and biomaterials to develop novel carriers capable of targeted navigation and precise drug release, significantly improving the bioavailability and efficacy of active ingredients. Furthermore, the introduction of artificial intelligence algorithms as intelligent engines to screen key targets and optimize compatibility regimens will facilitate personalized precision treatment paradigms based on patients' immune phenotypes. Ultimately, through the deep integration of molecular biology, immunology, pharmacology, and clinical medicine, we can accelerate the translation of fundamental research findings into clinical applications, thereby comprehensively improving the overall prevention and treatment capabilities of TCM in this field.

Osteoporosis is a metabolic bone disease closely associated with T cell immune regulation, with Th17/Treg imbalance representing its core immunopathological mechanism. Leveraging its multicomponent synergistic advantages, TCM improves the bone immune microenvironment and bone metabolism through multiple pathways, including regulating T cell subset balance, modulating key signaling pathways such as NF- κ B and Wnt/ β -catenin, and influencing the gut microbiota-immune axis. These actions provide new strategies for immune-targeted treatment of OP. Although current challenges include incomplete mechanistic understanding and a lack of high-level clinical evidence, the integration of advanced technologies such as multi-omics, nanoformulations, and artificial intelligence holds promise for facilitating the transition of TCM from experience-based to evidence-based medicine, offering safer and more effective therapeutic options for the prevention and treatment of OP.

Funding

Promotion and Application Demonstration of the Comprehensive Prevention and Treatment Platform for Bone Injuries in Traditional Chinese Medicine(Special Number: 2023A03007 ; Project Number: 2023A03007-6).

Disclosure statement

The authors declare no conflict of interest.

References

- [1] Rizzoli R, Biver E, Brennan-Speranza TC, 2021, Nutritional Intake and Bone Health. *Lancet Diabetes Endocrinol*,

- 9(9): 606–621.
- [2] Wang YT, Zheng SY, Luo Y, et al., 2025, Osteoimmunology and Aging: Mechanisms, Implications, and Therapeutic Perspectives. *Ageing Res Rev*, 111: 102822.
 - [3] Qi P, Xie R, Liu H, et al., 2024, Mechanisms of Gut Homeostasis Regulating Th17/Treg Cell Balance in PMOP. *Front Immunol*, 15: 1497311.
 - [4] Chen F, Li J, Wang H, et al., 2021, Anti-Tumor Effects of Chinese Medicine Compounds by Regulating Immune Cells in Microenvironment. *Front Oncol*, 11: 746917.
 - [5] Deng Z, Zhang Q, Zhao Z, et al., 2021, Crosstalk between Immune Cells and Bone Cells or Chondrocytes. *Int Immunopharmacol*, 101(Pt A): 108179.
 - [6] Li S, Liu G, Hu S, 2024, Osteoporosis: Interferon-Gamma-Mediated Bone Remodeling in Osteoimmunology. *Front Immunol*, 15: 1396122.
 - [7] Luo J, Li L, Shi W, et al., 2025, Oxidative Stress and Inflammation: Roles in Osteoporosis. *Front Immunol*, 16: 1611932.
 - [8] Fischer V, Haffner-Luntzer M, 2022, Interaction between Bone and Immune Cells: Implications for Postmenopausal Osteoporosis. *Semin Cell Dev Biol*, 123: 14-21.
 - [9] Cheng X, Chen Y, Zhou X, et al., 2025, Immunoporosis: The Hidden Link between Aging Immune Cells and Bone Fragility. *J Orthop Translat*, 53: 325–335.
 - [10] Zhou B, Li S, Song J, 2026, The Impact of Dyslipidemia on Skeletal Health - From an Immunoregulatory Perspective. *Front Immunol*, 17: 1774535.
 - [11] Chen L, Zhao Y, Qiu J, et al., 2024, Analysis and Validation of Biomarkers of Immune Cell-Related Genes in Postmenopausal Osteoporosis: An Observational Study. *Medicine (Baltimore)*, 103(19): e38042.
 - [12] Bhadriricha H, Patel V, Singh AK, et al., 2021, Increased Frequency of Th17 Cells and IL-17 Levels Are Associated with Low Bone Mineral Density in Postmenopausal Women. *Sci Rep*, 11(1): 16155.
 - [13] Takahara C, Tabuchi N, Inoue H, et al., 2026, The Differences in Gut Microbiota Due to Dietary Habits Affect the Onset of Disease Pathology in a Dextran Sulfate Sodium-Induced Colitis Model. *Biol Pharm Bull*, 49(3): 438–451.
 - [14] Qin X, Lian YE, Tang H, et al., 2025, *Lactobacillus rhamnosus* GG Mitigates Bone Loss Induced by Mechanical Unloading via Regulation of the Gut-Bone Axis. *Front Nutr*, 12: 1734220.
 - [15] Wang Z, Luo J, Yu T, et al., 2026, BMSC-Derived Exosomes Facilitate Osteogenesis and Ameliorate Ageing-Related Bone Loss Through Restoring Th17/Treg Homeostasis via the miR-21/Skp2/FoxO1 Axis. *Stem Cell Res Ther*, 2026.
 - [16] Lv J, Hao P, Zhou Y, et al., 2025, Role of the Intestinal Flora-Immunity Axis in the Pathogenesis of Rheumatoid Arthritis-Mechanisms Regulating Short-Chain Fatty Acids and Th17/Treg Homeostasis. *Mol Biol Rep*, 52(1): 617.
 - [17] Sun P, Zhang C, Huang Y, et al., 2022, Jiangu Granule Ameliorated OVX Rats Bone Loss by Modulating Gut Microbiota-SCFAs-Treg/Th17 Axis. *Biomed Pharmacother*, 150: 112975.
 - [18] Yan M, Yang M, Cai Y, et al., 2025, Progress in Multiaxial Coupling Mechanisms of Osteoporosis: Insights from Systems Medicine on Immune-Inflammatory Interactions, Hormonal Regulation, and Metabolic Imbalance. *Front Endocrinol (Lausanne)*, 16: 1705040.
 - [19] Bhardwaj A, Sapra L, Srivastava RK, 2026, Immunotherapeutic Potential of “Breg-Treg” vs “Th9-Th17” Cell Axis in Post-Menopausal Osteoporosis. *Int Rev Immunol*, 45(2): 77–98.
 - [20] Shen Y, Wang Z, Tan J, et al., 2021, TRAF6/ERK/p38 Pathway Is Involved in Interleukin-17-Mediated Autophagy to Promote Osteoclast Precursor Cell Differentiation. *Zhejiang Da Xue Xue Bao Yi Xue Ban*, 50(2): 162–170.
 - [21] Ni S, Fu W, Zhang L, et al., 2026, Circadian Rhythms Regulate Osteoclast Recycling Through Gut Microbiota-

- Dependent Th17 Cell Expansion. *Curr Res Microb Sci*, 10: 100561.
- [22] Takegahara N, Kim H, Choi Y, 2022, RANKL Biology. *Bone*, 159: 116353.
 - [23] Wu Y, Ai H, Xi Y, et al., 2023, Osteoclast-Derived Apoptotic Bodies Inhibit Naive CD8⁺ T Cell Activation via Siglec15, Promoting Breast Cancer Secondary Metastasis. *Cell Rep Med*, 4(9): 101165.
 - [24] Hua D, Yang J, Meng Q, et al., 2021, Soufeng Sanjie Formula Alleviates Collagen-Induced Arthritis in Mice by Inhibiting Th17 Cell Differentiation. *Chin Med*, 16(1): 39.
 - [25] Li X, Chen S, et al., 2026, Systems-Level Molecular and Immunological Evidence Identifies Th17/Treg Modulation as A Key Mechanism of CRSJ's Neuroprotection in Parkinson's Disease. *Front Aging Neurosci*, 18: 1764634.
 - [26] Zhang H, Liu J, Zhang P, et al., 2021, Herbal Formula Longteng Decoction Promotes the Regression of Synovial Inflammation in Collagen-Induced Arthritis Mice by Regulating Type 2 Innate Lymphocytes. *Front Pharmacol*, 12: 778845.
 - [27] Lan H, Qiu W, Wu J, et al., 2024, Formononetin Reverses Treg/Th17 Imbalance in Immune-Mediated Bone Marrow Failure Mice by Regulating the PI3K/Akt Signaling Pathway. *Chin Med*, 19(1): 55.
 - [28] Wang C, Shi S, Wang F, et al., 2026, A Biointerface-Engineered Gold Nanocluster Platform for Icariin Delivery: Dual-Pathway Modulation of Osteoblast and Osteoclast Dynamics in Osteoporosis Therapy. *Biomater Adv*, 183: 214773.
 - [29] Zeng M, Wu Y, Ren Y, et al., 2025, A New Phenolic Acid Isolated from *Salvia miltiorrhiza* Ameliorates OVA-Induced Allergic Asthma by Regulation of Th17/Treg Cells and Inflammation Through the TLR4 Pathway. *Chin J Nat Med*, 23(12): 100007.
 - [30] Zhang Z, Yang Z, Jia Z, et al., 2026, Optimized New Shengmai Powder Suppresses Ferroptosis in Ischemic Cardiomyocytes via cGMP-PKG Signalling. *Chin Med*, 21(1).
 - [31] Ilic J, Bold A, Knop S, 2026, The Role of Epigenetic Modifications in Hematological Cancers. *Front Oncol*, 16: 1744018.
 - [32] Li J, Ma Y, Li X, et al., 2022, Fermented *Astragalus* and Its Metabolites Regulate Inflammatory Status and Gut Microbiota to Repair Intestinal Barrier Damage in Dextran Sulfate Sodium-Induced Ulcerative Colitis. *Front Nutr*, 9: 1035912.
 - [33] Sapra L, Saini C, Mishra PK, et al., 2025, *Bacillus coagulans* Ameliorates Inflammatory Bone Loss in Post-Menopausal Osteoporosis via Modulating the "Gut-Immune-Bone" Axis. *Gut Microbes*, 17(1): 2492378.
 - [34] Li W, Ding Z, Chen Y, et al., 2022, Integrated Pharmacology Reveals the Molecular Mechanism of Gegen Qinlian Decoction Against Lipopolysaccharide-induced Acute Lung Injury. *Front Pharmacol*, 13: 854544.
 - [35] Ho TL, Lee KT, He YH, et al., 2025, C-X-C Motif Chemokine Ligand 13 Suppresses Osteoclast Differentiation Via Interference with RANKL-RANK Interaction. *Front Immunol*, 16: 1729222.
 - [36] Yifan G, Xiaohan X, Jie M, et al., 2026, Multi-Omics-Based Study on the Biological Characteristics of Kidney Renal Deficiency and Blood Stasis in Ankylosing Spondylitis. *J Tradit Chin Med*, 46(1): 183–194.
 - [37] Zihao L, Jie G, Jinyun S, et al., 2026, Network Pharmacological and Experimental Validation of the Mechanism of Chaihu Guizhi Ganjiang Decoction Regulating T Helper Cell 17/Regulatory T Cell Balance to Improve Autoimmune Hepatitis. *J Tradit Chin Med*, 46(1): 110–118.
 - [38] Zhang P, Lin L, Wang N, et al., 2025, Yougui Pills Prevent Ovariectomy-Induced Bone Loss by Suppressing Th17 Response and IL-17/NF-κB Pathway. *Ann Med*, 57(1): 2529576.
 - [39] Zhang H, Li Y, Yuan L, et al., 2021, Interleukin-35 Is Involved in Angiogenesis/Bone Remodeling Coupling

- Through T Helper 17/Interleukin-17 Axis. *Front Endocrinol (Lausanne)*, 12: 642676.
- [40] Gong S, Xu R, Wang Y, et al., 2025, Danggui Beimu Kushen Pill Alleviates Colitis-Induced Inflammation in Mice by Regulating the IL-6/IL-6R and IL-17A/IL-17RA Signaling Pathways. *Pharmaceuticals (Basel)*, 18(2): 141.
- [41] Gong N, Wang L, An L, et al., 2023, Exploring the Active Ingredients and Potential Mechanisms of Action of *Sinomenium acutum* in the Treatment of Rheumatoid Arthritis Based on Systems Biology and Network Pharmacology. *Front Mol Biosci*, 10: 1065171.
- [42] Zhang Y, He X, Wang K, et al., 2024, Irisin Alleviates Obesity-Induced Bone Loss by Inhibiting Interleukin 6 Expression via TLR4/MyD88/NF- κ B Axis in Adipocytes. *J Adv Res*, 69: 343–359.
- [43] Xia Y, Fan D, Li X, et al., 2021, Yi Shen Juan Bi Pill Regulates the Bone Immune Microenvironment via the JAK2/STAT3 Signaling Pathway *In Vitro*. *Front Pharmacol*, 12: 746786.
- [44] Zhuang C, Wang Z, Chen W, et al., 2021, Jintiang Capsules Ameliorate Osteoarthritis by Modulating Subchondral Bone Remodeling and Protecting Cartilage Against Degradation. *Front Pharmacol*, 12: 762543.
- [45] Li J, Cao H, Zhou X, et al., 2023, Advances in the Study of Traditional Chinese Medicine Affecting Bone Metabolism Through Modulation of Oxidative Stress. *Front Pharmacol*, 14: 1235854.
- [46] Peng Z, Xu R, You Q, 2022, Role of Traditional Chinese Medicine in Bone Regeneration and Osteoporosis. *Front Bioeng Biotechnol*, 10: 911326.
- [47] Shen D, Feng Y, Zhang X, et al., 2022, Antiosteoporosis Studies of 20 Medicine Food Homology Plants Containing Quercetin, Rutin, and Kaempferol: TCM Characteristics, *In Vivo* and *In Vitro* Activities, Potential Mechanisms, and Food Functions. *Evid Based Complement Alternat Med*, 2022: 5902293.
- [48] Liew KY, Chee HY, Abas F, et al., 2025, Curcumin-Like Diarylpentanoid Analogues Exhibit Antiviral and Anti-Inflammatory Activities in Influenza A Virus-Infected A549 Lung Epithelial Cells by Inhibiting Multiple Retinoic Acid-Inducible Gene I (RIG-I)-Mediated Pathways. *Viro J*, 22(1): 343.
- [49] Ahmed RH, Rashad Ahmed R, Galaly SR, et al., 2024, Mesenchymal Stem Cells and Curcumin Effectively Mitigate Freund's Adjuvant-Induced Arthritis via their Anti-Inflammatory and Gene Expression of COX-1, IL-6 and IL-4. *Endocr Metab Immune Disord Drug Targets*, 24(4): 468–488.
- [50] Zhu K, Yang C, Dai H, et al., 2019, Crocin Inhibits Titanium Particle-Induced Inflammation and Promotes Osteogenesis by Regulating Macrophage Polarization. *Int Immunopharmacol*, 76: 105865.
- [51] El Midaoui A, Ghzaïel I, Vervandier-Fasseur D, et al., 2022, Saffron (*Crocus sativus* L.): A Source of Nutrients for Health and for the Treatment of Neuropsychiatric and Age-Related Diseases. *Nutrients*, 14(3): 597.
- [52] de Molon RS, 2025, Therapeutic Potential of Tanshinones in Osteolytic Diseases: From Molecular and Cellular Pathways to Preclinical Models. *Dent J (Basel)*, 13(7): 309.

Publisher's note

Bio-Byword Scientific Publishing remains neutral with regard to jurisdictional claims in published maps and institutional affiliations.

Clinical Observation on the Efficacy of Minimally Invasive Treatment for Comminuted Fractures of Long Bones Using Adjustable Carbon Fiber Three-Dimensional External Fixator-Assisted Closed Reduction and Internal Fixation

Tuo Jia

Department of Orthopedics, Ward 3, Yan'an People's Hospital, Yan'an 716000, Shaanxi, China

Copyright: © 2026 Author(s). This is an open-access article distributed under the terms of the Creative Commons Attribution License (CC BY 4.0), permitting distribution and reproduction in any medium, provided the original work is cited.

Abstract: *Objective:* To observe the clinical efficacy of minimally invasive treatment for comminuted fractures of long bones using adjustable carbon fiber three-dimensional external fixator-assisted closed reduction and internal fixation, providing practical evidence for clinical treatment. *Methods:* Ninety patients with comminuted fractures of long bones admitted to the orthopedics department of our hospital from January 2024 to January 2026 were selected as the study subjects. They were randomly divided into an observation group and a control group using a random number table method, each with 45 patients. The control group underwent traditional open reduction and internal fixation, while the observation group underwent minimally invasive treatment using adjustable carbon fiber three-dimensional external fixator-assisted closed reduction and internal fixation. Surgical-related indicators (operative time, intraoperative blood loss, hospital stay), fracture healing status (fracture healing time, excellent and good rate of fracture healing), postoperative complications, and limb function recovery before and after treatment were compared between the two groups. *Results:* The observation group had significantly lower operative time, intraoperative blood loss, hospital stay, healing time, and complication rate compared to the control group (all $P < 0.05$). The excellent and good rate of fracture healing in the observation group was significantly higher than that in the control group ($P = 0.013 < 0.05$). At 3 and 6 months after treatment, the Johner-Wruhs scores of both groups were significantly higher than those before treatment, and the scores in the observation group were significantly higher than those in the control group (all $P < 0.001$). *Conclusion:* Minimally invasive treatment for comminuted fractures of long bones using adjustable carbon fiber three-dimensional external fixator-assisted closed reduction and internal fixation offers advantages such as minimal surgical trauma, less intraoperative bleeding, rapid postoperative recovery, good fracture healing, and fewer complications. It effectively promotes limb function recovery in patients, demonstrating definite clinical efficacy and warranting widespread application.

Keywords: Comminuted fracture of long bones; Adjustable carbon fiber three-dimensional external fixator; Closed reduction and internal fixation; Minimally invasive treatment

Online publication: May 14, 2026

1. Introduction

Comminuted fractures of long bones are common orthopedic traumatic injuries, mostly caused by high-energy violence, with the fracture ends fragmented into three or more pieces, often accompanied by soft tissue damage, poor stability, and high treatment difficulty. The core of clinical treatment is to restore anatomical alignment of the fracture ends, provide firm fixation, protect blood supply, promote healing, reduce complications, and maximize the restoration of limb function^[1,2]. Although traditional open reduction and internal fixation can achieve precise reduction, it involves significant surgical trauma, substantial blood loss, and is prone to damaging the blood supply, leading to complications such as delayed healing and nonunion, as well as slow postoperative recovery. Minimally invasive closed reduction and internal fixation have gradually been applied due to their minimal trauma and light disruption of the periosteal blood supply. However, they still face challenges in achieving precise reduction and stable fixation for complex fractures, with a continued risk of complications^[3]. The adjustable carbon fiber three-dimensional external fixator weighs only one-fifth of traditional metal frames, exhibits good biocompatibility, allows for six-directional fine adjustment of the fracture ends, precisely controls alignment errors, and provides firm three-dimensional fixation. To explore its clinical efficacy, this study compared the effects of minimally invasive treatment using this device-assisted closed reduction and internal fixation with traditional open reduction and internal fixation, and the results are reported as follows.

2. Materials and methods

2.1. General information

Ninety patients with comminuted fractures of long bones admitted to the orthopedics department of our hospital from January 2024 to January 2026 were selected as the study subjects. Inclusion criteria: (1) Diagnosed with comminuted fractures of long bones (femur, tibia, humerus) confirmed by X-ray and CT examinations, with the fracture ends fragmented into three or more pieces; (2) Time from injury to hospital admission ≤ 72 hours; (3) Aged 18 to 65 years, without severe dysfunction of the liver, kidney, heart, or lungs; (4) Without coagulopathy, osteoporosis, malignant tumors, or other diseases; (5) Patients and their families provided informed consent and signed the informed consent form. Exclusion criteria: (1) Open fractures or fractures combined with vascular and nerve injuries; (2) Old fractures or pathological fractures; (3) Patients with mental illnesses or those unable to cooperate with treatment and follow-up; (4) Patients allergic to the materials used in the surgery.

Patients were randomly divided into an observation group and a control group using a random number table method, with 45 patients in each group. In the observation group, there were 25 males and 20 females, aged 22 to 63 years, with an average age of 42.35 ± 8.76 years; the fracture sites were 18 femurs, 17 tibias, and 10 humeri. In the control group, there were 24 males and 21 females, aged 20 to 65 years, with an average age of 43.12 ± 8.95 years; the fracture sites were 17 femurs, 18 tibias, and 10 humeri. There were no statistically significant differences in general information such as gender, age, and fracture site between the two groups ($P > 0.05$), indicating comparability.

2.2. Treatment methods

The control group underwent traditional open reduction and internal fixation. Patients received general

anesthesia or epidural anesthesia, with a lateral decubitus position for femoral fractures and a supine position for others. An appropriate incision was made based on the fracture site, and the skin was incised layer by layer to the periosteum. The surrounding soft tissues were dissected to expose the fracture ends, and hematomas, bone fragments, and incarcerated tissues were cleared. After reduction with forceps, fixation was achieved using plates, screws, or intramedullary nails. Fluoroscopy confirmed firm alignment before the incision was irrigated, sutured, and a drainage tube was placed.

The observation group underwent minimally invasive treatment using adjustable carbon fiber three-dimensional external fixator-assisted closed reduction and internal fixation. After anesthesia, patients were placed in a supine position, and routine disinfection and draping were performed. Manual closed reduction of the fracture ends was performed under fluoroscopic guidance using a C-arm X-ray machine. Based on the fracture condition, an appropriate external fixator was selected, and 2–3 entry points were chosen near the proximal and distal ends of the fracture. Percutaneous pinning was performed for fixation, and the frame was installed and fine-tuned until satisfactory fracture alignment was achieved. Fluoroscopy confirmed the position before the frame was fixed.

Subsequently, for femoral and tibial fractures, minimally invasive intramedullary nail fixation was performed by making a 1–2 cm small incision to establish a medullary canal, inserting an intramedullary nail, and locking it in place. For humeral fractures, minimally invasive fixation with a mini-plate was performed by inserting the plate and screws through a subcutaneous tunnel, without the need for a drainage tube.

Both groups received antibiotics for 3–5 days postoperatively to prevent infection, along with symptomatic pain relief and swelling reduction. Early functional exercises were guided, and regular X-ray reviews were conducted to monitor fracture healing. In the observation group, the tightness of the external fixator could be adjusted 4–6 weeks postoperatively. Both groups gradually initiated weight-bearing exercises based on healing progress.

2.3. Observation indicators

2.3.1. Surgical-related indicators

The operative time (from the onset of anesthesia to the end of surgery), intraoperative blood loss, and hospital stay were recorded for both groups.

2.3.2. Fracture healing status

Regular postoperative X-ray reviews were conducted to record the fracture healing time (from the end of surgery to the appearance of continuous callus on X-ray, with a blurred fracture line and the patient able to bear normal weight). The healing quality was evaluated using the excellent and good rate: excellent indicated anatomical alignment and normal function; good indicated good alignment and basic functional recovery; fair indicated acceptable alignment but delayed healing; poor indicated poor alignment and abnormal healing. The excellent and good rate = (number of excellent + good cases) / total number of cases × 100%.

2.3.3. Postoperative complications

The occurrence of postoperative complications, including infection, delayed fracture healing, nonunion, internal fixation loosening, and joint stiffness, was observed and recorded in both groups. The complication rate was calculated as the number of complication cases / total number of cases × 100%.

2.3.4. Limb function recovery

The Johner-Wruhs score ^[4] was used to evaluate limb function before treatment, and at 3 and 6 months after treatment. This score includes aspects such as pain, deformity, joint range of motion, limb length, and functional recovery, with a total score ranging from 0 to 100. A higher score indicates better limb function recovery.

2.4. Statistical methods

Data analysis was performed using SPSS 27.0 statistical software. Measurement data were expressed as mean \pm standard deviation (SD), and comparisons between groups were made using independent sample t-tests. Count data were expressed as [n (%)], and comparisons were made using the χ^2 test. A *P*-value < 0.05 was considered statistically significant.

3. Results

3.1. Comparison of surgical-related indicators between the two groups

The operative time, intraoperative blood loss, and hospital stay in the observation group were significantly lower than those in the control group (all *P* < 0.001). See **Table 1**.

Table 1. Comparison of surgical-related indicators between the two groups

Group	Operation time (min)	Intraoperative blood loss (ml)	Hospital stay (d)
Observation group (<i>n</i> = 45)	68.45 \pm 10.23	89.36 \pm 15.78	7.62 \pm 1.85
Control group (<i>n</i> = 45)	95.78 \pm 12.56	186.54 \pm 20.31	11.35 \pm 2.42
<i>t</i>	11.318	25.353	8.196
<i>P</i>	<0.001	<0.001	<0.001

3.2. Comparison of fracture healing status between the two groups

The fracture healing time in the observation group was significantly shorter than that in the control group (*P* < 0.001); the excellent and good rate of fracture healing in the observation group was significantly higher than that in the control group (*P* = 0.013 < 0.05). See **Tables 2** and **3**.

Table 2. Comparison of fracture healing time between the two groups

Group	Fracture healing time (weeks)	<i>t</i>	<i>P</i>
Observation group (<i>n</i> = 45)	12.35 \pm 1.76	11.019	<0.001
Control group (<i>n</i> = 45)	16.89 \pm 2.13		

Table 3. Comparison of the excellent and good rate of fracture healing between the two groups [n (%)]

Group	Excellent	Good	Fair	Poor	Excellent + good rate (%)	χ^2	<i>P</i>
Observation group (<i>n</i> = 45)	28 (62.22)	15 (33.33)	2 (4.44)	0 (0.00)	43 (95.56)	6.154	0.013
Control group (<i>n</i> = 45)	18 (40.00)	17 (37.78)	7 (15.56)	3 (6.67)	35 (77.78)		

3.3. Comparison of the incidence of postoperative complications between the two groups

The incidence of postoperative complications in the observation group was significantly lower than that in the control group (*P* < 0.05). See **Table 4**.

Table 4. Comparison of the incidence of postoperative complications between the two groups [*n* (%)]

Group	Infection	Delayed fracture healing	Nonunion	Internal fixation loosening	Joint stiffness	Total incidence rate (%)	χ^2	<i>P</i>
Observation group (<i>n</i> = 45)	1 (2.22)	1 (2.22)	0 (0.00)	0 (0.00)	0 (0.00)	2 (4.44)	4.050	0.044
Control group (<i>n</i> = 45)	3 (6.67)	2 (4.44)	1 (2.22)	2 (4.44)	1 (2.22)	8 (20.00)		

3.4. Comparison of the recovery of limb function between the two groups before and after treatment

Three and six months post-treatment, the Johner-Wruhs scores of both groups showed a significant increase compared to pre-treatment levels, with the observation group achieving significantly higher scores than the control group (both $P < 0.001$). See **Table 5**.

Table 5. Comparison of Johner-Wruhs scores between the two groups before and after treatment

Group	Before treatment	3 months after treatment	6 months after treatment
Observation group (<i>n</i> = 45)	42.35 ± 5.78	78.45 ± 6.32	91.23 ± 4.15
Control group (<i>n</i> = 45)	43.12 ± 5.96	65.36 ± 7.18	80.57 ± 5.26
<i>t</i>	0.616	9.173	10.671
<i>P</i>	0.540	<0.001	<0.001

4. Discussion

Comminuted fractures of long bones pose significant clinical challenges due to severe fragmentation of the fracture ends, poor stability, and frequent association with soft tissue injuries. The key to improving treatment outcomes and promoting patient recovery lies in ensuring accurate fracture reduction and stable fixation while minimizing surgical trauma and preserving the periosteal blood supply. Traditional open reduction and internal fixation (ORIF) can achieve precise reduction of fracture ends, but it involves long surgical incisions, extensive trauma, and the need to strip a large amount of soft tissue and periosteum during surgery, which can easily damage the blood supply to the fracture site, leading to complications such as delayed fracture healing and nonunion. Additionally, the prolonged postoperative recovery period affects the restoration of limb function, limiting its clinical application to some extent ^[5,6].

With the advancement of minimally invasive orthopedic techniques, closed reduction and internal fixation (CRIF) has gradually replaced traditional ORIF as an important method for treating long bone fractures. This approach does not require extensive stripping of soft tissue and periosteum, resulting in less surgical trauma and intraoperative blood loss, effectively protecting the blood supply to the fracture site and promoting fracture healing ^[7]. However, in the treatment of comminuted fractures of long bones, due to the severe fragmentation of the fracture ends, manual closed reduction cannot precisely control the alignment of the fracture ends, and the fixation stability is insufficient, making it prone to issues such as fracture end displacement and loosening of internal fixation, which affect treatment outcomes.

The adjustable carbon fiber three-dimensional external fixator is a novel minimally invasive fixation device. Made of carbon fiber material, it offers advantages over traditional metal external fixators, including

lighter weight, better biocompatibility, and corrosion resistance. It also features multi-directional adjustment capabilities, enabling six-directional fine-tuning of the fracture ends, precisely controlling alignment errors within 0.5 mm, while providing firm three-dimensional fixation support to effectively maintain the stability of the fracture ends and prevent displacement^[8]. When combined with CRIF, it can fully leverage the advantages of both approaches: CRIF achieves minimally invasive fixation of the fracture ends, reducing surgical trauma; the adjustable carbon fiber three-dimensional external fixator assists in precise reduction, enhances fixation stability, and dynamically adjusts the fixation force according to the fracture healing process, achieving dynamic fixation. This balances “stability” and “healing,” promoting callus growth through moderate stress stimulation and shortening the fracture healing time.

The results of this study showed that the observation group had significantly shorter operative time, less intraoperative blood loss, and shorter hospital stay compared to the control group, indicating that minimally invasive treatment with the adjustable carbon fiber three-dimensional external fixator assisting CRIF results in less surgical trauma, less intraoperative bleeding, and faster postoperative recovery in patients. This is attributed to the fact that this approach does not require extensive stripping of soft tissue and involves simpler surgical procedures^[9]. The observation group also had a significantly shorter fracture healing time and a higher excellent and good rate of fracture healing compared to the control group, suggesting that this treatment regimen effectively promotes fracture healing and improves the quality of fracture healing. This is because the adjustable carbon fiber three-dimensional external fixator can precisely reduce the fracture ends, provide firm fixation, protect the blood supply to the fracture site, and dynamically adjust the fixation force to promote callus growth. In contrast, traditional ORIF delays fracture healing due to damage to the periosteal blood supply.

In terms of postoperative complications, the observation group had a significantly lower complication rate compared to the control group. The observation group only experienced one case of infection and one case of delayed fracture healing, while the control group had various complications such as infection, delayed fracture healing, nonunion, loosening of internal fixation, and joint stiffness. This is because minimally invasive treatment with the adjustable carbon fiber three-dimensional external fixator assisting CRIF causes less trauma and damage to soft tissue and periosteum, reducing the occurrence of complications such as infection and joint stiffness. Additionally, the firm three-dimensional fixation prevents fracture end displacement and reduces complications such as loosening of internal fixation and nonunion^[10]. Furthermore, the good biocompatibility of carbon fiber material significantly reduces the incidence of skin allergies and local inflammation compared to traditional steel structure brackets, further reducing the risk of complications.

5. Conclusion

In terms of limb function recovery, the Johner-Wruhs scores of the observation group were significantly higher than those of the control group at 3 and 6 months after treatment, indicating that this treatment regimen effectively promotes the recovery of limb function in patients. This is because this approach involves less trauma and faster postoperative recovery, allowing patients to engage in functional exercises early. Additionally, the high quality of fracture healing reduces factors affecting limb function such as malunion and joint stiffness. In contrast, traditional ORIF affects functional exercises and leads to poor limb function recovery due to slow postoperative recovery and multiple complications.

In summary, minimally invasive treatment of comminuted fractures of long bones with the adjustable carbon fiber three-dimensional external fixator assisting CRIF offers advantages such as less surgical trauma,

less intraoperative bleeding, faster postoperative recovery, better fracture healing, and fewer complications. It effectively promotes the recovery of limb function in patients and has definite clinical efficacy, making it worthy of promotion and application.

Funding

Yan'an Science and Technology Plan Project (2024SLSFGG-218)

Disclosure statement

The author declares no conflict of interest.

References

- [1] Lu W, An Y, Wang S, et al., 2026, Clinical Study on Modified Small Splint External Fixation for Comminuted Proximal Humeral Fractures. *Journal of Practical Traditional Chinese Medicine*, 42(02): 352–354.
- [2] Zhu S, Wang H, Chen Y, et al., 2024, Treatment of Comminuted Femoral Shaft Fractures in Older Children with a Bridge-Type Combined Internal Fixation System. *Journal of Clinical Orthopedics*, 27(05): 616.
- [3] Zhao F, Cao Y, 2026, Risk Factors and Countermeasures for Internal Fixation Failure in the Treatment of Intertrochanteric Fractures with Proximal Femoral Nail Antirotation. *Chinese Journal of Tissue Engineering Research*, 30(09): 2323–2333.
- [4] Zhou X, Jia J, Zhou Y, et al., 2024, Efficacy Analysis of Minimally Invasive Percutaneous Plate Fixation for Middle and Lower Tibial Fractures. *Journal of Hubei Medical College*, 43(04): 396–400.
- [5] Shao X, Zhao Y, 2026, Impact of Minimally Invasive Thoracoscopic Rib Fracture Internal Fixation on Rapid Postoperative Recovery in Patients with Multiple Rib Fractures. *Harbin Medical Journal*, 46(01): 71–73.
- [6] He S, Qing H, 2026, Short-Term Efficacy Observation of Reduction and Percutaneous Cannulated Screw Internal Fixation for Middle and Lower Humeral Spiral Fractures. *Da Yisheng (Journal of General Practitioners)*, 11(03): 66–68.
- [7] Zhu J, Wan X, Hu Z, et al., 2023, Comparative Study of Arthroscopic Small-Incision Surgery Versus Traditional Internal Fixation Reduction for Tibial Plateau Fractures. *Great Doctor*, 8(11): 8–10.
- [8] Zhao S, Ren Z, Li C, et al., 2017, Treatment of Tile C Pelvic Fractures with an Adjustable Pelvic External Fixator Combined with Lower Limb Skeletal Traction. *Electronic Journal of Clinical Medical Literature*, 4(50): 9771–9772.
- [9] Lu C, Wang H, Liu L, et al., 2014, Treatment of Distal Radius Fractures with Closed Reduction and an Adjustable External Fixator. *Anhui Medical Journal*, 35(10): 1395–1397.
- [10] Cheng E, Liu Y, Cai F, et al., 2022, Treatment of Open Proximal Phalangeal Fractures with Metacarpophalangeal Joint Dislocation Using an Adjustable Miniature External Fixator Combined with Limited Kirschner Wire Internal Fixation. *Journal of Practical Hand Surgery*, 36(01): 14–18.

Publisher's note

Bio-Byword Scientific Publishing remains neutral with regard to jurisdictional claims in published maps and institutional affiliations.

Single-Row Versus Double-Row Rotator Cuff Repair: A Systematic Review and Meta-Analysis of Structural Integrity and Functional Outcomes

Delger, Xiubin Wu*

Xijing Hospital, Xilinhot 026000, Xilingol League, Inner Mongolia Autonomous Region, China

**Author to whom correspondence should be addressed.*

Copyright: © 2026 Author(s). This is an open-access article distributed under the terms of the Creative Commons Attribution License (CC BY 4.0), permitting distribution and reproduction in any medium, provided the original work is cited.

Abstract: *Background:* Double-row rotator cuff repair is often used to improve tendon healing. However, its effect on clinical outcomes is still not clearly established. *Methods:* A systematic review and meta-analysis was performed following PRISMA guidelines. This study compared single-row and double-row repair. Structural integrity and functional outcomes were evaluated. Structural failure was defined as any non-intact repair, including both partial- and full-thickness defects. Odds ratios (ORs) and mean differences (MDs) with 95% confidence intervals (CIs) were calculated using a random-effects model. *Results:* Eight comparative studies were included. Six contributed to structural analysis, and six reported functional outcomes. Among these, four were included in the quantitative synthesis for functional results. Structural failure occurred in 42.7% of shoulders after single-row repair and 26.4% after double-row repair. This corresponds to an absolute reduction of about 16%, which is significant in practice. Double-row repair reduced the risk of structural failure (OR 0.47, 95% CI 0.29 to 0.75; $I^2 = 0\%$). In contrast, postoperative Constant scores were similar between groups (MD -0.08, 95% CI -3.98 to 3.82; $I^2 = 0\%$). *Conclusion:* Double-row repair improves structural integrity. But it does not seem to improve functional outcomes, at least within the current sample size. This indicates that structural healing and clinical recovery may not fully align.

Keywords: Rotator cuff tear; Single-row repair; Double-row repair; Structural integrity; Retear; Constant score; Arthroscopic repair; Meta-analysis

Online publication: May 14, 2026

1. Introduction

Rotator cuff tears are common. They often cause shoulder pain, weakness, and limited function, especially in older patients. When conservative treatment fails, surgery is usually needed. The goal is to repair the tendon and improve function. Even with better arthroscopic techniques, structural failure after surgery is still a concern.

The repair method is an important factor in rotator cuff surgery. Single-row repair is widely used

because it is simple and reliable. Double-row repair was developed to better restore the natural tendon footprint. It increases the contact area and pressure between the tendon and bone ^[1]. Biomechanical studies show that double-row repair provides stronger fixation and better contact properties ^[2].

However, the clinical value of double-row repair is still unclear. Imaging studies often show better structural healing with double-row repair. But clinical studies do not always show better functional outcomes. This raises a question: Does better healing really lead to better function?

Structural integrity and functional outcome are related, but they are not the same. Imaging mainly reflects tendon healing. Functional recovery depends on many factors, such as pain, range of motion, muscle strength, and rehabilitation ^[3]. Because of this, better structural results do not always lead to better functional recovery, especially in the short to mid term.

Interpretation of the existing literature is further complicated by heterogeneity in study design, including variation in tear size, patient selection, imaging modality, and follow-up duration. In addition, structural and functional outcomes are often analyzed separately, and few studies have explicitly examined their relationship within a unified analytical framework ^[4]. Recent comparative studies have continued to report inconsistent findings, and an updated synthesis focusing on the relationship between structural and functional outcomes remains warranted.

This study compares single-row and double-row repair. It focuses on structural integrity and functional outcomes, and how they relate to each other. It is expected that double-row repair reduces structural failure. However, it may not lead to a clear improvement in functional outcomes.

2. Methods

2.1. Study design

This study was conducted as a systematic review and meta-analysis of comparative studies evaluating single-row and double-row rotator cuff repair, in accordance with the Preferred Reporting Items for Systematic Reviews and Meta-Analyses (PRISMA) guidelines. A study protocol was developed prior to data extraction.

A systematic literature search was conducted in PubMed, Embase, and the Cochrane Library from database inception to April 20, 2026. The search strategy included combinations of Medical Subject Headings (MeSH) and free-text terms related to “rotator cuff,” “single-row,” and “double-row” repair. Only studies published in English were included. Reference lists of included studies were also manually screened to identify additional relevant studies.

2.2. Study selection

Study selection was performed independently by two reviewers based on predefined eligibility criteria. Titles and abstracts were initially screened, followed by full-text review of potentially eligible studies. Discrepancies were resolved through discussion.

2.3. Eligibility criteria

Studies were eligible if they met the following criteria: (1) direct comparison of single-row and double-row rotator cuff repair; (2) reporting postoperative structural integrity assessed by imaging and/or postoperative functional outcomes; and (3) involving human subjects.

Studies without a direct comparison group were excluded to avoid indirect comparisons across

heterogeneous populations. Postoperative imaging was required for inclusion in the structural analysis, as tendon integrity was defined as the primary structural endpoint ^[5]. Studies reporting only intraoperative findings were excluded, as these do not reflect healing status.

No restrictions were placed on tear size, repair configuration, or imaging modality in order to maximize study inclusion and reflect real-world clinical variability.

Review articles, case reports, biomechanical studies, cadaveric studies, and studies without sufficient extractable data were excluded. When multiple publications involved overlapping cohorts, the report with the most complete outcome data or longest follow-up was included to avoid duplication.

2.4. Data extraction

Data extraction was performed independently by two reviewers using a predefined collection form. Discrepancies were resolved through discussion and verification against the original reports.

The following information was recorded when available: first author, year of publication, study design, sample size, follow-up duration, tear size, repair technique, imaging modality, and reported outcomes.

For structural analysis, the number of postoperative failures and the number of shoulders assessed by imaging were extracted for each group. Structural failure was defined as any non-intact repair, including both partial-thickness defects and full-thickness retears, to ensure consistency across studies despite potential differences in clinical relevance. When tendon integrity was reported in multiple categories, these were collapsed into intact versus non-intact repair to allow consistent pooling across studies.

For functional analysis, postoperative Constant scores were extracted together with measures of variance. Postoperative values were prioritized over change scores to allow comparison of final functional status between techniques. Studies reporting normalized Constant scores relative to the contralateral shoulder were described separately and not pooled with raw scores in the primary meta-analysis due to differences in scale and interpretability.

For studies reporting different sample sizes for structural and functional outcomes, data were extracted separately for each endpoint based on the most appropriate reported population.

For structural outcomes, the denominator was defined as the number of shoulders that underwent postoperative imaging rather than the number initially treated to reduce bias associated with incomplete imaging follow-up.

Missing variance data were recorded during extraction. Studies without sufficient variance data were not included in the quantitative synthesis of continuous outcomes.

2.5. Risk of bias assessment

Risk of bias in randomized controlled trials was assessed using the Cochrane Risk of Bias tool. Nonrandomized comparative studies were evaluated using the Newcastle–Ottawa Scale.

Differences in imaging modality and reporting criteria were considered potential sources of measurement bias for structural outcomes. For functional outcomes, variability related to follow-up duration and evaluator-dependent scoring was considered.

Studies were categorized as having low, moderate, or high risk of bias based on their overall methodological profile. Studies were not excluded solely on the basis of risk of bias, but study quality was considered during interpretation. Sensitivity analysis was performed to evaluate the influence of nonrandomized studies.

2.6. Statistical analysis

Quantitative synthesis was performed using a random-effects model to account for expected clinical and methodological variability across studies. For structural outcomes, odds ratios (ORs) with 95% confidence intervals (CIs) were calculated. For functional outcomes, mean differences (MDs) with 95% CIs were used for postoperative Constant scores. Statistical heterogeneity was assessed using the I^2 statistic.

For dichotomous outcomes, event counts were derived from reported healing categories when necessary. For continuous outcomes, means and standard deviations were extracted when available. Studies that reported mean postoperative Constant scores without corresponding variance data were described qualitatively but were not included in the pooled mean-difference analysis.

Sensitivity analysis was performed by excluding nonrandomized studies to assess the robustness of the pooled estimates. Statistical significance was defined as a two-sided P -value < 0.05 .

Publication bias was not formally assessed due to the limited number of included studies (<10), as funnel plot-based methods are not considered reliable in small meta-analyses.

All statistical analyses were performed using Review Manager (RevMan, version 5.4; The Cochrane Collaboration).

3. Results

A total of 168 records were identified through database searching, with an additional four records identified through manual screening. After removal of duplicates, 140 records remained for title and abstract screening, of which 120 were excluded. Twenty full-text articles were assessed for eligibility, and 14 were excluded after full-text review, primarily due to lack of direct comparison, absence of postoperative imaging outcomes, or insufficient extractable data. In total, eight studies were included in the systematic review, with six contributing to the structural integrity analysis and six reporting functional outcomes, of which four were included in the quantitative synthesis.

The characteristics of the included studies are summarized in **Table 1**. Eight comparative studies were identified, including five randomized controlled trials and three nonrandomized comparative studies. Sample sizes varied across studies, and follow-up duration ranged from 12 to 24 months.

Structural integrity was assessed using magnetic resonance imaging (MRI), magnetic resonance arthrography (MRA), ultrasonography, and computed tomography (CT) arthrography. Functional outcomes were primarily reported using the Constant score.

Table 1. Characteristics of included studies

Study	Year	Design	Sample size(SR/DR)	Follow-up	Imaging modality	Outcomes
Franceschi	2007	RCT	30/30 (26/26 analyzed)	24 m	MRA	Structural
Burks	2009	RCT	20/20	12 m	MRI	Structural + Constant
Koh	2011	RCT	24/23	24 m	MRI	Structural + Constant
Lapner	2012	RCT	48/42 (39/37 analyzed)	24 m	US/MRI	Structural + Constant
Ma	2012	RCT	27/26	24 m	MRA	Structural
Charousset	2007	Comparative	35/31	24 m	CT arthrography	Structural + Constant
Grasso	2009	Comparative	37/35	24 m	MRI	Constant
Aydin	2010	Comparative	34/34	24 m	MRI	Constant

Risk of bias assessment is summarized in **Table 2**. Among randomized studies, most showed low risk of selection bias, although allocation concealment and blinding were not consistently reported. Nonrandomized studies demonstrated a higher risk of bias, particularly with respect to selection and comparability between groups.

Table 2. Risk of bias assessment

Study	Study design	Selection bias	Comparability	Outcome assessment	Follow-up completeness	Overall
Franceschi	RCT	Low	Low	Low	Low	Low
Burks	RCT	Low	Unclear	Unclear	Low	Moderate
Koh	RCT	Low	Unclear	Unclear	Low	Moderate
Lapner	RCT	Low	Low	Low	Low	Low
Ma	RCT	Unclear	Unclear	Unclear	Low	Moderate
Charousset	Comparative	High	Moderate	Low	Low	High
Grasso	Comparative	Moderate	Moderate	Low	Low	Moderate
Aydin	Comparative	Moderate	Moderate	Low	Low	Moderate

Structural failure was reported in all six studies included in the structural analysis. Across the pooled sample, failure occurred in 73 of 171 shoulders (42.7%) in the single-row group and 43 of 163 shoulders (26.4%) in the double-row group, corresponding to an absolute reduction of approximately 16%.

At the study level, failure rates in the single-row group ranged from 10% to 60%, whereas rates in the double-row group ranged from 10% to 39% (**Table 3**). Most studies reported lower failure rates in the double-row group, although the magnitude of difference varied across studies. Greater absolute differences were observed in studies with higher baseline failure rates, although this observation was not formally tested. Pooled analysis showed that double-row repair reduced structural failure (OR 0.47, 95% CI 0.29–0.75; $I^2 = 0\%$), with no evidence of statistical heterogeneity (**Table 4**).

Table 3. Study-level data for structural failure

Study	DR events	DR total	SR events	SR total
Franceschi	8	26	12	26
Burks	2	20	2	20
Koh	7	23	15	24
Lapner	8	37	13	39
Ma	6	26	10	27
Charousset	12	31	21	35

Table 4. Pooled analysis of structural failure

Outcome	Studies	Patients (SR/DR)	Events (SR/DR)	OR	95% CI	I^2
Re-tear	6	171/163	73/43	0.47	0.29–0.75	0%

After exclusion of the nonrandomized study, the pooled estimate remained similar (OR 0.48, 95% CI 0.28–0.83; $I^2 = 0\%$), indicating that the overall result was stable (**Table 5**).

Table 5. Sensitivity analysis

Outcome	Studies	OR	95% CI	I ²	Interpretation
Re-tear (excluding Charousset)	5	0.48	0.28–0.83	0%	Stable

Functional outcomes were reported in six studies using the Constant score; however, only four provided sufficient variance data for inclusion in the pooled analysis. Two studies reported mean values without standard deviations and were therefore summarized qualitatively but not included in the quantitative synthesis (**Table 6**).

Pooled analysis excluding the study reporting normalized Constant scores (Grasso *et al.*, 2009) showed no difference between techniques (MD –0.08, 95% CI –3.98 to 3.82; I² = 0%). The pooled estimate was centered near zero, indicating no detectable difference in functional outcome. One study (Grasso, 2009) reported normalized Constant scores rather than raw values, which may affect comparability with other studies.

Table 6. Study-level data for Constant score

Study	DR n	DR mean	DR SD	SR n	SR mean	SR SD
Grasso*	35	104.9	21.8	37	100.5	17.8
Burks	20	74.4	18.4	20	77.8	9.0
Koh	31	82.5	21.9	31	85.4	13.8
Lapner	42	86.3	14.2	48	85.6	14.0
Aydin	34	78.8	NA	34	82.2	NA
Charousset	31	82.7	NA	35	80.7	NA

Normalized Constant score; not included in pooled analysis.

NA indicates that standard deviation was not reported in the original study. Studies without variance data were not included in the pooled mean-difference analysis.

Values for Grasso (2009) were reported as normalized Constant scores relative to the contralateral shoulder and may exceed 100. These data were not included in the pooled meta-analysis due to a lack of comparability with raw Constant scores (**Table 7**).

Table 7. Pooled analysis of Constant score

Outcome	Studies	MD	95% CI	I ²
Constant score	4	-0.08	–3.98 to 3.82	0%

Double-row repair was associated with a reduction in structural failure compared with single-row repair. No statistically significant difference was observed in functional outcome as measured by the Constant score, although this finding should be interpreted in the context of limited sample size in the functional analysis.

4. Discussion

4.1. Principal findings

The principal finding of this meta-analysis is that double-row rotator cuff repair was associated with a lower rate of postoperative structural failure compared with single-row repair, whereas no statistically significant

difference was observed in functional outcome, which may reflect limited statistical power rather than true equivalence as measured by the Constant score, although this finding should be interpreted in the context of limited sample size in the functional analysis. The structural advantage was consistent in magnitude and direction across studies, and the pooled estimate remained stable after sensitivity analysis.

The observed reduction in structural failure corresponds to an absolute difference of approximately 16%, indicating a clinically meaningful effect. However, this structural advantage was not accompanied by a detectable improvement in functional outcome, which may reflect limited statistical power rather than true equivalence ^[6]. These findings suggest that structural integrity and clinical recovery represent related but distinct endpoints after rotator cuff repair and should be interpreted separately.

4.2. Structural success versus clinical success

Clinical scores reflect overall shoulder function rather than tendon healing alone. As a composite outcome, the Constant score integrates pain, motion, and strength, and may improve despite the presence of structural defects. Conversely, an anatomically intact repair does not uniformly translate into superior clinical performance, particularly within short- to mid-term follow-up.

The present analysis demonstrates a consistent reduction in structural failure with double-row repair, yet without a corresponding improvement in postoperative Constant score. Rather than representing a contradiction, this finding may reflect a fundamental dissociation between anatomical healing and early functional recovery.

Functional outcomes after rotator cuff repair are determined by a composite of factors including pain relief, restoration of range of motion, neuromuscular compensation, and strength recovery. Among these, early improvements in pain and mobility may dominate patient-reported outcomes, potentially masking the contribution of tendon integrity within short- to mid-term follow-up. Consequently, structural failure—particularly when partial—may not translate into measurable deficits in composite functional scores.

This interpretation is further supported by the observation that structural failure was defined as a binary composite endpoint encompassing both partial defects and full-thickness retears ^[7]. These entities likely differ in biomechanical consequence and clinical relevance. Pooling them into a single category may attenuate the observable association between tendon integrity and functional outcome, thereby biasing results toward functional equivalence.

In addition, the relationship between structural integrity and function is likely time-dependent. While early functional recovery is driven primarily by pain resolution and mobility, the long-term trajectory may be more strongly influenced by tendon durability, muscle strength preservation, and prevention of tear progression ^[8]. The follow-up duration of the included studies (12–24 months) may therefore be insufficient to capture delayed functional divergence between repair constructs.

Taken together, these findings suggest that structural integrity and clinical outcome should not be interpreted as interchangeable endpoints, but rather as related yet temporally and mechanistically distinct dimensions of treatment effect.

4.3. Interpretation of functional equivalence: Absence of evidence versus evidence of absence

The lack of a statistically significant difference in Constant score should be interpreted with caution. The pooled analysis included a limited number of studies with available variance data, resulting in relatively

wide confidence intervals. As such, the present findings should be considered as an absence of evidence for a functional difference rather than definitive evidence of equivalence. Future studies with larger sample sizes and longer follow-up are required to determine whether subtle but clinically meaningful differences exist.

Implications for surgical decision-making: toward a goal-oriented framework

The dissociation between structural and functional outcomes has direct implications for surgical decision-making. Rather than favoring a uniform repair strategy, the choice between single-row and double-row fixation may be better conceptualized as goal-dependent.

When the primary objective is to maximize structural durability—such as in larger tears, compromised tissue quality, or patients with higher functional demands—double-row repair may be preferred due to its lower risk of structural failure^[9]. Conversely, when the clinical priority is short-term functional recovery, the current evidence does not demonstrate a measurable advantage of double-row repair, suggesting that single-row fixation remains a reasonable and potentially more efficient option.

This goal-oriented framework highlights the importance of aligning surgical technique with the intended outcome domain, and underscores the need for future studies to stratify patients according to factors such as tear size, tissue quality, and functional demand^[10].

4.4. Strengths of the present study

This study has several strengths. Structural and functional outcomes were analyzed separately, preserving conceptual clarity in a field where these endpoints are often combined. The structural findings were consistent across studies, with low statistical heterogeneity and stable sensitivity analysis, strengthening confidence in the robustness of the observed effect. In addition, the analysis was restricted to comparative studies, improving interpretability relative to indirect comparisons across heterogeneous populations.

4.5. Limitations

Several limitations should be considered. First, structural failure was defined as a binary outcome by grouping partial-thickness defects and full-thickness retears as non-intact repairs. These conditions differ in biological and clinical significance, and this classification may have attenuated the relationship between structural integrity and functional outcome.

Second, important effect modifiers such as tear size, tissue quality, and chronicity were not consistently reported across studies and could not be accounted for in the analysis. As a result, the pooled estimates likely represent an average treatment effect across heterogeneous patient populations.

Third, structural integrity was assessed using different imaging modalities (MRI, MRA, ultrasonography, and CT arthrography), which have variable sensitivity for detecting partial defects and may have introduced measurement heterogeneity.

Fourth, the functional analysis was based on a limited number of studies with incomplete variance reporting, resulting in reduced statistical power and relatively wide confidence intervals. Therefore, the absence of a statistically significant difference should be interpreted with caution.

Finally, most included studies reported short- to mid-term follow-up (12–24 months). Any potential long-term functional benefits associated with improved structural integrity, particularly in terms of strength preservation or prevention of tear progression, may not have been captured.

Future studies should focus on stratifying patients according to key clinical variables and incorporating

longer-term follow-up to better define the relationship between structural integrity and functional outcome.

5. Conclusion

Double-row rotator cuff repair is associated with a lower rate of structural failure compared with single-row repair; however, this structural advantage does not translate into a measurable improvement in short- to mid-term functional outcome based on the available evidence.

These findings highlight that structural integrity and clinical recovery represent complementary but non-equivalent dimensions of outcome after rotator cuff repair. While anatomical healing reflects the durability of the repair construct, functional recovery is influenced by a broader set of factors, including pain, mobility, and neuromuscular adaptation.

From a clinical perspective, the choice of repair technique should therefore be aligned with the primary treatment objective. Double-row repair may be preferred when structural durability is a priority, whereas single-row repair remains a reasonable option when the focus is on short-term functional recovery and procedural efficiency.

Future research should aim to clarify the long-term functional implications of improved structural integrity and to identify patient subgroups most likely to benefit from more complex repair strategies.

Disclosure statement

The authors declare no conflict of interest.

References

- [1] Franceschi F, Ruzzini L, Longo UG, et al., 2007, Equivalent Clinical Results of Arthroscopic Single-Row and Double-Row Suture Anchor Repair for Rotator Cuff Tears: A Randomized Controlled Trial. *The American Journal of Sports Medicine*, 35(8): 1254–1260.
- [2] Burks RT, Crim J, Brown N, et al., 2009, A Prospective Randomized Clinical Trial Comparing Arthroscopic Single- and Double-Row Rotator Cuff Repair: Magnetic Resonance Imaging and Early Clinical Evaluation. *The American Journal of Sports Medicine*, 37(4): 674–682.
- [3] Koh KH, Kang KC, Lim TK, et al., 2011, Prospective Randomized Clinical Trial of Single-Versus Double-Row Suture Anchor Repair in 2- to 4-cm Rotator Cuff Tears: Clinical and Magnetic Resonance Imaging Results. *Arthroscopy: The Journal of Arthroscopic & Related Surgery*, 27(4): 453–462.
- [4] Ma HL, Chiang ER, Wu HTH, et al., 2012, Clinical Outcome and Imaging of Arthroscopic Single-Row and Double-Row Rotator Cuff Repair: A Prospective Randomized Trial. *Arthroscopy: The Journal of Arthroscopic & Related Surgery*, 28(1): 16–24.
- [5] Lapner PL, Sabri E, Rakhra K, et al., 2012, A Multicenter Randomized Controlled Trial Comparing Single-Row with Double-Row Fixation in Arthroscopic Rotator Cuff Repair. *JBJS*, 94(14): 1249–1257.
- [6] Charousset C, Grimberg J, Duranthon LD, et al., 2007, Can a Double-Row Anchorage Technique Improve Tendon Healing in Arthroscopic Rotator Cuff Repair? A Prospective, Nonrandomized, Comparative Study of Double-Row and Single-Row Anchorage Techniques with Computed Tomographic Arthrography Tendon Healing Assessment. *The American Journal of Sports Medicine*, 35(8): 1247–1253.
- [7] Grasso A, Milano G, Salvatore M, et al., 2009, Single-Row Versus Double-Row Arthroscopic Rotator Cuff Repair:

A Prospective Randomized Clinical Study. *Arthroscopy: The Journal of Arthroscopic & Related Surgery*, 25(1): 4–12.

- [8] Aydin N, Kocaoglu B, Guven O, 2010, Single-Row Versus Double-Row Arthroscopic Rotator Cuff Repair in Small- to Medium-Sized Tears. *Journal of Shoulder and Elbow Surgery*, 19(5): 722–725.
- [9] Carbonel I, Martinez AA, Calvo A, et al., 2012. Single-Row Versus Double-Row Arthroscopic Repair in the Treatment of Rotator Cuff Tears: A Prospective Randomized Clinical Study. *International Orthopaedics*, 36(9): 1877–1883.
- [10] Imam M, Sallam A, Ernstbrunner L, et al., 2020. Three-Year Functional Outcome of Transosseous-Equivalent Double-Row vs. Single-Row Repair of Small and Large Rotator Cuff Tears: A Double-Blinded Randomized Controlled Trial. *Journal of Shoulder and Elbow Surgery*, 29(10): 2015–2026.

Publisher's note

Bio-Byword Scientific Publishing remains neutral with regard to jurisdictional claims in published maps and institutional affiliations.

Effects of Grape Seed Extract on NF- κ B Expression in Synoviocytes of Mice with Rheumatoid Arthritis

Fan Li, Shun Yuan, Qun Kong, Jingzheng Wang, Zhuoran Li, Chanjuan Liu, Yue Wang, Qingjun Ding*

Qilu Institute of Technology, Jinan 250200, Shandong, China

**Author to whom correspondence should be addressed.*

Copyright: © 2026 Author(s). This is an open-access article distributed under the terms of the Creative Commons Attribution License (CC BY 4.0), permitting distribution and reproduction in any medium, provided the original work is cited.

Abstract: *Objective:* To investigate the effects of grape seed extract (GSE) on NF- κ B expression and inflammatory injury in synoviocytes of mice with rheumatoid arthritis (RA), so as to provide experimental evidence for the natural drug therapy of RA. *Methods:* RA mouse model was established by collagen induction. The mice were randomly divided into a normal control group, a model group, and low-/medium-/high-dose GSE groups, and received intragastric intervention for 48 hours. Synoviocytes were isolated and cultured *in vitro*. The mRNA and protein expressions of NF- κ B/p65 were detected by qRT-PCR and Western blot, respectively. The secretion levels of TNF- α , IL-6, and IL-1 β were detected by ELISA, and the pathological changes of synovial tissue were observed by HE staining. *Results:* Compared with the model group, the expression of NF- κ B/p65 in each GSE dose group decreased in a dose-dependent manner ($P < 0.05$ or $P < 0.01$). The expression and secretion of downstream inflammatory factors were significantly down-regulated, and the pathological injury of synovial tissue was significantly improved, with the most significant effect in the high-dose group. *Conclusion:* GSE can inhibit the NF- κ B signaling pathway, down-regulate the release of inflammatory factors, and alleviate synovial inflammation and pathological injury in RA mice. It is expected to be a potential natural drug for the treatment of RA.

Keywords: Grape seed extract; Rheumatoid arthritis; Synoviocytes; Nuclear factor- κ B; Inflammatory factors

Online publication: May 14, 2026

1. Introduction

Rheumatoid arthritis (RA) is an autoimmune disease characterized by chronic inflammation and hyperplasia of joint synovium. The global prevalence rate is 0.5–1%, and it mostly occurs in middle-aged women. Its pathological process is accompanied by abnormal proliferation of synoviocytes and massive release of inflammatory factors, which eventually lead to the destruction of articular cartilage and bone, causing joint

deformity and even disability ^[1]. At present, the clinical treatment of RA mainly relies on disease-modifying antirheumatic drugs, biological agents, glucocorticoids, etc. However, such drugs have problems such as obvious side effects, high treatment costs, and easy drug resistance. Therefore, searching for safe, efficient, and economical natural therapeutic drugs has become a research hotspot in this field ^[2].

As a core transcription factor regulating inflammation, nuclear factor-kappa B (NF-κB) plays a key role in the pathological process of RA. In RA synovial tissue, abnormal activation of NF-κB can trigger the cascade release of downstream inflammatory factors such as TNF-α, IL-6, and IL-1β, forming a vicious inflammatory cycle, promoting synovial hyperplasia and joint structure destruction ^[3]. Inhibiting the activation of the NF-κB signaling pathway has become an important target for the research and development of new therapeutic drugs for RA.

Grape seed extract (GSE) is a natural polyphenol extract from grape seeds, and its main active component is proanthocyanidins, which have significant antioxidant, anti-inflammatory, and immunomodulatory properties ^[4]. In recent years, studies have found that GSE can alleviate the pathological injury of various inflammatory diseases such as cardiovascular diseases and nervous system diseases by inhibiting the activation of NF-κB ^[5]. However, the regulatory effect and molecular mechanism of GSE on NF-κB expression in synoviocytes of RA mice are still not fully understood ^[6].

In this study, RA mouse model was used as the research object to investigate the effects of different concentrations of GSE on NF-κB expression in synoviocytes and the release of downstream inflammatory factors, aiming to provide experimental evidence for the clinical application of GSE in the treatment of RA and open up a new direction for the research and development of natural drugs for RA.

2. Materials and methods

2.1. Experimental animals

Sixty SPF-grade C57BL/6 female mice, aged 6–8 weeks, weighing 18–22 g, were selected. The mice were raised in the animal room of the School of Medicine, Qilu Institute of Technology, under constant temperature and humidity, with a 12-hour light-dark cycle, free access to food and water, and adaptive feeding for 1 week before the experiment.

2.2. Experimental reagents and instruments

Grape seed extract; complete Freund's adjuvant, incomplete Freund's adjuvant; primers for NF-κB/p65, TNF-α, IL-6, IL-1β; qRT-PCR kit, RNA extraction kit; Western blot-related antibodies, HRP-labeled secondary antibody; ELISA detection kit; ultra-low temperature refrigerator; real-time fluorescent quantitative PCR instrument; protein electrophoresis instrument, membrane transfer instrument; microplate reader; inverted microscope; high-speed refrigerated centrifuge.

2.3. Experimental methods

2.3.1. Establishment and grouping of RA mouse model

Sixty mice were randomly divided into a normal control group ($n = 10$) and a model establishment group ($n = 50$). The RA model was established in the model establishment group by collagen induction: type II collagen was mixed with complete Freund's adjuvant in equal volume, and after full emulsification, it was injected intradermally at the base of the mouse tail, with the initial immunization dose of 100 μg per mouse; on day

21, booster immunization was performed with the emulsion of type II collagen and incomplete Freund's adjuvant at a dose of 50 µg per mouse. The normal control group was injected with the same volume of normal saline. After booster immunization, the joint symptoms of mice were observed weekly, and the modeling effect was evaluated according to the arthritis index (AI) scoring standard. A score ≥ 4 was judged as successful modeling [7].

After successful modeling, the modeled mice were randomly divided into RA model group, low-dose GSE group, medium-dose GSE group, and high-dose GSE group, with 10 mice in each group.

The normal control group and RA model group were given the same volume of normal saline by gavage, and each GSE group was given 10, 50, 100 µg/mL GSE solution by gavage, respectively, with a gavage volume of 0.2 mL/10 g body weight, once a day for 48 consecutive hours.

2.3.2. Isolation and culture of synoviocytes

Twenty-four hours after the last administration, the mice were sacrificed by cervical dislocation. The ankle synovial tissues of mice were separated under sterile conditions, rinsed 3 times with phosphate buffer, cut into pieces of about 1 mm³, digested with 0.25% trypsin in a 37°C incubator for 30 minutes, and then the digestion was terminated with DMEM medium containing 10% fetal bovine serum. The mixture was filtered through a 200-mesh sieve, and the filtrate was collected and centrifuged at 1,000 r/min for 5 minutes.

The supernatant was discarded, and the cells were resuspended in DMEM complete medium. The cell concentration was adjusted to 1×10^6 cells/mL, inoculated into 6-well culture plates, and cultured in a 37°C, 5% CO₂ incubator. Subsequent experiments were performed when the cells adhered and fused to 70–80%.

2.3.3. Detection of mRNA expression of NF-κB/p65 and inflammatory factors by qRT-PCR

Synoviocytes cultured in each group were collected, and total cellular RNA was extracted using an RNA extraction kit. The purity and concentration of RNA were detected by a nucleic acid protein detector [8]. RNA was reverse-transcribed into cDNA according to the instructions of the qRT-PCR kit, and real-time fluorescent quantitative PCR amplification was performed using cDNA as a template [9].

PCR reaction system: 2×SYBR Green Mix 10 µL, upstream and downstream primers 0.5 µL each, cDNA template 2 µL, RNase-free H₂O 7 µL, total system 20 µL. Reaction conditions: pre-denaturation at 95°C for 30 s; denaturation at 95°C for 5 s, annealing at 60°C for 30 s, 40 cycles; final extension at 72°C for 5 min. Using β-actin as the internal reference gene, the relative expression of the target gene was calculated by the 2^{-(ΔΔCt)} method. The primer sequences of each gene are shown in **Table 1**.

Table 1. Primer sequences

Gene name	Forward primer (5'→3')	Reverse primer (5'→3')	Product length (bp)
<i>NF-κB/p65</i>	GAGCAAGAGCAAGAAGATGG	GCTGGTGATGGTGATGGTAA	215
<i>TNF-α</i>	CCCTCACACTCAGATCATCTTCT	GCTACGACGTGGGCTACAG	198
<i>IL-6</i>	CCAGAGTCATTGAGAGCAATG	TTGGATGGTCTTGGTCCTTA	203
<i>IL-1β</i>	GAAATGCCACCTTTTGACAGTG	TGGATGCTCTCATCAGGACAG	220
<i>β-actin</i>	GGCTGTATTCCCCTCCATCG	CCAGTTGGTAACAATGCCATGT	189

2.3.4. Detection of NF-κB/p65 protein expression by Western blot

Synoviocytes in each group were collected, lysed on ice for 30 minutes with RIPA lysis buffer (containing

1% protease inhibitor), centrifuged at 12,000 r/min, 4°C for 15 minutes, and the supernatant was collected. Protein concentration was determined by BCA method. Equal amounts of protein (50 µg/well) were subjected to SDS-PAGE electrophoresis.

After electrophoresis, the protein was transferred to a PVDF membrane, blocked with 5% skimmed milk at room temperature for 2 hours, and incubated with primary antibodies (NF-κB/p65 1:1,000, β-actin 1:2,000) overnight at 4°C. The membrane was washed 3 times with TBST for 10 minutes each, incubated with HRP-labeled secondary antibody (1:5,000) at room temperature for 1 hour, and washed 3 times with TBST again.

Development was performed using an ECL chemiluminescence kit, and images were taken with a gel imaging system. Using β-actin as an internal reference, the gray value of the target protein band was analyzed with ImageJ software, and the relative expression was calculated ^[10].

2.3.5. Detection of inflammatory factor secretion by ELISA

The culture supernatant of synoviocytes in each group was collected, and the operation was performed according to the instructions of the TNF-α, IL-6, and IL-1β ELISA detection kits. Standard wells and sample wells were set up, and the absorbance (OD value) at 450 nm was measured on a microplate reader after adding the corresponding reagents. The concentration of each inflammatory factor was calculated according to the standard curve.

2.3.6. Observation of synovial tissue pathological morphology by HE staining

The ankle synovial tissues of mice in each group were taken, fixed with 4% paraformaldehyde for 24 hours, routinely dehydrated, cleared, waxed, embedded, and made into 5 µm-thick paraffin sections. HE staining was performed, and neutral gum was used for sealing. The pathological morphology of synovial tissues was observed under an inverted microscope, including synoviocyte proliferation, inflammatory cell infiltration, tissue edema, etc., and pathological scoring was performed ^[11].

2.4. Statistical analysis

SPSS 26.0 statistical software was used for data analysis. Measurement data were expressed as mean ± standard deviation (SD). One-way ANOVA was used for comparison among multiple groups, and LSD-t test was used for pairwise comparison between groups. $P < 0.05$ was considered statistically significant, and $P < 0.01$ was considered extremely statistically significant.

3. Results

3.1. Effects of GSE on arthritis index in RA mice

Mice in the normal control group had no joint swelling or deformity, and the AI score was 0. Mice in the model group began to show symptoms such as joint swelling and limited activity 2–3 weeks after booster immunization, and the AI score gradually increased. Four weeks after modeling, the AI score was ≥ 4 , and the modeling success rate was 84% (42/50). A total of 50 mice were finally included in the experiment (10 in the normal control group, 10 in the model group and each GSE dose group).

Compared with the RA model group, the joint swelling symptoms of mice in each GSE intervention group were significantly relieved, and the AI score was significantly reduced ($P < 0.01$), and the AI score of the high-dose GSE group was the lowest ($P < 0.01$), as shown in **Table 2**.

Table 2. Comparison of arthritis index scores in mice of each group (mean \pm SD, $n = 10$, score)

Group	AI score
Normal control group	0.00 \pm 0.00
RA model group	6.23 \pm 0.58**
Low-dose GSE group	4.15 \pm 0.42*#
Medium-dose GSE group	2.87 \pm 0.35**#
High-dose GSE group	1.52 \pm 0.28*** \triangle

Note: Compared with the normal control group, $P < 0.01$; compared with the RA model group, * $P < 0.05$, ** $P < 0.01$; compared with the low-dose GSE group, $\triangle P < 0.01$; compared with the medium-dose GSE group, $\blacktriangle P < 0.01$ (the same below).

3.2. Effects of GSE on NF- κ B/p65 mRNA and protein expression in synoviocytes of RA mice

qRT-PCR results showed that compared with the normal control group, the relative expression of NF- κ B/p65 mRNA in synoviocytes of mice in the RA model group was significantly increased ($P < 0.01$); compared with the RA model group, the relative expression of NF- κ B/p65 mRNA in each GSE intervention group was significantly decreased ($P < 0.01$), and showed a gradual downward trend with the increase of GSE concentration. The down-regulation effect of the high-dose GSE group was the most significant ($P < 0.01$).

Western blot results were consistent with qRT-PCR results. Compared with the normal control group, the relative expression of NF- κ B/p65 protein in synoviocytes of mice in the RA model group was extremely significantly increased ($P < 0.01$); the expression level of NF- κ B/p65 protein in each GSE intervention group was significantly lower than that in the RA model group ($P < 0.01$) in a dose-dependent manner, and the effect of the high-dose GSE group was the best ($P < 0.01$).

3.3. Effects of GSE on mRNA expression of downstream inflammatory factors in synoviocytes of RA mice

Compared with the normal control group, the relative mRNA expressions of TNF- α , IL-6, and IL-1 β in synoviocytes of mice in the RA model group were extremely significantly increased ($P < 0.01$); compared with the RA model group, the mRNA expression levels of the above inflammatory factors in each GSE intervention group were significantly down-regulated ($P < 0.05$ or $P < 0.01$). The down-regulation effect of the high-dose GSE group was significantly better than that of the low- and medium-dose groups ($P < 0.01$), and the medium-dose group was better than the low-dose group ($P < 0.01$).

3.4. Effects of GSE on the secretion of inflammatory factors in the culture supernatant of synoviocytes of RA mice

ELISA results showed that the concentrations of TNF- α , IL-6, and IL-1 β in the culture supernatant of synoviocytes of mice in the normal control group were very low; compared with the normal control group, the concentrations of each inflammatory factor in the RA model group were extremely significantly increased ($P < 0.01$); compared with the RA model group, the concentrations of inflammatory factors in each GSE intervention group were significantly decreased ($P < 0.05$ or $P < 0.01$), and gradually decreased with the increase of GSE concentration, showing an obvious dose-effect relationship ($P < 0.01$).

3.5. Effects of GSE on the pathological morphology of synovial tissue of RA mice

Compared with the RA model group, the pathological injury of synovial tissue in each GSE intervention

group was significantly improved, the degree of synoviocyte proliferation was reduced, inflammatory cell infiltration was decreased, tissue edema was subsided, and the pathological score was significantly reduced ($P < 0.01$); among them, the synovial tissue morphology of the high-dose GSE group was close to normal, with only a small amount of inflammatory cell infiltration, and the pathological score was the lowest ($P < 0.01$). See **Table 3**.

Table 3. Comparison of synovial tissue pathological scores in mice of each group (mean \pm SD, $n = 10$, score)

Group	Pathological score
Normal control group	0.32 ± 0.11
RA model group	$7.85 \pm 0.62^{**}$
Low-dose GSE group	$5.12 \pm 0.45^{*}\#$
Medium-dose GSE group	$3.05 \pm 0.38^{**}\#$
High-dose GSE group	$1.26 \pm 0.21^{**}\# \triangle \blacktriangle$

4. Discussion

Rheumatoid arthritis is characterized by chronic inflammation and abnormal proliferation of synovium. Abnormal activation of the NF- κ B signaling pathway is a key molecular mechanism mediating synovial inflammation^[12]. Activation of this pathway can significantly promote the massive expression and release of pro-inflammatory factors such as TNF- α , IL-6, and IL-1 β , triggering an inflammatory cascade, aggravating synovial hyperplasia and destruction of articular cartilage and bone. Targeted inhibition of the NF- κ B pathway has become an important research direction for the anti-inflammatory treatment of RA^[13].

The main active component of GSE is proanthocyanidins, which have strong antioxidant and anti-inflammatory activities. Previous studies have confirmed that GSE can reduce the injury of various inflammatory diseases by regulating the NF- κ B pathway, but its regulatory effect and dose-effect on NF- κ B in RA synoviocytes remain unclear^[14].

The results of this study showed that GSE could down-regulate the mRNA and protein expression of NF- κ B/p65 in synoviocytes of RA mice in a dose-dependent manner, and the high-dose inhibition effect was the most significant, which could directly block the activation of the NF- κ B pathway. At the same time, GSE could significantly reduce the transcription and secretion levels of downstream inflammatory factors, alleviate the pathological injury of synovial tissue, reduce the arthritis index, and improve joint swelling symptoms. Compared with traditional antirheumatic drugs, GSE has the advantages of high safety, wide sources, and small side effects, and has the potential to be developed as an adjuvant natural drug for RA^[15].

5. Conclusion

In conclusion, grape seed extract can inhibit the expression of NF- κ B in synoviocytes of RA mice in a dose-dependent manner, thereby down-regulating the release of its downstream inflammatory factors TNF- α , IL-6, and IL-1 β , reducing the inflammatory response and pathological injury of synovial tissue, and improving the joint symptoms of mice. Its mechanism may be related to the regulation of the NF- κ B signaling pathway. Grape seed extract is expected to be a potential natural drug for the treatment of RA. This study provides new experimental evidence and research ideas for the natural drug therapy of RA, and also lays a foundation for

the clinical application and high-value utilization of grape seed extract.

Funding

This paper was the research result of the 2024 University-level Science and Technology Project of Qilu Institute of Technology (Project Name: Experimental Study on the Effects of Grape Seed Extract on NF- κ B Expression in Synoviocytes of RA Mice; Project No.: QIT24NN0724).

Disclosure statement

The authors declare no conflict of interest.

References

- [1] Xie Y, Wang N, Cao NN, et al., 2025, Grape Seed Extract Inhibits Chondrocyte Apoptosis by Regulating miR-539-5p in Rat Growth Plate. *Chinese Journal of Integrated Traditional and Western Medicine*, 45(04): 447–453.
- [2] Sun Z, Liu YQ, Dong H, et al., 2023, Effects of Grape Seed Extract on Endocrine Metabolism in Menopausal Model Mice. *Journal of Medical College of Yanbian University*, 46(04): 252–254.
- [3] Li D, Xu SL, Wang Y, et al., 2023, Protective Mechanism of Grape Seed Extract on Cerebral Ischemia-Reperfusion Injury in Rats through NF- κ B/TLR4 Signaling Pathway. *Chinese Journal of Integrative Medicine on Cardio-Cerebrovascular Disease*, 21(19): 3527–3531.
- [4] Lei JQ, Tian YX, Li ZG, et al., 2023, Molecular Mechanism of Grape Seed Extract Proanthocyanidins Inhibiting Proliferation, Migration and Invasion of Hepatocellular Carcinoma Hep3B Cells by Regulating EMT via LncRNA NBR2/miR-650. *Chinese Journal of Gerontology*, 43(17): 4307–4312.
- [5] Zhang SS, Wang N, Li YJ, 2024, Grape Seed Extract Inhibits Apoptosis of Rat Growth Plate Chondrocytes and Promotes Tibial Growth. *Chinese Journal of Tissue Engineering Research*, 28(16): 2494–2499.
- [6] Zhang ZX, Guo JQ, Zhu CH, 2023, Study on Antioxidant Effect of Grape Seed and Vitamin C on D-Galactose Model Mice. *China Food Additives*, 34(01): 208–213.
- [7] Sun J, Zou YJ, Sun X, et al., 2024, Study on Anti-*Helicobacter pylori* Effect and Mechanism of Grape Seed Extract and Fucoidan Composition. *Food and Fermentation Industries*, 50(18): 279–283.
- [8] Ding QJ, Niu JP, Ding HL, et al., 2025, Analysis of Molecular Action Path of Grape Seed Extract Regulating NF- κ B. *Sino-Foreign Food Industry*, (21): 79–81.
- [9] Feng SL, Tan XG, 2025, Effects of Red Bean Coix Seed Fulxia Dampness-Removing and Detoxification Tea Combined with Grape Seed Extract on People with Phlegm-Dampness Constitution. *Western Journal of Traditional Chinese Medicine*, 38(12): 126–128.
- [10] Jia SZ, 2025, Evaluation Test of Antioxidant Function of Only 100® Grape Seed Extract Tablets in Human Trial. *Shanghai Light Industry*, (01): 61–63.
- [11] Ma J, Li T, Lin L, et al., 2024, Biological Function of Grape Seed Extract and Its Application in Livestock and Poultry Production. *Chinese Journal of Animal Nutrition*, 36(09): 5441–5450.
- [12] Li JF, Diao JJ, Chen ZH, et al., 2024, Analysis of Chemical Constituents of Grape Seed Extract and Determination of Multi-Component Content Based on UHPLC-MS/MS. *Food and Fermentation Industries*, 50(20): 303–312.
- [13] Ding QJ, Lv JW, Ding HL, et al., 2024, Experimental Study on Inhibitory Effect of Grape Seed Extract on

Bacterial Biofilm. Sino-Foreign Food Industry, (11): 49–51.

- [14] Geng Z, Fu JL, Guo WT, 2023, Preparation and Antibacterial Property of Grape Seed Extract Composite Film. Hubei Agricultural Sciences, 62(11): 118–124 + 130.
- [15] Zhou XH, 2023, Research Progress on Nutritional Composition and Biological Function of Grape Seed Extract. Food and Machinery, 39(07): 228–233 + 240.

Publisher's note

Bio-Byword Scientific Publishing remains neutral with regard to jurisdictional claims in published maps and institutional affiliations.

Comparison of the Clinical Effect of Collagenase Lysis with Different Administration Routes in Treating Lumbar Disc Herniation

Junhong Liu

Department of Pain, Liuzhou People's Hospital Affiliated to Guangxi Medical University, Liuzhou 545006, Guangxi, China

Copyright: © 2026 Author(s). This is an open-access article distributed under the terms of the Creative Commons Attribution License (CC BY 4.0), permitting distribution and reproduction in any medium, provided the original work is cited.

Abstract: *Objective:* To observe and discuss the clinical effect of collagenase lysis in the treatment of lumbar disc herniation through different administration routes. *Methods:* Sixty patients with lumbar disc herniation admitted to Liuzhou People's Hospital from February 2023 to February 2024 were selected, including 31 males and 29 females. They were divided into A and B groups according to the random number table method. Group A was injected through sacral hiatus route combined with intervertebral foramen safety triangle route ($n = 30$), and Group B was injected only through sacral hiatus route ($n = 30$). The VAS score, ODI index, and the efficacy of Macnab were observed before operation, 3 days, 1 month, and 3 months after operation, and the results were summarized and compared. *Results:* Compared with Group B (only through the sacral hiatus route), the VAS score, ODI index, and the efficacy evaluation of Macnab in Group A (through the sacral hiatus route combined with the intervertebral foramen safety triangle route) were significantly better, and the differences were statistically significant ($P < 0.05$). *Conclusion:* Multi-path collagenase lysis is more effective than single-path collagenase lysis.

Keywords: Puncture; Collagenase; Clinical observation; Lumbar disc herniation

Online publication: May 14, 2026

1. Introduction

Lumbar disc herniation (LDH) is commonly encountered in clinical pain departments and is generally considered a degenerative spinal disease. Epidemiological surveys indicate that LDH is highly prevalent among middle-aged and elderly populations, with low back pain and sciatica being its most common concurrent symptoms, significantly impacting the daily lives of elderly patients and thereby drawing considerable attention from scientific research in geriatric medicine, geriatric nursing, and other geriatric healthcare fields^[1]. As times change, the demographic most affected by LDH is gradually becoming younger, no longer limited to the middle-aged and elderly. Moreover, patients discharged after treatment

for lumbar disc herniation often face a lengthy treatment cycle and incur substantial costs during treatment, posing a considerable burden on the social healthcare system ^[2]. Collagenase chemonucleolysis (CCNL) is a minimally invasive interventional treatment commonly used in clinical settings for LDH patients who do not respond well to conventional conservative treatments. Since its introduction in 1968, CCNL has garnered widespread attention due to its minimal invasiveness, effectiveness, and relatively low cost. However, due to the development of new technologies and commercial competition, its application has gradually decreased abroad. In contrast, in China, continuous research and improvement of this method have led to its widespread use as a common treatment for LDH in clinical practice ^[3]. Depending on the injection route, CCNL can be classified into various types. This study takes the injection of collagenase chemonucleolysis through sacral hiatus route combined with intervertebral foramen safe triangle route as an example. By comparing the clinical effects of combined injection and the sacral hiatus route alone, we explore the impact of different injection routes on the clinical efficacy of CCNL.

2. Materials and methods

2.1. General information

This study selected 60 patients with LDH admitted to Liuzhou People's Hospital from February 2023 to February 2024, comprising 31 males and 29 females, aged between 50 and 70 years. They were divided into two groups, A and B, using a random number method. Patients in Group A underwent catheter injection surgery via the sacral hiatus route combined with the intervertebral foramen safe triangle route ($n = 30$), while patients in Group B underwent catheter injection surgery via the anterior space approach through sacral hiatus puncture ($n = 30$). The physical conditions of the two groups of patients were similar, with no significant differences in various data ($P > 0.05$), indicating comparability. See **Table 1**.

This study has been approved by the Ethics Committee of Liuzhou People's Hospital, and all patients fully understood the research content and signed informed consent forms.

Table 1. General information of the two groups of patients

Group	Number of cases	Age (years)	Male/Female	Body mass index (kg/m ²)	ASA grade ratio (I/II)	Operation time (min)	Medical history (years)	Lesion location	
								L5–S1	L4–5
A	30	59.6 ± 5.3	16/14	21.27 ± 2.4	9/21	48.5 ± 7.0*	14.5 ± 3.2	5	25
B	30	60.1 ± 5.3	15/15	22.0 ± 2.2	1/2	35.4 ± 4.5	14.6 ± 2.5	6	24
<i>t</i>	/	-3.65	/	-1.24	/	8.65	-0.18	/	/
<i>P</i>	/	0.716	/	0.220	/	<0.01	0.859	/	/

2.2. Diagnostic indicators

Based on the *Guidelines for Diagnosis, Treatment, and Rehabilitation Management of Lumbar Disc Herniation* ^[4], pain scores and various indicators were recorded and compared before surgery, as well as 3 days, 1 month, and 3 months after surgery. The indicators to be compared include: the Oswestry Disability Index (ODI), Visual Analog Scale (VAS), and the modified Macnab criteria for evaluating therapeutic efficacy.

2.3. Inclusion criteria

- (1) Meet the diagnostic criteria for mild to moderate lumbar disc herniation with radiculopathy as confirmed by MRI examination ^[5];
- (2) Aged between 50 and 70 years old;
- (3) Able to communicate normally with medical staff and accurately describe pain and symptoms;
- (4) Able to actively cooperate with treatment and complete all measures in the study;
- (5) No severe allergic reactions to medications used in surgery and acceptable for collagenase chemonucleolysis treatment;
- (6) Informed consent obtained from both the patient and their family for participation in this study.

2.4. Exclusion criteria

- (1) Patients with sudden worsening of symptoms and signs, presenting with motor dysfunction and cauda equina syndrome;
- (2) Patients with other major diseases such as cancer, hypertension, coronary heart disease, etc.;
- (3) Patients who have previously received other spinal interventional treatments;
- (4) Patients with infections or organ failure leading to organ dysfunction;
- (5) Patients with abnormal blood coagulation function who cannot undergo surgery;
- (6) Patients who withdraw from the study for various reasons.

2.5. Instruments and medications

2.5.1. Instruments

- (1) Medical angiography X-ray machine (DSA, Siemens Healthineers, Arsis One);
- (2) 18-gauge epidural needle (BD, USA, State Food and Drug Administration Import License No. 2005-3153190).

2.5.2. Medications

- (1) Collagenase for injection (Yuanda Life Sciences Co., Ltd., National Medical Products Administration Approval No. H10960178);
- (2) 1% lidocaine hydrochloride injection (Hubei Tiansheng Pharmaceutical Co., Ltd., National Medical Products Administration Approval No. H42021839);
- (3) Dexamethasone sodium phosphate for injection (Cisen Pharmaceutical Co., Ltd., National Medical Products Administration Approval No. H37021969);
- (4) Hismanal (Loratadine tablets; Chengdu Yongkang Pharmaceutical Co., Ltd., National Medical Products Administration Approval No. H20051618);
- (5) Iodotren injection (contrast agent; Yangtze River Pharmaceutical Group Co., Ltd., National Medical Products Administration Approval No. H10970358);
- (6) Betamethasone sodium phosphate for injection (Ma'anshan Fengyuan Pharmaceutical Co., Ltd., National Medical Products Administration Approval No. H20060968).

2.6. Surgical methods

Group A: Catheter injection surgery via the sacral hiatus pathway combined with the safe triangle pathway of the intervertebral foramen;

Group B: Catheter injection surgery with catheter placement in the anterior epidural space via the sacral hiatus puncture approach.

2.6.1. Preoperative preparation

Both groups underwent the same preoperative preparation, including routine examinations to ensure normal vital signs and suitability for surgery. Patients received an intravenous injection of 5 mg dexamethasone before surgery.

2.6.2. Procedure

Group A: (1) Puncture point localization: The patient was placed in a prone position. Under DSA guidance, the optimal puncture point was identified, and the puncture angle and depth were calculated and marked. (2) Local anesthesia with 1% lidocaine was administered. Using an 18-gauge epidural needle, under DSA guidance, the needle was inserted at the predetermined optimal puncture point, adjusting the angle as needed to reach the predetermined depth. (3) 2 ml of contrast agent was injected, and anteroposterior and lateral vertebral canal angiography images were taken to confirm catheter position (see **Figure 1**). (4) After confirming that the needle tip was located in the anterior epidural space, a catheter was placed (or the puncture needle was oriented towards the intervertebral foramen with its spoon-shaped side facing it). 3 ml of 1.3% lidocaine was injected, and the patient's response was observed for 10–15 minutes. If no spinal anesthesia occurred, collagenase for injection (4 ml of collagenase diluent dissolving 1,200 U of collagenase powder) was injected (see **Figure 2**). (5) After observing for 1 hour postoperatively for no allergic reactions or other complications, the patient was instructed to maintain a supine position for approximately 8 hours, with the body slightly tilted forward and the affected side down. Absolute bed rest was required for at least 24 hours.

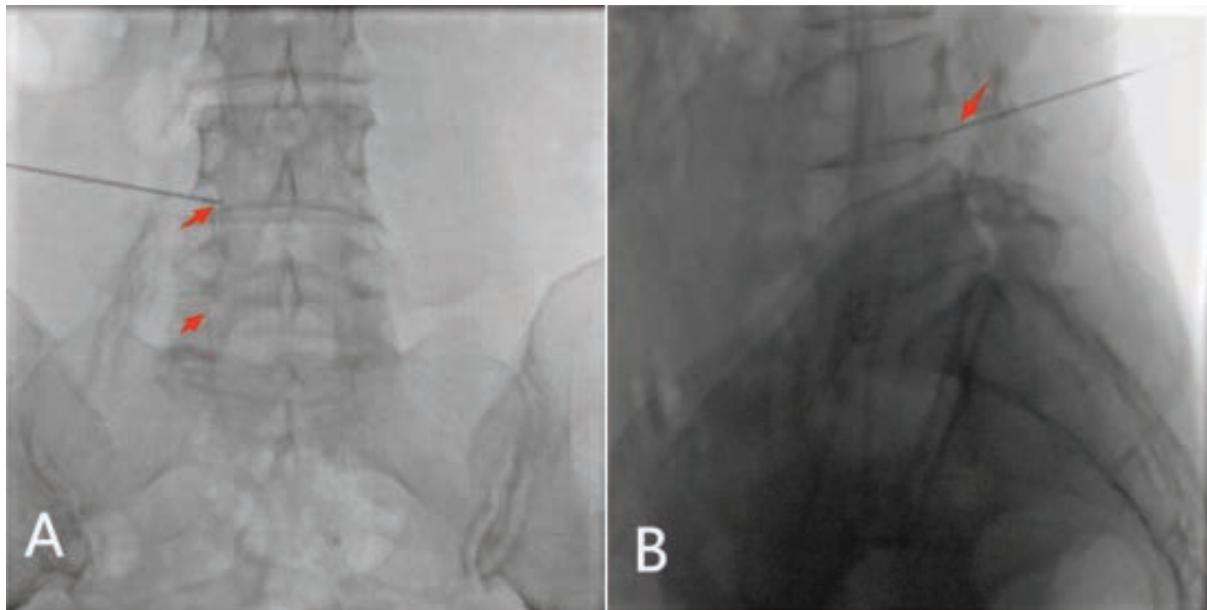


Figure 1. Sacral hiatus route combined with intervertebral foramen safety triangle route

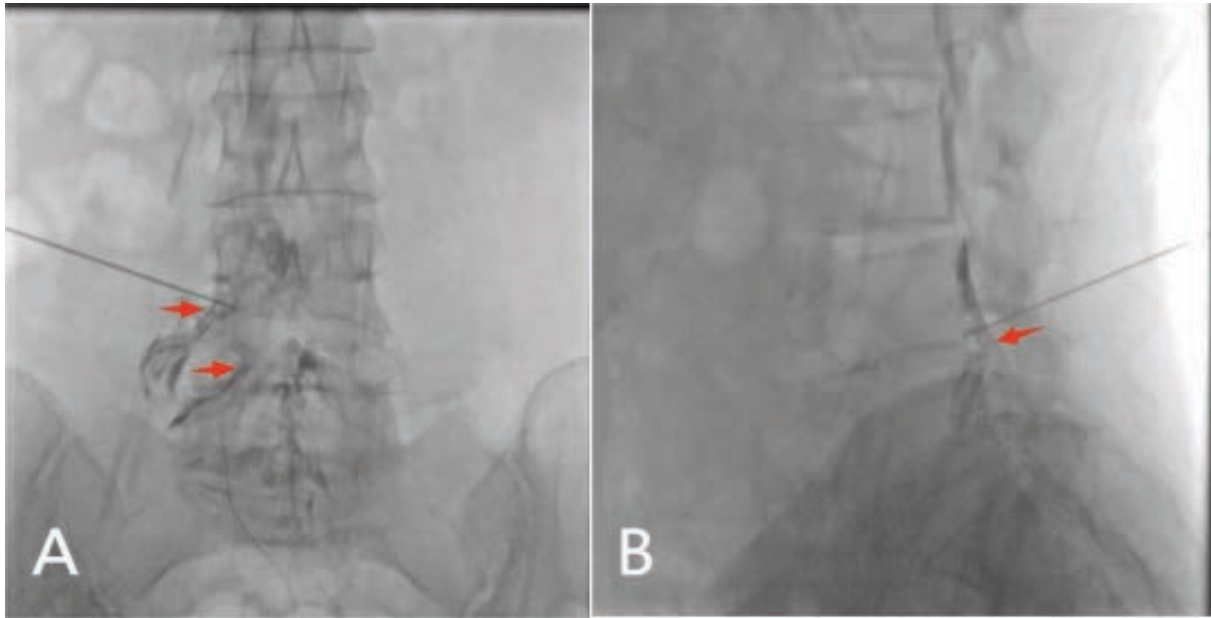


Figure 2. Intraoperative imaging (A: Puncture needle to target, nerve root development; B: Anterior epidural space imaging)

Group B: (1) Puncture point localization: Under DSA guidance, identified the puncture point at the sacral hiatus, calculated the puncture angle and depth, and marked them accordingly; (2) Disinfected the skin at the affected area and draped it with a sterile towel. Using an 18-gauge beveled intradiscal needle, punctured through the sacrococcygeal ligament to reach the periosteum. The needle was initially inserted perpendicular to the skin at a 90° angle, then adjusted to tilt caudally, forming a 15–30° angle upwards with the skin. The needle was inserted approximately 5–7 cm into the skin, with the puncture depth exceeding the plane of the posterior. See **Figures 3** and **4**.

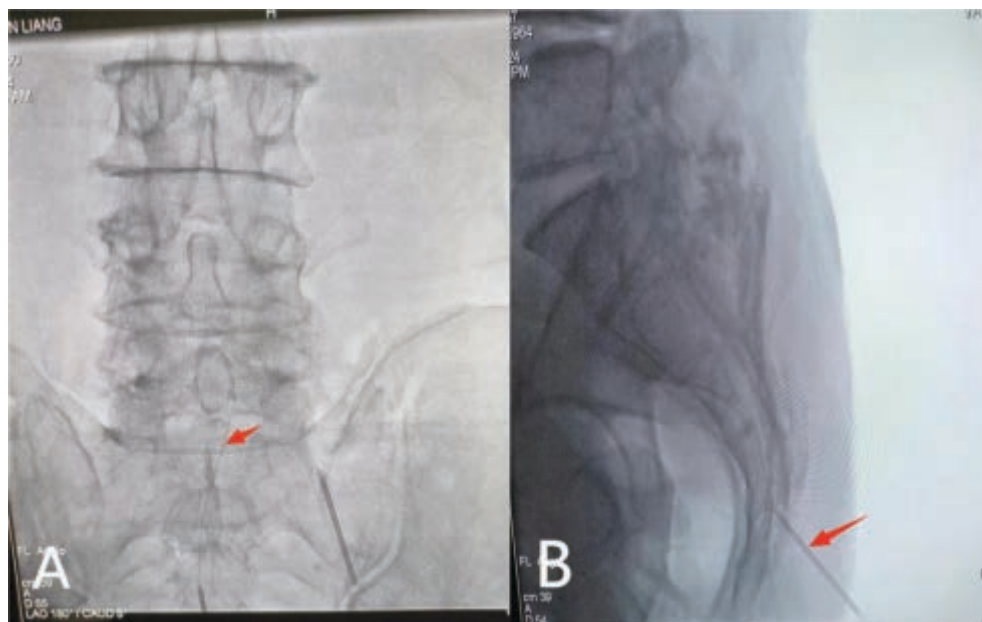


Figure 3. Gap before sacral hiatus puncture approach (A: Right position; B: Lateral position)

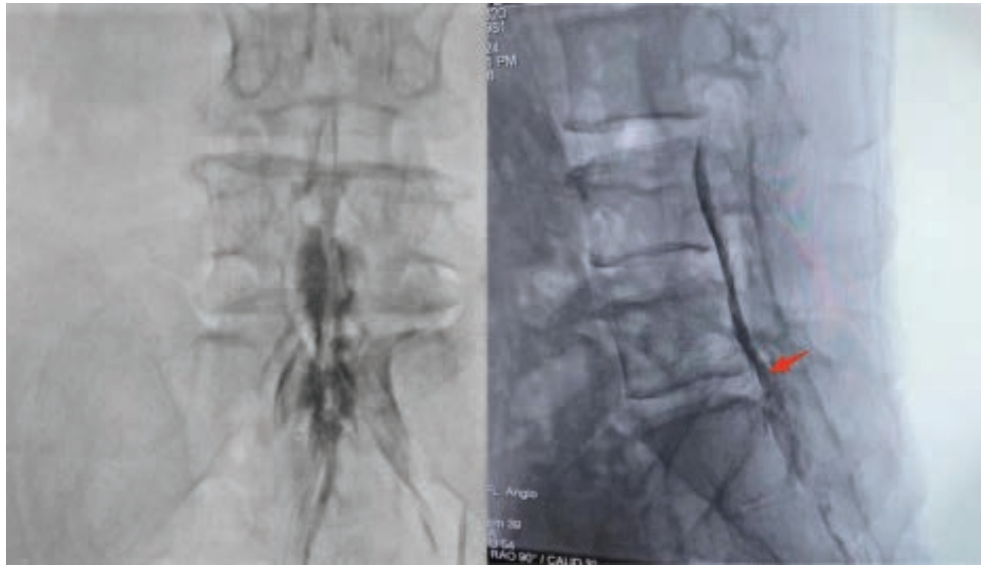


Figure 4. Puncture imaging of sacral hiatus (lumbar L5/S1)

2.6.3. Prevention and emergency management of complications

Early prevention: After CCNL surgery, complications such as nervous system edema, intervertebral space infection, and deep vein thrombosis of the lower extremities are prone to occur^[6]. To ensure the safety of the surgery, it is necessary to strictly control the patient's diet before the operation and provide relevant bowel training. Studies have shown that the patient's psychological state has a certain impact on postoperative recovery, so professional psychological counseling should be provided before surgery. The patient's vital signs should be closely monitored during the puncture process. After surgery, infrared radiation should be applied locally while keeping the affected area clean and dry. Medications should be administered strictly according to medical advice to prevent postoperative infection, and patients should be assisted in performing functional exercises safely and correctly^[7].

Emergency management: Accidental entry into the subarachnoid space is an emergency that may occur during the collagenase dissolution treatment process. Experiments have shown that accidental entry into the subarachnoid space carries a certain risk of spinal cord injury, leading to lower limb paralysis and causing serious consequences. Therefore, once it occurs, the following emergency measures should be taken immediately: (1) The characteristic of accidental entry into the subarachnoid space is that the cerebrospinal fluid in the cavity is pink or bloody. If the puncture point is selected at or below the collagenase injection level and this characteristic appears, a diagnosis can be made. First, withdraw 10 ml of cerebrospinal fluid, then inject 10 ml of normal saline, wait for 2 minutes, and repeat the above operation until the cerebrospinal fluid becomes clear. The replacement can be repeated once after 24 hours, generally replacing more than 50 ml. (2) Factors such as advanced age with spinal stenosis, high-level herniation causing obstruction, cerebrospinal fluid leakage, and arachnoid adhesion may all prevent cerebrospinal fluid replacement. If relevant situations occur, replacement can be performed under CT guidance. The patient should lie prone on the diagnostic bed, and the needle should be inserted at the L3–4; L4–5 ligamentum flavum area, with the needle tip placed in the center of the dural sac. At this time, fluid overflow can be seen at the needle tip, confirming entry into the subarachnoid space. Inject 10 ml of normal saline with a syringe, remove the

syringe, wait for about 10 ml to automatically overflow, continue to inject 10 ml of saline, and repeat the above operation 5–6 times.

2.6.4. Postoperative follow-up and observation

Patients were followed up after surgery, and their indicators and recovery status were recorded at three time points: 3 days, 1 month, and 3 months after surgery.

2.7. Observation of treatment efficacy and safety

2.7.1. Efficacy evaluation

- (1) The Visual Analog Scale (VAS) is used to assess the degree of pain. Patients mark their pain intensity on a scale according to their own perception, with scores ranging from 0 to 10, increasing from painless to severe pain. The higher the score, the more severe the pain. A score of 0 is considered painless, and 10 is the highest level of unbearable pain. A mean score of 2.57 ± 1.54 is considered mild, 5.18 ± 1.41 is considered moderate, and 8.41 ± 1.35 is considered severe.
- (2) The modified Macnab method is used to evaluate the efficacy, which is divided into four grades: excellent, good, fair, and poor, based on the degree of pain relief and recovery of daily life activities. “Excellent” means that the patient can resume normal life without medication and has no pain symptoms; “good” means significant improvement, with the patient’s life basically returning to normal; “fair” means that symptoms have improved but still affect life to a certain extent; “poor” means no significant improvement. Poor results are considered ineffective treatment. The results are summarized and the proportion is calculated.
- (3) The Oswestry Disability Index (ODI) is used to evaluate functional impairment. Patients fill out a test form with a maximum possible score of 50, with 5 points for each question. The ODI index is calculated using the formula $(\text{actual score}/\text{maximum possible score}) \times 100\%$ (if any questions are left unanswered, the maximum possible score should be reduced by the score of the unanswered questions). The higher the score, the more severe the functional impairment^[8].

2.7.2. Safety observation

- (1) Observe whether the patient experiences any discomfort in the digestive system, nervous system, immune system, etc., after surgery, and whether the vital signs are normal.
- (2) Observe whether the patient develops complications such as infection or adverse reactions such as allergies after surgery.

2.8. Statistical analysis methods

Data were processed using SPSS 27.1 statistical software. Measurement data were tested using the two independent sample t-test and expressed as mean \pm standard deviation (SD). Count data were tested using the χ^2 test, with a test standard of $\alpha = 0.05$. If $P < 0.05$, the difference was considered statistically significant.

3. Results

3.1. Pain status

The preoperative P -value of $0.250 > 0.05$ for the two groups of patients indicates no significant difference

in preoperative VAS scores. The VAS scores of both Group A and Group B on the 3rd day, 1 month, and 3 months after surgery were significantly lower than those before surgery ($P < 0.05$). The VAS scores of both groups dropped below 3 at 3 months after surgery, indicating that both groups had effective treatment with good results. Comparing the VAS scores of Group A and Group B, the preoperative average score of Group A was 8.6 ± 0.3 , which dropped to 1.5 ± 0.3 at 3 months after surgery; the preoperative average score of Group B was 8.5 ± 0.3 , which was 1.9 ± 0.3 at 3 months after surgery. The improvement rate of postoperative scores in Group A was slightly higher than that in Group B (see **Table 2**).

Table 2. Comparison of VAS scores before and after surgery in the two groups of patients (mean \pm SD)

Group	Number of cases	Preoperative	3rd day postoperative	1 month postoperative	3 months postoperative
A	30	8.6 ± 0.3	2.7 ± 0.3	1.8 ± 0.3	1.5 ± 0.3
B	30	8.5 ± 0.3	3.1 ± 0.2	2.2 ± 0.3	1.9 ± 0.3
<i>t</i>	/	1.161	-7.198	-5.541	-8.591
<i>P</i>	/	0.250	<0.01	<0.01	<0.01

* $P < 0.05$ compared with preoperative values

3.2. Functional impairment status

The preoperative P -value of $0.937 > 0.05$ for the two groups of patients indicates no significant difference in preoperative ODI scores. The ODI scores on the 3rd day, 1 month, and 3 months after surgery were significantly lower than those before surgery in both groups ($P < 0.05$). The ODI scores of both groups dropped below 45 at 3 months after surgery, indicating that both groups had effective treatment with good results. Comparing the ODI scores of Group A and Group B, the preoperative average score of Group A was 76.4 ± 6.8 , which dropped to 20.6 ± 2.3 at 3 months after surgery; the preoperative score of Group B was 76.6 ± 6.1 , which decreased to 23.4 ± 2.3 at 3 months after surgery. The improvement rate of postoperative scores in Group A was slightly higher than that in Group B (see **Table 3**).

Table 3. Comparison of ODI scores before and after surgery in the two groups of patients (mean \pm SD)

Group	Number of cases	Preoperative	3rd day postoperative	1 month postoperative	3 months postoperative
A	30	76.4 ± 6.8	34.5 ± 3.3	23.8 ± 3.8	20.6 ± 2.3
B	30	76.6 ± 6.1	40.5 ± 3.0	26.5 ± 2.8	23.4 ± 2.3
<i>t</i>	/	-0.80	-6.937	-3.216	-4.853
<i>P</i>	/	0.937	<0.01	<0.05	<0.01

* $P < 0.05$ compared with preoperative values

3.3. Modified Macnab efficacy assessment

At the 3-month postoperative Macnab efficacy evaluation, Group A had 0 cases classified as “poor,” with an excellent and good rate of 100%; Group B had 1 case classified as “poor,” with an excellent and good rate of 76.7%. Furthermore, compared with Group B, Group A had a higher number of cases rated as “excellent” and “good,” indicating a more favorable treatment outcome in Group A (see **Table 4**, **Figures 5** and **6**).

Table 4. Efficacy evaluation of the two groups of patients at 3 months postoperatively

Group	Number of cases	Excellent	Good	Fair	Poor	Excellent and good rate (%)
A	30	20	10	0	0	100
B	30	15	8	6	1	76.7
χ^2	/	/	/	/	/	10.643
<i>P</i>	/	/	/	/	/	<0.05

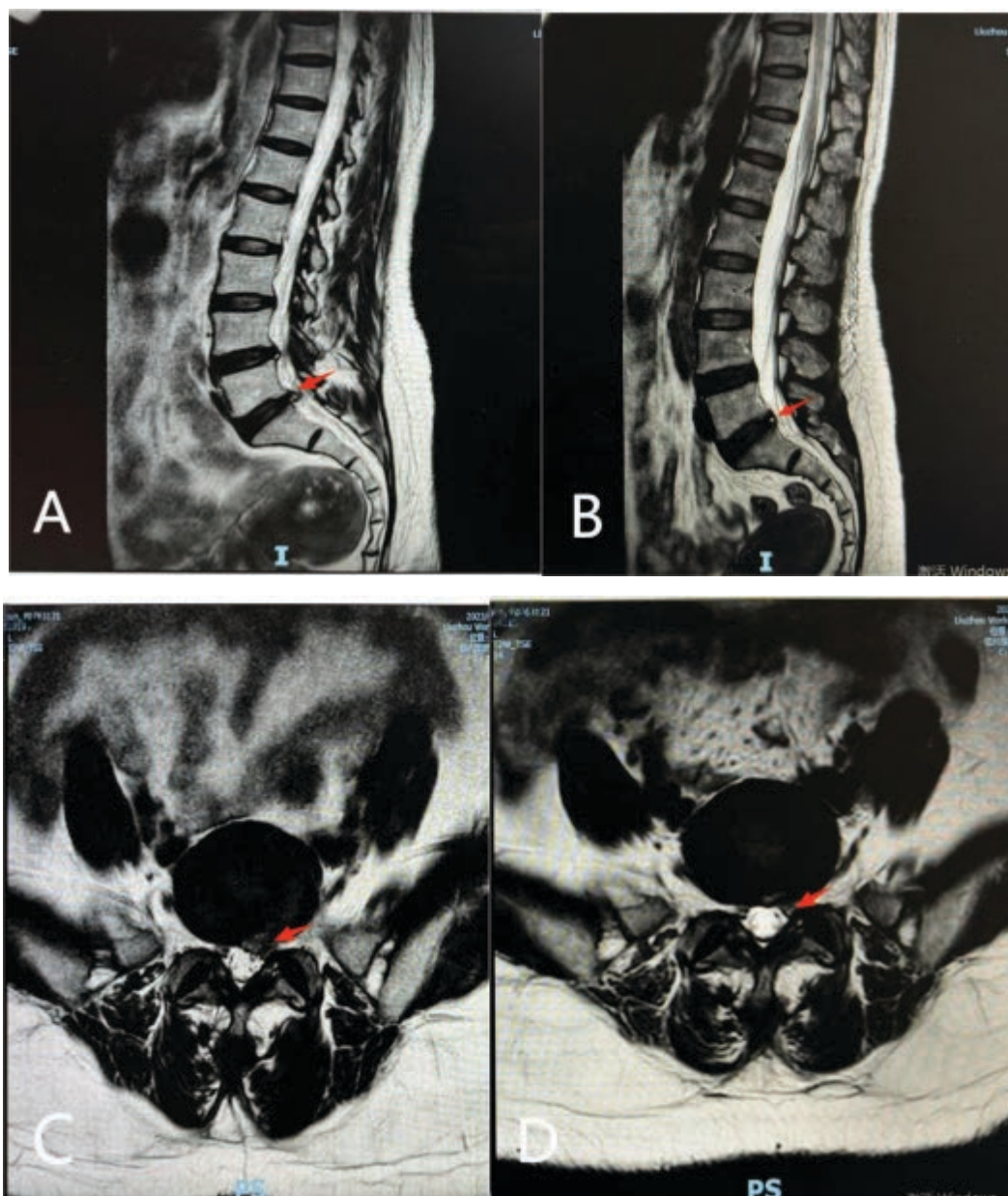


Figure 5. Preoperative and postoperative images of Group A (A, C: preoperative; B, D: 3 months after surgery)

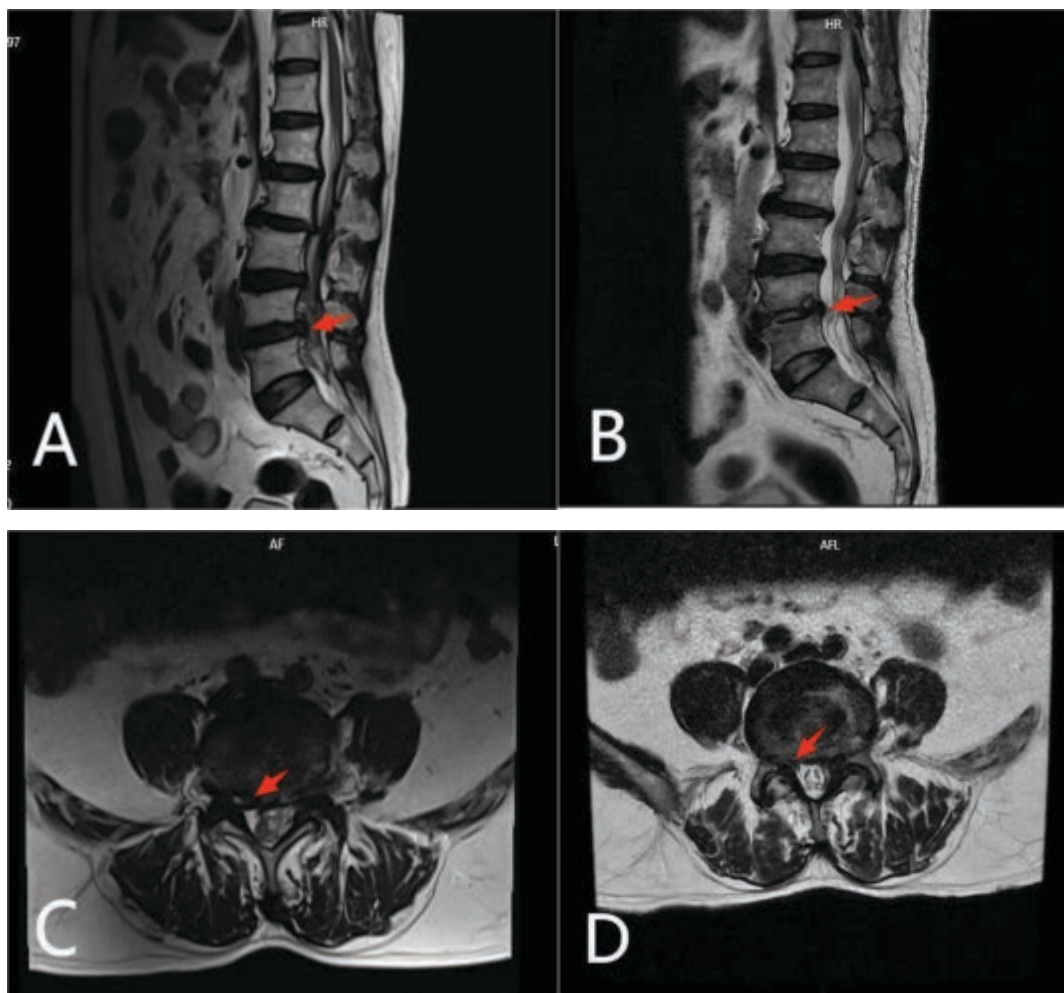


Figure 6. Preoperative and postoperative images of Group B (A, C: preoperative; B, D: 3 months after surgery)

3.4. Safety evaluation

Neither group of patients experienced nerve root injury, neurological edema, intervertebral space infection, deep vein thrombosis of the lower extremities, or other complications. In Group A, only one patient experienced minor bleeding during the operation, which ceased after emergency hemostasis, allowing normal subsequent treatment to proceed. Group B did not experience any bleeding during the operation. Neither group exhibited weakness or numbness in the lower extremities postoperatively. Both groups demonstrated satisfactory safety profiles.

4. Discussion

Collagenase chemonucleolysis involves inserting a puncture needle into the affected area and injecting collagenase, which reaches the herniated site through puncture injection. Activated by proenzyme activators within the intervertebral disc, collagenase disrupts the internal structure, causing the α -chain to break at 3/4 of the distance from the amino acid, ultimately degrading into amino acids that flow into the bloodstream and are neutralized and absorbed by plasma^[9]. Additionally, collagenase can inhibit the activity of phospholipase A2, a substance typically associated with tissue inflammation, thereby providing both analgesic and anti-

inflammatory effects at the affected site, resulting in an excellent therapeutic outcome for lumbar disc herniation ^[10–13]. Theoretically, when the herniation is small and the annulus fibrosus is intact, collagenase can be injected into the intervertebral disc for intradiscal injection ^[14]. However, this method is prone to causing injury, poses greater challenges in postoperative care, and has a higher recurrence rate compared to extradiscal injection, making extradiscal injection more commonly used in clinical practice ^[15]. In this study, both groups underwent extradiscal injection.

In this study, both Group A and Group B demonstrated favorable therapeutic effects during the 3-month postoperative follow-up, indicating the superior efficacy of collagenase chemonucleolysis in the clinical treatment of lumbar disc herniation. Since its initial proposal in 1999, the treatment concept of “targeted injection, enzyme dissolution of substrate” has gained widespread acceptance through numerous clinical trials and case observations. Adverse reactions following collagenase surgery have been continuously reduced with the development of treatment methods, while treatment efficacy has improved, with lower costs and minimal trauma. This not only contributes to the conservation of medical resources but also meets the requirements of the Diagnosis-Related Groups (DRG) policy ^[16].

In this study, Group A, which underwent a combination of sacral hiatus and intervertebral foramen safe triangle approach, showed superior results in terms of VAS score, ODI index, and Macnab efficacy evaluation compared to Group B, which underwent only sacral hiatus approach injection. This suggests that multi-path combined collagenase chemonucleolysis has better clinical efficacy than single-puncture path collagenase chemonucleolysis. This may be because multi-path combined collagenase chemonucleolysis has more puncture targets than single-path methods, covering a larger area on the surface of the herniated lesion, promoting the infiltration of collagenase through weak points to dissolve the herniated lesion compressing the nerve root, thereby enhancing the therapeutic effect ^[17]. This also suggests that collagenase chemonucleolysis should be performed according to the principles of low dose and multiple targets in actual clinical practice.

5. Conclusion

In summary, the results of this study indicate that multi-path combined collagenase chemonucleolysis has superior clinical efficacy compared to single-path collagenase chemonucleolysis. However, it should be noted that multi-path combined collagenase chemonucleolysis requires injection punctures at more sites than single-path methods, thereby increasing the surgical risk. In actual clinical treatment, a comprehensive consideration of efficacy and safety should be undertaken, taking into account the patient’s personal wishes and specific circumstances, to reasonably assess risks and select the appropriate puncture path. This study is a single-center clinical observational study, and due to the selection of samples only from our hospital, it inevitably has the limitation of a small sample size. Additionally, due to time constraints, the follow-up in this study only extended to 3 months postoperatively, which is a relatively short period. To more comprehensively and specifically validate the conclusions, further in-depth studies with larger sample sizes and more comprehensive approaches are needed to refine the conclusions of this study.

Disclosure statement

The author declares no conflict of interest.

References

- [1] Wang J, Fu Z, Song W, et al., 2022, Observation on the Efficacy of Percutaneous Discectomy Combined with Collagenase Chemonucleolysis in the Treatment of Giant Cervical Disc Herniation. *Chinese Journal of Pain Medicine*, 28(4): 314–316.
- [2] Li J, Lu P, 2023, Reevaluation and Prognosis Analysis of Radiofrequency Ablation in the Treatment of Lumbar Disc Herniation in Elderly Patients. *Science & Technology Review*, 41(13): 49–55.
- [3] Spinal Source Pain Group, Pain Society, Chinese Medical Association, 2020, Chinese Pain Expert Consensus on the Diagnosis and Treatment of Lumbar Disc Herniation. *Chinese Journal of Pain Medicine*, 26(1): 2–6.
- [4] Lang H, 2024, Analysis of Costs and Influencing Factors in 3520 Hospitalized Patients with Lumbar Disc Herniation. *Chinese Medical Record*, 25(5): 71–74.
- [5] Basic Research and Translation Group, Spinal Cord Professional Committee, Chinese Rehabilitation Medical Association, 2022, Guidelines for the Diagnosis, Treatment, and Rehabilitation Management of Lumbar Disc Herniation. *Chinese Journal of Surgery*, 60(5): 401–405.
- [6] Liu X, Yao B, Zhao S, et al., 2023, Clinical Observation of Radiofrequency Combined with a Small Amount of Collagenase Targeted Injection in the Treatment of Lumbar Disc Herniation. *Chinese Journal of Pain Medicine*, 29(4): 307–310.
- [7] Shi X, Lv Z, Hu L, et al., 2023, Historical Review and Development of Minimally Invasive Interventional Treatment with Collagenase Chemonucleolysis. *Journal of Air Force Military Medical University*, 44(10): 1006–1010.
- [8] Sheng M, Li S, 2020, Application Effect of Predictive Nursing in the Care of Patients After Collagenase Chemonucleolysis for Lumbar Disc Herniation. *Chinese Journal of Civil Health*, 32(8): 157–158.
- [9] Pain Society, Chinese Medical Association, Pain Physician Branch, Chinese Medical Doctor Association, 2023, Chinese Expert Consensus on Perioperative Nursing for Lumbar Disc Collagenase Chemonucleolysis. *Chinese Journal of Pain Medicine*, 29(11): 801–804.
- [10] Zhao J, Zhang R, Zhu B, et al., 2023, Comparison of the Efficacy of Transforaminal Endoscopic Spine System and Collagenase Chemonucleolysis in the Treatment of Extreme Lateral (Type II) Lumbar Disc Herniation. *Chinese Journal of Pain Medicine*, 29(2): 113–119.
- [11] Tang H, Chen S, 2023, Effects of Different Injection Methods of Collagenase on Serum TIMP-2, MMP-9 Expression, and Pain Scores in Patients with Lumbar Disc Herniation. *Journal of Neck and Low Back Pain*, 44(5): 836.
- [12] Song Y, Wang C, Fang B, et al., 2019, Research Progress and Application of Collagenase. *CIESC Journal*, 70(9): 3213–3227.
- [13] Han L, Li T, Chen L, et al., 2023, Effect of Collagenase Chemonucleolysis on Residual Pain After Transforaminal Lumbar Endoscopic Discectomy. *Journal of Pain Research*, 16(1): 1257–1265.
- [14] Ma W, Zhao X, Shi P, et al., 2022, Observation on the Application Effect of CT Manifestations of Lumbar Disc Herniation and Collagenase Chemonucleolysis. *Imaging Research and Medical Application*, 6(14): 41–43.
- [15] Zhang X, 2024, Effects of Radiofrequency Ablation Combined with Collagenase on Serum Pain Mediator Levels and Lumbar Function in Patients with Lumbar Disc Herniation. *Practical Journal of Integrated Traditional Chinese and Western Medicine*, 24(5): 58–74.
- [16] Danazumi MS, 2020, Physiotherapy Management of Lumbar Disc Herniation with Radiculopathy: A Narrative

Review. Nigerian Journal of Experimental and Clinical Biosciences, 7(2): 93–100.

- [17] Liu C, Chai Y, Ouyang L, 2023, Efficacy and Safety Evaluation of Percutaneous Transforaminal Endoscopic Spine System in the Treatment of Lumbar Disc Herniation with Nerve Root Canal Stenosis. Jiangxi Medical Journal, 58(5): 581–589.

Publisher's note

Bio-Byword Scientific Publishing remains neutral with regard to jurisdictional claims in published maps and institutional affiliations.

Observation on the Therapeutic Effect of Core Stability Training of Lumbar and Back Muscles Combined with Dynamic Joint Mobilization on Patients with Sacroiliac Joint Dysfunction

Huiqian Yan*, Jinpu Ge

Key Laboratory of Emergency and Trauma of Ministry of Education, Department of Rehabilitation Medicine, The First Affiliated Hospital, Hainan Medical University, Haikou 570102, Hainan, China

**Author to whom correspondence should be addressed.*

Copyright: © 2026 Author(s). This is an open-access article distributed under the terms of the Creative Commons Attribution License (CC BY 4.0), permitting distribution and reproduction in any medium, provided the original work is cited.

Abstract: *Objective:* To explore the clinical efficacy of core stability training of the lumbodorsal muscles combined with dynamic joint mobilization in patients with sacroiliac joint dysfunction. *Methods:* From October 2023 to December 2025, 38 patients with sacroiliac joint dysfunction were randomly divided into a training group ($n = 13$), a treatment group ($n = 12$), and a combined intervention group ($n = 13$). The training group received core stability training of the lumbodorsal muscles, the treatment group received Mulligan's technique, and the combined intervention group first received core stability training of the lumbodorsal muscles followed by Mulligan's technique. Before treatment and after six weeks of treatment, evaluations were conducted using the Numeric Pain Rating Scale (NPRS), the Oswestry Disability Index (ODI score), lumbar range of motion (ROM), and pressure pain threshold (PPT). *Results:* After six weeks of treatment, both the treatment group and the combined intervention group showed a decrease in NPRS scores compared to before intervention ($P < 0.05$). All three groups showed a decrease in ODI scores compared to before intervention ($P < 0.05$), with the combined intervention group having lower NPRS scores than the training group ($P < 0.05$) and lower lumbar extension ROM than the treatment group ($P < 0.05$). *Conclusion:* Core stability training of the lumbodorsal muscles combined with dynamic joint mobilization can effectively alleviate pain and improve dysfunction in patients with sacroiliac joint dysfunction, demonstrating good clinical application value.

Keywords: Sacroiliac joint dysfunction; Core stability training of the lumbodorsal muscles; Dynamic joint mobilization

Online publication: May 14, 2026

1. Introduction

Low back pain is a common musculoskeletal disorder, and sacroiliac joint dysfunction is a common subtype^[1]. Clinical treatments include exercise, manual therapy, medication, and surgery, among which core stability

training is widely used ^[2]. However, the efficacy of a single type of training is limited, and evidence for combined treatments remains insufficient. This study adopts core stability training combined with dynamic joint mobilization to evaluate its clinical efficacy.

2. Subjects and methods

2.1. General information

Thirty-eight patients with sacroiliac joint dysfunction who visited the Rehabilitation Medicine Department of the First Affiliated Hospital of Hainan Medical University in Haikou City from October 2023 to December 2025 were selected as the study subjects, including 8 males (21.1%) and 30 females (78.9%), with an average age of 38.76 ± 10.44 years. The 38 patients were randomly divided into a training group (13 cases), a treatment group (12 cases), and a combined intervention group (13 cases) using a random number table method. This study was approved by the hospital's Medical Ethics Committee (Ethics Approval Number: 2023-KYL-164).

2.2. Inclusion and exclusion criteria

Inclusion criteria: (1) Meeting the relevant diagnostic criteria of the 2021 Chinese Expert Consensus on the Diagnosis and Treatment of Sacroiliac Joint Pain, with diagnosis supported by CT or MRI examination; (2) Presenting with unilateral or bilateral persistent dull pain or needle-like pain; (3) Showing asymmetry in gait, shoulders, or pelvis on physical examination, with significant tenderness within 2 cm of the posterior superior iliac spine; (4) Having at least 3 positive results in sacroiliac joint pain provocation tests; (5) Negative results in the straight leg raise test and neurological examination. Exclusion criteria: (1) Spinal pathologies (e.g., infection, tumor, osteoporosis, fracture, structural deformity, inflammatory disease), radicular pain/radiculopathy (e.g., radicular syndrome or cauda equina syndrome), recent fracture or surgery in the lumbosacral or pelvic region; (2) Fear of manual therapy, etc.

2.3. Treatment methods

All three groups received treatment for 6 weeks, 3 times a week.

2.3.1. Training group

The training group received core stability training of the lumbodorsal muscles, mainly including the following exercises ^[3,4]: (1) Transversus abdominis training: The patient lies supine with hips and knees flexed, adjusts breathing, and actively contracts the abdomen during exhalation to draw the abdominal wall inward toward the spine. (2) Bird-dog exercise: In a quadrupod position, alternately lift the opposite upper and lower limbs while maintaining trunk stability. (3) Side bridge training: Lie on the side, support the body with the elbow and foot, and maintain the trunk in a straight line. (4) Bridge exercise: Lie supine with knees flexed, contract the gluteal and lumbodorsal muscles to elevate the pelvis. Each exercise is performed 10–15 times per set, 3 sets each time. As tolerance increases, a balance pad or Swiss ball can be used to increase training difficulty.

2.3.2. Treatment group

The treatment group received Mulligan's dynamic joint mobilization (Mobilisations With Movements, MWM) ^[5]. The direction of sacroiliac joint dysfunction is determined based on motion palpation: posteromedial MWM is used for anterior iliac dysfunction, and anterolateral MWM is used for posterior iliac dysfunction. Treatment is performed within a pain-free or significantly reduced pain range, with each movement repeated 6–10 times, 3 sets each time, approximately 10 minutes per session.

2.3.3. Combined intervention group

The combined intervention group received dynamic joint mobilization combined with core stability training, with the same treatment content and dosage as the above two groups. The combined treatment aims to first correct abnormal joint position and movement patterns through manual therapy, then consolidate pelvic and lumbar stability through core stability training to reduce recurrence.

2.4. Observation indicators

2.4.1. Pain perception

The degree of pain was assessed using the 0–10 Numeric Pain Rating Scale (NPRS) ^[6], with higher scores indicating more severe pain.

2.4.2. Functional disability

The degree of lumbodorsal-related functional disability was assessed using the Oswestry Disability Index (ODI) ^[7], with higher scores indicating more severe functional disability.

2.4.3. Range of motion

Lumbar flexion and extension range of motion (ROM) ^[8] were measured.

2.4.4. Pressure pain threshold

The pressure pain threshold (PPT) ^[9] was measured using a handheld push-pull dynamometer, recording the pressure value when the patient first felt pain, measured separately on the left and right sides.

2.5. Statistical methods

Statistical analysis was performed using SPSS 20.0 software. Measurement data conforming to a normal distribution were expressed as mean \pm standard deviation (SD). Paired sample t-tests were used for within-group comparisons, one-way analysis of variance was used for between-group comparisons, and the LSD method was used for post-hoc pairwise comparisons. A *P*-value <0.05 was considered statistically significant.

3. Results

3.1. Comparison of general information among the three groups

There were no significant differences in general information such as gender, age, and body mass index among the three groups (*P* > 0.05). See **Table 1**.

Table 1. Comparison of general information among the three groups of subjects (mean \pm SD)

	Training group	Treatment group	Combined intervention group
Number of participants (persons)	13	12	13
Age (years)	38.76 \pm 10.44	40.00 \pm 8.84	38.23 \pm 12.99
Male/Female	3/10	2/10	3/10
Height (cm)	164.31 \pm 6.51	165.17 \pm 8.96	166.77 \pm 8.72
Body weight (kg)	58.02 \pm 6.01	57.17 \pm 7.79	58.81 \pm 7.09
Body mass index (kg/m ²)	21.71 \pm 2.08	20.99 \pm 2.69	21.10 \pm 1.39

3.2. Comparison of NPRS scores among the three groups of patients

In this study, a comparison of the pre-intervention NPRS scores among the three groups of patients revealed no significant differences ($P > 0.05$). After the intervention, both the treatment group and the combined intervention group showed a decrease in NPRS scores compared to their pre-intervention levels ($P < 0.05$), with the combined intervention group having significantly lower NPRS scores than the training group ($P < 0.05$). See **Table 2**.

Table 2. NPRS (points, mean \pm SD) of the three groups before and after intervention

	Training group ($n = 13$)	Treatment group ($n = 12$)	Combined intervention group ($n = 13$)
Before intervention	3.62 \pm 1.33	4.29 \pm 2.07	3.5 \pm 1.29
After intervention	3.15 \pm 0.99 ^a	2.00 \pm 1.54 ^b	1.65 \pm 1.41
<i>P</i> value	0.273	0.005	0.010

Note: ^a indicates that the comparison between the combined intervention group and the training group shows $P < 0.05$; ^b indicates that the comparison between the combined intervention group and the treatment group shows $P < 0.05$.

3.3. Comparison of ODI scores among the three groups of patients

In this study, there was no significant difference in ODI scores among the three groups of patients before intervention ($P > 0.05$). After intervention, the ODI scores of all three groups decreased compared to those before intervention ($P < 0.05$), with no significant difference among the three groups ($P > 0.05$). See **Table 3**.

Table 3. ODI scores (points, mean \pm SD) before and after intervention for three groups of subjects

	Training group ($n = 13$)	Treatment group ($n = 12$)	Combined intervention group ($n = 13$)
Preintervention	36.15 \pm 11.49	36.00 \pm 7.68	36.77 \pm 9.64
Postintervention	30.00 \pm 9.06	28.67 \pm 7.24	27.54 \pm 10.43
<i>P</i> value	<0.001	<0.001	<0.001

3.4. Comparison of forward flexion range of motion (ROM) among the three groups of patients

In this study, there was no significant difference in forward flexion ROM among the three groups of patients before and after intervention ($P > 0.05$). See **Table 4**.

Table 4. Range of motion (ROM) in forward flexion ($^{\circ}$, mean \pm SD) before and after the intervention for three groups of participants

	Training group ($n = 13$)	Treatment group ($n = 12$)	Combined intervention group ($n = 13$)
Pre-intervention	27.64 \pm 5.13	28.33 \pm 4.40	28.61 \pm 5.29
Post-intervention	27.08 \pm 7.96	26.70 \pm 4.46	29.59 \pm 5.98
<i>P</i> value	0.785	0.414	0.590

3.5. Comparison of extension range of motion (ROM) among the three groups of patients

When comparing the extension ROM before and after intervention among the three groups of patients, no significant differences were observed among the groups ($P > 0.05$). After intervention, the extension ROM in the combined intervention group was significantly lower than that in the treatment group ($P < 0.05$). See **Table 5**.

Table 5. Extension ROM ($^{\circ}$, mean \pm SD) before and after intervention among the three groups of subjects

	Training group ($n = 13$)	Treatment group ($n = 12$)	Combined intervention group ($n = 13$)
Pre-intervention	13.72 \pm 2.80	14.86 \pm 3.93	15.56 \pm 4.29
Post-intervention	15.85 \pm 3.41 ^a	17.08 \pm 4.14 ^b	14.23 \pm 4.24
<i>P</i> value	0.073	0.188	0.260

Note: ^a indicates a significant difference ($P < 0.05$) between the combined intervention group and the training group; ^b indicates a significant difference ($P < 0.05$) between the combined intervention group and the treatment group.

3.6. Comparison of left PPT among the three groups

When comparing the left PPT of the three groups before and after intervention, there were no significant differences among the three groups ($P > 0.05$). See **Table 6**.

Table 6. Left PPT of subjects in the three groups before and after intervention (mean \pm SD)

	Training group ($n = 13$)	Treatment group ($n = 12$)	Combined intervention group ($n = 13$)
Pre-intervention	2.10 \pm 1.04	2.13 \pm 0.88	1.95 \pm 0.48
Post-intervention	2.29 \pm 1.09	2.10 \pm 0.51	2.20 \pm 0.44
<i>P</i> value	0.334	0.898	0.198

3.7. Comparison of right PPT among the three groups

When comparing the right PPT of the three groups before and after the intervention, there were no significant differences observed among the three groups ($P > 0.05$). See **Table 7**.

Table 7. Right PPT of subjects in the three groups before and after intervention (mean \pm SD)

	Training group ($n = 13$)	Treatment group ($n = 12$)	Combined intervention group ($n = 13$)
Pre-intervention	2.27 \pm 1.15	2.11 \pm 0.62	2.06 \pm 0.45
Post-intervention	2.11 \pm 1.01	2.19 \pm 0.49	2.20 \pm 0.42
<i>P</i> value	0.445	0.707	0.366

4. Discussion

The stability of the sacroiliac joint relies on the combined action of joint structure, ligament system, muscular system, and neural control system. When ligaments are lax, pelvic alignment is abnormal, or local stabilizing muscles are insufficiently controlled, the sacroiliac joint may experience minor dislocation and abnormal stress distribution, thereby inducing lumbosacral pain, functional limitations, and abnormal movement patterns^[10,11].

Mulligan's mobilization with movement emphasizes the application of appropriate assisted gliding during the patient's active movement to correct abnormal joint positions or movement trajectories^[12,13]. This method can restore local mechanical balance with minimal pain induction, reduce mechanical stimulation of the joint capsule, ligaments, and surrounding soft tissues, thereby alleviating pain. In addition to mechanical effects, manual therapy may also produce analgesic effects through neurophysiological mechanisms such as modulating central and peripheral pain transmission and activating descending inhibitory systems^[14–17]. Core stability training primarily targets deep stabilizing muscles such as the transverse abdominis, multifidus, pelvic floor muscles, and diaphragm. By enhancing the activation capacity and synergistic contraction level of these muscle groups, it can strengthen the dynamic stability of the lumbar-pelvic complex, improve posture control and load transfer efficiency, and reduce compensatory pain caused by insufficient stability^[13,18]. For patients with sacroiliac joint dysfunction, relying solely on passive treatment may be difficult to maintain long-term efficacy, while core stability training can provide continuous support at the functional level^[19].

The results of this study show that both the treatment group and the combined intervention group outperformed the training group in terms of pain improvement, and the NPRS score of the combined intervention group was lower than that of the training group after treatment, indicating that mobilization with movement has a more direct effect on pain relief, while combined treatment can further enhance efficacy. The ODI results showed that all three groups improved functional impairment, suggesting that both exercise therapy and manual therapy contribute to enhancing patients' daily activity capabilities. The combined group showed a numerically greater improvement in ODI, indicating that the treatment approach of "manual correction combined with active stabilization" has certain advantages.

However, this study revealed that after intervention, the extension range of motion (ROM) in the combined intervention group was significantly lower than that in the treatment group, possibly related to the increased lumbar stability resulting from core stability training of the lumbar and back muscles. Future research needs to further explore the impact of core stability training on lumbar stability. Although there was an upward trend in PPT, it did not reach statistical significance, possibly due to factors such as a small sample size, short treatment duration, and significant individual differences in pain sensitivity. The pressure pain threshold is greatly influenced by local tissue status, psychological factors, and the degree of central sensitization, and short-term intervention may not fully reflect its changes^[20,21]. Future research could appropriately expand the sample size, increase follow-up observations, and incorporate objective indicators such as surface electromyography, ultrasound, or motor control assessment to more comprehensively elucidate the mechanism of combined treatment.

5. Conclusion

In summary, core stability training of the lumbar and back muscles combined with mobilization with

movement can reduce pain and improve functional impairment in patients with sacroiliac joint dysfunction. However, due to the small sample size in this study, future research could expand the sample size and increase follow-up duration to further track the efficacy of core stability training of the lumbar and back muscles combined with mobilization with movement in treating sacroiliac joint dysfunction.

Funding

Youth Cultivation Fund Project of the First Affiliated Hospital of Hainan Medical University (HYYFYYPY202307)

Disclosure statement

The authors declare no conflict of interest.

References

- [1] Katz V, Schofferman J, Reynolds J, 2003, The Sacroiliac Joint: A Potential Cause of Pain After Lumbar Fusion to the Sacrum. *Journal of Spinal Disorders Techniques*, 16(1): 96–99.
- [2] Cohen S, Chen Y, Neufeld N, 2013, Sacroiliac Joint Pain: A Comprehensive Review of Epidemiology, Diagnosis and Treatment. *Expert Review of Neurotherapeutics*, 13(1): 99–116.
- [3] Training Bureau of the State General Administration of Sports, Physical Fitness Training Center of the National Team, 2017, *Manual of Body Functional Training Movements*, People's Sports Publishing House, Beijing.
- [4] Zhang G, Chen Y, Zhang Y, et al., 2015, Observation on the Efficacy of Manual Therapy Combined with Core Stability Training in the Treatment of Lumbar Disc Herniation. *Chinese Journal of Physical Medicine and Rehabilitation*, 37(07): 536–538.
- [5] Mulligan BR, 2004, *Manual Therapy: NAGS, SNAGS, MWMS, etc.*, 5th Edition, OPTH.
- [6] Von Korff M, Jensen MP, Karoly P, 2000, Assessing Global Pain Severity by Self-Report in Clinical and Health Services Research. *Spine*, 25(24): 3140–3151.
- [7] Fairbank JC, Couper J, Davies JB, et al., 1980, The Oswestry Low Back Pain Disability Questionnaire. *Physiotherapy*, 66(8): 271–273.
- [8] Saur PM, Ensink FB, Frese K, et al., 1996, Lumbar Range of Motion: Reliability and Validity of the Inclinator Technique in the Clinical Measurement of Trunk Flexibility. *Spine*, 21(11): 1332.
- [9] Orakifar N, Kamali F, Pirouzi S, et al., 2012, Sacroiliac Joint Manipulation Attenuates Alpha-Motoneuron Activity in Healthy Women: A Quasi-Experimental Study. *Archives of Physical Medicine Rehabilitation*, 93(1): 56–61.
- [10] Yang X, Zhang X, Liu H, et al., 2016, Research Progress in Manual Therapy for Sacroiliac Joint Dislocation. *Chinese Journal of Traditional Chinese Orthopedics and Traumatology*, 24(08): 77–79.
- [11] Spinal-Derived Pain Group of the Pain Society of the Chinese Medical Association, Feng Z, Zheng Y, et al., 2021, Chinese Expert Consensus on the Diagnosis and Treatment of Sacroiliac Joint Pain. *Chinese Journal of Pain Medicine*, 27(2): 7.
- [12] Exelby L, 2002, The Mulligan Concept: Its Application in the Management of Spinal Conditions. *Man Ther*, 7(2): 64–70.
- [13] Gibbons J, 2018, *Functional Anatomy of the Pelvis and Sacroiliac Joint - A Manual Therapy Guide* [Zhu Y, Wang X,

Li C, Trans.], Beijing Science and Technology Press, Beijing.

- [14] Imamura M, Chen J, Matsubayashi S, et al., 2013, Changes in Pressure Pain Threshold in Patients with Chronic Nonspecific Low Back Pain. *Spine*, 38(24): 2098–2107.
- [15] Palsson TS, Graven-Nielsen T, 2012, Experimental Pelvic Pain Facilitates Pain Provocation Tests and Causes Regional Hyperalgesia. *Pain*, 153(11): 2233–2240.
- [16] O'Neill S, Manniche C, Graven-Nielsen T, et al., 2007, Generalized Deep-Tissue Hyperalgesia in Patients with Chronic Low-Back Pain. *Eur J Pain*, 11(4): 415–420.
- [17] Aoyagi K, He J, Nicol A, et al., 2019, A Subgroup of Chronic Low Back Pain Patients With Central Sensitization. *The Clinical Journal of Pain*, 35(11): 869–879.
- [18] Stathopoulos N, Dimitriadis Z, Koumantakis GA, 2019, Effectiveness of Mulligan's Mobilization With Movement Techniques on Range of Motion in Peripheral Joint Pathologies: A Systematic Review With Meta-analysis Between 2008 and 2018. *J Manipulative Physiol Ther*, 42(6): 439–449.
- [19] Zhang Z, Huang Z, 2008, A New Concept in Rehabilitation Treatment for Low Back Pain - Spinal Segmental Stability Training. *Chinese Journal of Rehabilitation Medicine*, (03): 279–282.
- [20] Bialosky J, Bishop M, Price D, et al., 2009, The Mechanisms of Manual Therapy in the Treatment of Musculoskeletal Pain: A Comprehensive Model. 14(5): 531–538.
- [21] Moss P, Sluka K, Wright A, 2007, The Initial Effects of Knee Joint Mobilization on Osteoarthritic Hyperalgesia. *Man Ther*, 12(2): 109–118.

Publisher's note

Bio-Byword Scientific Publishing remains neutral with regard to jurisdictional claims in published maps and institutional affiliations.

Research Progress on Subchondral Bone Lesions in Knee Osteoarthritis

Yunlong Li¹, Xiaoqiang Su^{2*}

¹The First Clinical Medical College of Shaanxi University of Chinese Medicine, Xianyang 712046, Shaanxi, China

²Spine Department, Xi'an Affiliated Hospital of Shaanxi University of Chinese Medicine, Xi'an 710021, Shaanxi, China

**Corresponding author:* Xiaoqiang Su, 1005639367@qq.com

Copyright: © 2026 Author(s). This is an open-access article distributed under the terms of the Creative Commons Attribution License (CC BY 4.0), permitting distribution and reproduction in any medium, provided the original work is cited.

Abstract: This article reviews the research on subchondral bone lesions in knee osteoarthritis. Subchondral bone is closely related to articular cartilage in terms of embryonic development and anatomical structure, and the two form bone-cartilage units. These units interact and crosstalk with each other in biomechanics and molecular biology. Subchondral bone lesions include various pathological forms. There are certain research prospects for the prevention and treatment of knee osteoarthritis targeting the subchondral bone.

Keywords: Knee osteoarthritis; Subchondral bone; Bone-cartilage unit

Online publication: May 14, 2026

1. Introduction

Knee osteoarthritis (KOA) is a disease characterized mainly by the degeneration of articular cartilage. With the aging of the population and the increase in the number of obese people, the number of KOA patients has increased, which has brought a great burden to society and families ^[1,2]. Drug and non-drug treatments for KOA can effectively relieve joint pain, but they cannot effectively reverse the pathological process of KOA. As the severity of the disease increases, it can cause significant pain and joint function limitations, and in severe cases, surgical treatment is required ^[3]. KOA is currently also regarded as a disease of the entire joint, in which subchondral bone is closely related to articular cartilage. Studies have shown that the integrity and homeostasis of articular cartilage may depend on the biomechanical and molecular biological interactions with subchondral bone ^[4]. There are certain research prospects for the prevention and treatment of KOA through the regulation of subchondral bone.

2. Embryonic development and tissue structure of subchondral bone

The femur and tibia in the knee joint originate from bone marrow mesenchymal stem cells in the embryo.

These stem cells form “blastema,” which contains a small amount of type I collagen matrix and transforms into a cartilage structure in the early fetal stage. The extracellular components of this structure are mainly type II collagen^[5]. During the terminal differentiation of cartilage, it hypertrophies and forms blood vessels and bone mineralization, thereby causing the process of endochondral ossification and creating the main ossification center. After birth, three cartilaginous interfaces are formed at the tibia and femoral ends of the knee joint, namely the chondroepiphyseal bone, the growth plate epiphyseal bone, and the growth plate metaphysis bone. The articular cartilage is located at the top of the subchondroepiphyseal bone. During growth and development, the epiphyses expand into the chondroprimordium until a very thin calcified layer is formed deep within the cartilage, thus forming calcified cartilage. The perivascular bone beneath the calcified cartilage gradually deposits to form subchondral bone plates and the supporting trabeculae below. At this stage, a wavy structure forms at the junction of the cartilage and the subchondral bone. This is conducive to the close combination of the two and the dispersion of the stress in the upper cartilage^[6]. From the perspective of embryonic development and anatomical structure, cartilage and subchondral bone have a close relationship and may influence each other pathologically.

3. Bone-cartilage units and KOA

Bone and articular cartilage form the “bone-cartilage unit,” which includes hyaline cartilage, hyaline line, calcified cartilage, and subchondral bone. This unit is a complex functional unit. There is mutual interference between molecules at the junction of articular cartilage and subchondral bone. Abnormal remodeling of subchondral bone caused by KOA can lead to vascular and nerve invasion of the junction area between articular cartilage and subchondral bone. Cartilage damage and vascular invasion can increase the diffusion of small molecules in this area and enhance the cross-interference between articular cartilage and subchondral bone molecules^[7,8]. In terms of biomechanics, abnormal subchondral bone remodeling caused by KOA, such as bone destruction, bone sclerosis, and thickening of subchondral bone plates, may damage the mechanical characteristics of subchondral bone, leading to the loss of mechanical balance between cartilage and subchondral bone, thereby aggravating the degeneration of overlying articular cartilage^[9].

4. Manifestations and treatment of subchondral bone lesions in KOA

4.1. Subchondral bone destruction

Animal studies have shown that in the early stage of KOA, the activity of osteoclasts in subchondral bone increases, leading to subchondral bone resorption and the formation of a large number of cavities. Osteoclasts can also secrete netrin-1, which promotes the innervation of sensory nerves in subchondral bone, thereby aggravating joint pain^[10]. Studies have found that in the early stage of KOA, the expression of prostaglandin E2 (PGE2) in subchondral bone and prostanoid 4 (EP4) in osteoclasts increases. PGE2 can promote the differentiation of osteoclasts through EP4, causing the destruction of subchondral bone structure and sensory nerve innervation related to pain^[11]. Not all animal studies showed enhanced activity of osteoclasts in the early subchondral bone of KOA. Studies found that in the same mouse, through the left knee anterior cruciate ligament transection to simulate KOA, in the early stage, the subchondral bone of the left knee joint shows enhanced osteoclast activity, while the right knee joint on the opposite side only shows weak osteoblast changes. This may be somewhat different from the spontaneous KOA in humans^[12]. This also indicates that

the enhanced activity of subchondral osteoclasts in the early stage of KOA in animal studies may be related to the abnormal load caused by mechanical damage resulting from surgical modeling. Zoledronate belongs to the bisphosphonate class of drugs and has the effect of inhibiting osteoclast generation. Zoledronate can alleviate the early subchondral bone mass loss in KOA rabbits, thereby improving the bone microstructure and alleviating the degeneration of articular cartilage^[13]. Clinical studies have also found that zoledronate can alleviate joint pain and limited joint movement in patients with KOA, and can reduce the use of non-steroidal anti-inflammatory drugs^[14]. Some studies have found that the preventive use of alendronate can alleviate the early subchondral bone destruction of KOA and relieve cartilage degeneration. Although the use of alendronate two weeks after modeling can reduce subchondral bone destruction, it cannot effectively relieve cartilage degeneration^[15]. Because the main mechanism of bisphosphonate drugs is to inhibit the activity of osteoclasts, the timing of treating subchondral bone lesions in KOA is crucial. However, if the cartilage has already undergone degeneration, while the use of bisphosphonate drugs at this time can alleviate abnormal bone remodeling, the damage to the cartilage is already irreversible.

4.2. Subchondral bone sclerosis

As KOA progresses and subchondral bone undergoes continuous bone remodeling, subchondral bone gradually thickens and its bone density increases, leading to subchondral bone sclerosis^[16]. Stromal cell-derived factor-1 α (SDF-1 α) is closely related to bone metabolism. In KOA mice, SDF-1 α in subchondral bone and peripheral blood slightly increased in the second week after modeling, but significantly increased in the eighth week. High levels of SDF-1 α promote the proliferation of bone marrow mesenchymal stem cells, thereby indirectly leading to an increase in osteoblast differentiation and bone formation, and causing subchondral bone hardening^[17]. Transforming growth factor- β (TGF- β) is a key factor for maintaining the normal structure of articular cartilage, but it is also involved in the pathological process of KOA. Abnormal remodeling of subchondral bone in KOA can cause an increase in the production of TGF- β , leading to degeneration of articular cartilage and excessive osteogenesis^[18]. Vasoactive intestinal peptide (VIP) is related to bone metabolism. VIP can promote osteogenic formation. The expression of VIP in subchondral bone significantly increases in patients with severe KOA. The use of VIP antagonists in KOA mice can alleviate the hardening of subchondral bone and the degeneration of articular cartilage^[19]. Metformin is a hypoglycemic drug, but it can also affect bone metabolism through its anti-inflammatory effect. Research has found that metformin can alleviate the degeneration of cartilage in KOA mice and also reduce the hardening of subchondral bone, thereby exerting a therapeutic effect on KOA^[20]. Compared with drug treatment, physical therapy may have more research prospects. Some studies have found that low-intensity ultrasound can reduce cartilage degeneration and repair cartilage, as well as alleviate the hardening of subchondral bone^[21].

4.3. Subchondral bone marrow lesions

Bone marrow lesions (BMLs) are the imaging features of the subchondral bone region of the knee joint on MRI, manifested as low-signal areas in T1-weighted images and high-signal areas in T2-weighted images. BMLs include pathological changes such as subchondral bone marrow edema, hemorrhage, necrosis, and bone remodeling, which are seen in diseases such as fractures, bone contusions, and KOA. Therefore, BMLs are not a specific manifestation of KOA, but there is a significant positive correlation between BMLs and articular cartilage injury. Moreover, BMLs can occur in the early stage of KOA, even before articular

cartilage degeneration ^[22,23]. A study has found that after a 3-year follow-up, the proportion of total knee arthroplasty in KOA patients with BMLs was significantly higher than that in patients without BMLs. Moreover, the larger the range of BMLs in KOA patients, the higher the proportion of total knee arthroplasty. This also indicates that BMLs are one of the risk factors for the progression of KOA ^[24]. In terms of treatment, injecting calcium phosphate into the BMLs of KOA patients can alleviate joint pain and improve joint function, but the impact on patients' long-term prognosis remains uncertain. In patients with KOA, the increase in the range of BMLs is closely related to the aggravation of joint pain. After neridronate injection treatment is given to patients with acute joint pain and BMLs in KOA, the BML score can be reduced and joint pain can be improved ^[25].

5. Conclusion

Subchondral bone and articular cartilage form the bone-cartilage unit, and the two are closely related in physiology and pathology. The lesions of subchondral bone in KOA can be observed in animal studies as abnormal activation of osteoclasts in the early stage and abnormal osteogenesis in the late stage leading to subchondral bone hardening. However, whether there is abnormal activation of osteoclasts in the subchondral bone of early KOA in humans requires further research. The BMLs of subchondral bone are closely related to the progression of KOA disease. The treatment of KOA by targeting BMLs has certain research prospects.

Disclosure statement

The authors declare no conflict of interest.

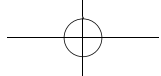
References

- [1] Sharma L, 2021, Osteoarthritis of the Knee. *N Engl J Med*, 384(1): 51–59.
- [2] Helmick CG, Felson DT, Lawrence RC, et al., 2008, Estimates of the Prevalence of Arthritis and Other Rheumatic Conditions in the United States. Part I. *Arthritis Rheum*, 58(1): 15–25.
- [3] Gelber AC, 2024, Knee Osteoarthritis. *Ann Intern Med*, 177(9): Itc129–itc144.
- [4] Kasaeian A, Roemer FW, Ghotbi E, et al., 2023, Subchondral Bone in Knee Osteoarthritis: Bystander or Treatment Target? *Skeletal Radiol*, 52(11): 2069–2083.
- [5] Sasano Y, Mizoguchi I, Kagayama M, et al., 1992, Distribution of Type I Collagen, Type II Collagen and PNA Binding Glycoconjugates During Chondrogenesis of Three Distinct Embryonic Cartilages. *Anat Embryol (Berl)*, 186(3): 205–213.
- [6] Hoemann CD, Lafantaisie-Favreau CH, Lascau-Coman V, et al., 2012, The Cartilage-Bone Interface. *J Knee Surg*, 25(2): 85–97.
- [7] Walsh DA, McWilliams DF, Turley MJ, et al., 2010, Angiogenesis and Nerve Growth Factor at the Osteochondral Junction in Rheumatoid Arthritis and Osteoarthritis. *Rheumatology (Oxford)*, 49(10): 1852–1861.
- [8] Pan J, Wang B, Li W, et al., 2012, Elevated Cross-Talk Between Subchondral Bone and Cartilage in Osteoarthritic Joints. *Bone*, 51(2): 212–217.
- [9] Goldring MB, Goldring SR, 2010, Articular Cartilage and Subchondral Bone in the Pathogenesis of Osteoarthritis. *Ann N Y Acad Sci*, 1192: 230–237.

- [10] Zhu S, Zhu J, Zhen G, et al., 2019, Subchondral Bone Osteoclasts Induce Sensory Innervation and Osteoarthritis Pain. *J Clin Invest*, 129(3): 1076–1093.
- [11] Jiang W, Jin Y, Zhang S, et al., 2022, PGE2 Activates EP4 in Subchondral Bone Osteoclasts to Regulate Osteoarthritis. *Bone Res*, 10(1): 27.
- [12] Zhu J, Zhu Y, Xiao W, et al., 2020, Instability and Excessive Mechanical Loading Mediate Subchondral Bone Changes to Induce Osteoarthritis. *Ann Transl Med*, 8(6): 350.
- [13] She G, Zhou Z, Zha Z, et al., 2017, Protective Effect of Zoledronic Acid on Articular Cartilage and Subchondral Bone of Rabbits with Experimental Knee Osteoarthritis. *Exp Ther Med*, 14(5): 4901–4909.
- [14] Ealahi T, Azad MAK, Islam MN, et al., 2025, Zoledronic Acid in the Treatment of Primary Knee Osteoarthritis: A Randomized Clinical Trial. *Cureus*, 17(5): e85087.
- [15] Mohan G, Perilli E, Parkinson IH, et al., 2013, Pre-Emptive, Early, and Delayed Alendronate Treatment in a Rat Model of Knee Osteoarthritis: Effect on Subchondral Trabecular Bone Microarchitecture and Cartilage Degradation of the Tibia, Bone/Cartilage Turnover, and Joint Discomfort. *Osteoarthritis Cartilage*, 21(10): 1595–1604.
- [16] Ren P, Niu H, Cen H, et al., 2021, Biochemical and Morphological Abnormalities of Subchondral Bone and Their Association with Cartilage Degeneration in Spontaneous Osteoarthritis. *Calcif Tissue Int*, 109(2): 179–189.
- [17] Meng Z, Xin L, Fan B, 2023, SDF-1 α Promotes Subchondral Bone Sclerosis and Aggravates Osteoarthritis by Regulating the Proliferation and Osteogenic Differentiation of Bone Marrow Mesenchymal Stem Cells. *BMC Musculoskelet Disord*, 24(1): 275.
- [18] Zhao W, Wang T, Luo Q, et al., 2016, Cartilage Degeneration and Excessive Subchondral Bone Formation in Spontaneous Osteoarthritis Involves Altered TGF- β Signaling. *J Orthop Res*, 34(5): 763–770.
- [19] Kanemitsu M, Nakasa T, Shirakawa Y, et al., 2020, Role of Vasoactive Intestinal Peptide in the Progression of Osteoarthritis Through Bone Sclerosis and Angiogenesis in Subchondral Bone. *J Orthop Sci*, 25(5): 897–906.
- [20] Feng XF, Zhang RK, Qi WZ, et al., 2019, Metformin Intervenes in Cartilage and Subchondral Bone Changes in the Early Stage of Osteoarthritis in a Mouse Model of Osteoarthritis. *Chinese Journal of Tissue Engineering Research*, 23(19): 3031–3036.
- [21] Li X, Sun Y, Zhou Z, et al., 2019, Mitigation of Articular Cartilage Degeneration and Subchondral Bone Sclerosis in Osteoarthritis Progression Using Low-Intensity Ultrasound Stimulation. *Ultrasound Med Biol*, 45(1): 148–159.
- [22] Xu L, Hayashi D, Roemer FW, et al., 2012, Magnetic Resonance Imaging of Subchondral Bone Marrow Lesions in Association with Osteoarthritis. *Semin Arthritis Rheum*, 42(2): 105–118.
- [23] Moradi K, Mohammadi S, Roemer FW, et al., 2024, Progression of Bone Marrow Lesions and the Development of Knee Osteoarthritis: Osteoarthritis Initiative Data. *Radiology*, 312(3): e240470.
- [24] Scher C, Craig J, Nelson F, 2008, Bone Marrow Edema in the Knee in Osteoarthritis and Association with Total Knee Arthroplasty within a Three-Year Follow-Up. *Skeletal Radiology*, 37(7): 609–617.
- [25] Varenna M, Zucchi F, Failoni S, et al., 2015, Intravenous Neridronate in the Treatment of Acute Painful Knee Osteoarthritis: A Randomized Controlled Study. *Rheumatology (Oxford)*, 54(10): 1826–1832.

Publisher's note

Bio-Byword Scientific Publishing remains neutral with regard to jurisdictional claims in published maps and institutional affiliations.



Integrated Services Platform of International Scientific Cooperation

Innoscience Research (Malaysia), which is global market oriented, was founded in 2016. Innoscience Research focuses on services based on scientific research. By cooperating with universities and scientific institutes all over the world, it performs medical researches to benefit human beings and promotes the interdisciplinary and international exchanges among researchers.

Innoscience Research covers biology, chemistry, physics and many other disciplines. It mainly focuses on the improvement of human health. It aims to promote the cooperation, exploration and exchange among researchers from different countries. By establishing platforms, Innoscience integrates the demands from different fields to realize the combination of clinical research and basic research and to accelerate and deepen the international scientific cooperation.

Cooperation Mode



Clinical Workers



In-service Doctors



Foreign Researchers



Hospital



University



Scientific institutions

OUR JOURNALS



The *Journal of Architectural Research and Development* is an international peer-reviewed and open access journal which is devoted to establish a bridge between theory and practice in the fields of architectural and design research, urban planning and built environment research.

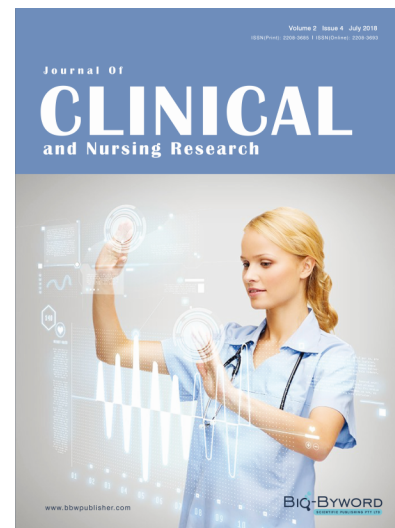
Topics covered but not limited to:

- Architectural design
- Architectural technology, including new technologies and energy saving technologies
- Architectural practice
- Urban planning
- Impacts of architecture on environment

Journal of Clinical and Nursing Research (JCNR) is an international, peer reviewed and open access journal that seeks to promote the development and exchange of knowledge which is directly relevant to all clinical and nursing research and practice. Articles which explore the meaning, prevention, treatment, outcome and impact of a high standard clinical and nursing practice and discipline are encouraged to be submitted as original article, review, case report, short communication and letters.

Topics covered by not limited to:

- Development of clinical and nursing research, evaluation, evidence-based practice and scientific enquiry
- Patients and family experiences of health care
- Clinical and nursing research to enhance patient safety and reduce harm to patients
- Ethics
- Clinical and Nursing history
- Medicine



Journal of Electronic Research and Application is an international, peer-reviewed and open access journal which publishes original articles, reviews, short communications, case studies and letters in the field of electronic research and application.

Topics covered but not limited to:

- Automation
- Circuit Analysis and Application
- Electric and Electronic Measurement Systems
- Electrical Engineering
- Electronic Materials
- Electronics and Communications Engineering
- Power Systems and Power Electronics
- Signal Processing
- Telecommunications Engineering
- Wireless and Mobile Communication

